

Electronic Thesis and Dissertation Repository

7-24-2019 10:30 AM


Enhanced Carbon Fiber-Epoxy Composites for Rowing Racing Shells

Rayehe Samimi
The University of Western Ontario

Supervisor
Charpentier, Paul A.
The University of Western Ontario

Graduate Program in Chemical and Biochemical Engineering
A thesis submitted in partial fulfillment of the requirements for the degree in Master of Engineering Science
© Rayehe Samimi 2019

Follow this and additional works at: <https://ir.lib.uwo.ca/etd>

 Part of the [Other Chemical Engineering Commons](#), [Other Materials Science and Engineering Commons](#), [Polymer Science Commons](#), and the [Structural Materials Commons](#)

Recommended Citation

Samimi, Rayehe, "Enhanced Carbon Fiber-Epoxy Composites for Rowing Racing Shells" (2019). *Electronic Thesis and Dissertation Repository*. 6276.
<https://ir.lib.uwo.ca/etd/6276>

This Dissertation/Thesis is brought to you for free and open access by Scholarship@Western. It has been accepted for inclusion in Electronic Thesis and Dissertation Repository by an authorized administrator of Scholarship@Western. For more information, please contact wlsadmin@uwo.ca.

Abstract

This thesis investigates the thermomechanical properties of two commercial composites using carbon fiber reinforcement in epoxy resins for manufacturing marine based rowing racing shells. The main goal of this project was to investigate how to control the resin properties and curing temperatures to improve the final product properties including adhesion, toughness modulus and tensile strength. Moreover, an efficient curing process was required by our supporting company to be used at low temperatures to enhance the curing characteristics and to provide improved mechanical properties. Accordingly, the current research tries to improve the manufacturing curing process and build up high performance structure with enhanced properties for low weight racing hulls.

Using a vacuum bagging only technique (VBO), the composite prepregs were cured by an improved ramp rate of 3°C/min. Numerous thermomechanical devices (e.t TGA, DSC, DMA and Instron) were used to check for weigh loss and mechanical properties of the carbon fiber-epoxy resin prepregs.

The results of this thesis showed that utilizing the autoclave curing technique (OoA), an epoxy matrix composite could be prepared with the thermomechanical properties of the carbon fiber prepregs improved and the curing cycle shortened. A void- free and pinhole-free composite surface was obtained with enhanced mechanical properties using a ramp rate of 3°C/min and holding time after the curing process of 2 hours and 50 minutes with an onset curing temperature of 121°C.

Keywords

Carbon fiber- epoxy resin, composite prepregs, Vacuum bagging technique (VBO), TGA, DSC, DMA, Instron, Out of Autoclave curing (OoA)

Summary for lay audience

This dissertation investigates the thermomechanical properties of two commercial composites using carbon fiber reinforcement in epoxy resins for manufacturing marine based rowing racing shells. The main goal was to examine how to control the resin properties and curing temperatures to improve the final product properties and illuminating the possible voids and pinholes on the surface of the composites.

An efficient curing process was required by our supporting company to be used at low temperatures to enhance the curing characteristics and to provide improved mechanical properties. Using a vacuum bagging only technique (VBO), the composite prepregs were baked, which will be called curing, by an improved ramp rate of 3°C/min. Numerous thermomechanical devices (e.t TGA, DSC, DMA and Instron) were used to check for weight loss and mechanical properties of the carbon fiber- epoxy resin prepregs.

All in all, the results of this thesis showed that utilizing the autoclave curing technique (OoA), an epoxy matrix composite could be prepared with the thermomechanical properties of the carbon fiber prepregs improved and the curing cycle shortened. A void- free and pinhole-free composite surface was obtained with enhanced mechanical properties using a ramp rate of 3°C/min and holding time after the curing process of 2 hours and 50 minutes with an onset curing temperature of 121°C.

Co-Authorship Statement

This dissertation is prepared in the integrated-article format. Manuscripts that have been previously published, or submitted for publication, or finalized for submission form the body of this dissertation which are presented with some adjustments in Chapters 2 through 4.

Title: Optimizing the carbon fiber- epoxy resin matrix composites to improve the thermomechanical properties. **Authors:** Rayehe Samimi, Sahar Samimi, Mehdi Bagheri, Paul A. Charpentier. The experimental works were conducted by Rayehe Samimi under the guidance of advisor Dr. Paul A. Charpentier. The statistical planning was guided by Dr. Sahar Samimi. Mehdi Bagheri helped for the microscopic figures. The draft of this manuscript was written by Rayehe Samimi. Modifications were carried out under the close supervision of Dr. Paul A. Charpentier. The final version of this article was presented as a poster in **Interamerican congress of Chemical Engineering incorporating the 68th Canadian chemical engineering conference** at Toronto, ON, Canada, 2018.

Title: Improving and comparing the mechanical properties of two commercial prepregs by optimizing the carbon fiber- epoxy resin matrix composites. **Authors:** Rayehe Samimi, Bode Oyeneeye, Paul A. Charpentier, Amin Rizkalla. The experimental works were conducted by Rayehe Samimi under the guidance of advisor Dr. Paul A. Charpentier. Bode Oyeneeye helped in the experimental set up and design. The hardness tests were done in Dr. Rizkalla's lab under his supervision. The draft of this manuscript was written by Rayehe Samimi and corrected by Dr. Paul A. Charpentier. This manuscript is under preparation for publication.

Dedication

To my beloved family whom are always my emotional support through thick and thin...
Mostly my darling sister, Sahar, who is truly both my mentor and heroine from now to the
eternity...

Acknowledgments

I would like to express my deep gratitude to Professor Paul A. Charpentier for his tremendous guidance, encouragement, and support. The completion of this dissertation would not have been possible without his incomparable assistance and invaluable effort.

I gratefully thank Hudson Boat works for their impressive advice and help in for technical supports, material supplies and cutting several samples for the matter of this project. Also, I would like to express my appreciation and sincere respect to Dr. Sahar Samimi for her invaluable advice and positive comments in this thesis.

I gratefully thank Dr. Bode Oyeneeye and Mehdi Bagheri for their valuable help during both Instron runs and microscopic results and Dr. Amin Rizkalla for his great support on training the hardness device and giving the permission to run more samples using numerous mechanical techniques. Also, I thank Dr. William Z. Xu for his help in training me for the DMA device and Yixing Tang for training sessions on the TGA and DSC devices.

I would also thank all my colleagues in Charpentier's Lab (past and present) for their support, cooperation and helpful discussion specifically Dr. Sahar Samimi, Dr. William Z. Xu, Dr. Bode Oyeneeye and support of Devon Machin, Shaun Fraser and Mohammad Osama.

More importantly, I would like to thank my true friends and wonderful family members specially my beloved sister and brother in law Sahar and Alireza. Also, without the unconditional love and support, tremendous patience and understanding of my parents, Mohammad and Soheila, I would not have been able to triumph my goals.

At last, I would like to mention that this work has been carried out with support from The Ontario Centres of Excellence (OCE).

Table of Contents

Abstract.....	i
Summary for lay audience	ii
Co-Authorship Statement.....	iii
Dedication.....	iv
Acknowledgments.....	v
List of Tables	ix
List of Figures	xi
List of Abbreviations, Symbols and Nomenclature	xvii
Chapter 1	1
1 Literature Review and experimental analysis and methods.....	1
1.1 Into the marine world and boat industry	1
1.2 Epoxy Resin	2
1.3 Carbon fiber	5
1.4 Nomex honeycomb	8
1.5 Matrix.....	10
1.6 Composites.....	11
1.7 Vacuum oven curing system.....	12
1.7.1 Prepregs and the Vacuum Bagging Only method (VBO).....	13
1.8 The relationship of DOE method and the materials (Chapter II).....	14
1.8.1 Central composite design.....	15
1.8.2 Reaching the optimization phase using the central composite design	16
1.8.3 Analysis of variance (ANOVA) for the statistical analysis technique	17

1.8.4	The relationship of the mechanical properties on behavior of the prepregs after the curing process (Chapter III).....	17
1.8.5	Tensile properties of the composite prepregs	18
1.8.6	Statistical analysis using the Holm-Sidak method (t-test)	26
1.9	Scope of the research	26
1.10	References.....	27
Chapter 2.....		31
2	Optimizing the carbon fiber- epoxy resin matrix composites to improve the thermomechanical properties	31
2.1	Abstract.....	31
2.2	Introduction.....	32
2.3	Experimental objectives.....	34
2.3.1	Sample preparation	34
2.3.2	Methodology.....	35
2.4	Results and discussion	41
2.4.1	Comparison of PID and Ramp and Soak curing technique	41
2.4.2	The response surface design of analysis	42
2.4.3	Checking basic mechanical properties for both two commercial prepregs	53
2.4.4	Comparison of both A and B prepregs	62
2.4.5	Differential Scanning Calorimetry (DSC)	64
2.4.6	DMA results for curing type B samples in lab scale	69
2.4.7	Optical Microscopic figures for both types of prepregs	72

2.5 Summary	73
2.6 References	74
Chapter 3	77
3 Improving and comparing the mechanical properties of two commercial prepregs by optimizing the carbon fiber- epoxy resin matrix composites.....	77
3.1 Abstract	77
3.2 Introduction.....	78
3.3 Experimental objectives.....	80
3.3.1 Sample preparation	80
3.3.2 Methodology.....	82
3.4 Results and discussion	84
3.4.1 The Central composite design (CCD) as the DOE technique for the optimization condition	84
3.4.2 Thermal gravimetry analysis (TGA) for both A and B prepregs indicating the mechanical behavior status of the composites	95
3.4.3 Glass transition point values using the (DMA).....	102
3.4.4 Tensile Strength	106
3.4.5 Elongation percentage to break.....	108
3.4.6 Young’s Modulus.....	110
3.4.7 Modulus of toughness	112
3.4.8 Hardness.....	113
3.5 Summary	116
3.6 References	118
Chapter 4.....	120

4	Conclusions and Recommendations	120
4.1	Conclusions.....	120
4.2	Recommendations for future works.....	122
	Curriculum Vitae	123

List of Tables

Table 2.1: Levels of variables for central composite experimental design.....	37
Table 2.2: Design runs using central composite design.....	37
Table 2.3: The results of ANOVA analysis of the developed models.....	43
Table 2.4: Constrains on the first optimization using the central composite design .	45
Table 2.5: Suitable solutions possible for central composite design optimum value for both types of A and B samples.....	46
Table 3.1: Constraints on the second phase optimization using the central composite design	89
Table 3.2: Propriate solutions possible for central composite design optimum value for both types of A and B samples in the second phase optimization.	90
Table 3.3: Addressing types of the prepregs using special relationship between onset curing temperature and the glass transition temperature.....	98
Table 3.4: The t-test results for the tensile strength results using the Holm-Sidak method for the two types of prepregs .	110
Table 3.5: The t-test results for the hardness value using the Holm-Sidak method by the design expert software for the curing conditions using two types of prepregs.....	112
Table 3.6: The t-test results for the Young's modulus value using the Holm-Sidak method by the design expert software for the curing conditions using two types of prepregs.....	114
Table 3.7: The t-test results for the hardness value using the Holm-Sidak method by the design expert software for the curing conditions using two types of prepregs.....	117

List of Figures

Figure 1.1: Numerous usages of polymer composite materials from the automotive to marine industry ²	1
Figure 1.2: The SHARK production being viewed from different angles ⁵	2
Figure 1.3: The chemical structure of the Bisphenol A (BPA) ¹	3
Figure 1.4: Curing Stages of the Epoxy resin: a) Epoxy resin uncured, b) Epoxy resin partially cured but still fusible, c) Epoxy resin becoming infusible (gel point) around 60% cured, d) Epoxy resin (fully-cured, infusible).....	4
Figure 1.5: a) Dyhard UR500 epoxy resin accelerator, b) Dyhard S100 curing agent, c) EPM104 epoxy resin, d) the overview of the three commercial components together.	5
Figure 1.6: Sample of the unidirectional commercial prepreg being used for this research. ...	7
Figure 1.7: The woven carbon fiber fabrics as the reinforcement materials, fillers, before the curing process.	7
Figure 1.8: Types of the numerous pinholes and voids the supplied prepregs were suffering from in the seat section of the rowing halls.	8
Figure 1.9: The Nomex honeycomb texture used for this dissertation.	9
Figure 1.10: a) The visual components of a matrix, b) the matrix components using carbon fiber, epoxy resin and Nomex honeycomb, and c) the cured matrix being used for the experiment, measuring the thermomechanical properties.	11
Figure 1.11: Schematic definition of both a) Isotropic and, b) Anisotropic structure of materials.....	12
Figure 1.12: a) Response surface with no curvature, b) Response surface with curvature ²⁹ . 15	
Figure 1.13: Stress-Strain Curves for a polymer.	20
Figure 1.14: Tensile strength at break point for polymers using the stress-strain curve.	21

Figure 1.15: The amount of elongation at break point using the stress-strain curve.	22
Figure 1.16: The Young's modulus using the stress-strain curve.....	22
Figure 1.17: The toughness modulus area for polymers using the stress-strain curve.	24
Figure 1.18: A typical diamond structure that the indenters would leave on the surface of the samples during the hardness test.....	25
Figure 1.19: a) Buehler MicroMet 5100 series device for hardness testing. b) The mounted sample being used for the hardness test using the paraffin wax.....	26
Figure 2.1: Assembly for curing Prepreg, a) without core, b) with honeycomb core.	5
Figure 2.2: Conventional curing technique using oven 1) The Vacuum Bagging process (VBO), 2) Installation of the direct vacuum line inside the oven, 3) Installation of the controller for the oven, 4) Final cured prepreg product after using the VBO technique.....	6
Figure 2.3: Orientation of the unidirectional carbon fibers for each layer of the prepreg composite matrix construction for both type A and B samples.	7
Figure 2.4: Testing mode using the DMA device for both prepregs ⁹	10
Figure 2.5: Curing conditions using: a) PID mode starting from the room temperature and increasing it manually, b-e) Ramp and Soak technique respectively using the values of 2, 3, 4 and 5 °C/min as the ramping factor starting from room temperature and increasing its value gradually with specific slope according to the ramp values.	13
Figure 2.6: a) Desirability plot and contour in A prepreg (Optimum point number 1), b) Desirability plot and contour in B prepreg (Optimum point number 5), c) Storage modulus plot and contour in A prepreg (Optimum point number 1), d) Storage modulus plot and contour in B prepreg (Optimum point number 5), e) Loss modulus plot and contour in A prepreg (Optimum point number 1), f) Loss modulus plot and contour in B prepreg (Optimum point number 5), g) Stiffness plot and contour in A prepreg (Optimum point number 1), h) Stiffness plot and contour in B prepreg (Optimum point number 5), i) Tan δ	

plot and contour in A prepreg (Optimum point number 1), j) Tan δ plot and contour in B prepreg (Optimum point number 5).....	21
Figure 2.7: Predicted vs. actual values of a) Storage modulus, b) Loss modulus, c) Stiffness and d) Tan δ as four responses of this central composite design of experiment.....	24
Figure 2.8: DMA results for A and B prepregs: a) Storage Modulus no- core, b) Storage modulus- with core, c) Stiffness-no core, d) Stiffness- with core, e) Tan δ - no core and f) Tan δ - no core.	27
Figure 2.9: Typical tan δ profile of cured prepreg without honeycomb core. Where ΔT is the temperature difference at 12h , and h is the height of the tan δ peak	29
Figure 2.10: Tan δ profile of type A prepreg and B <i>in solvent</i> prepreg without and with honeycomb core a) A prepregs at 115, 121 and 150 °C temperature without core, b) A prepregs at 115, 121 and 150 °C temperature with core, c) B prepregs at 115, 121 and 150 °C temperature without core and d) B prepregs at 115, 121 and 150 °C temperature with core.	32
Figure 2.11: TGA analysis of type A (top) and B (bottom) prepregs.....	35
Figure 2.12: Heat flow of A and B prepregs isothermal at 121 °C (top, after weight adjustment) and peak temperature, 155 °C and 145 °C, respectively.	36
Figure 2.13: Curing enthalpy of A and B prepregs (after weight adjust according to TGA result).	37
Figure 2.14: Glass transition temperature of A and B prepregs after dynamic curing.	38
Figure 2.15: Curing profile for A (top) and B prepregs (bottom) at peak temperature using <i>temperature jump</i> method. Mass corrected to the resin content in prepreg.....	39
Figure 2.16: DMA results for type B prepregs cured in lab scale. a) Storage Modulus, b) Loss modulus, c) Stiffness and d) Tan δ	42
Figure 2.17: Optical Microscopic structure of both A and B prepregs in different conditions: a) A with Ramp 2 °C/min, Holding time of 2 hours and 50 minutes. b) B with Ramp 2 °C/min,	

Holding time of 2 hours and 50 minutes. c) A with Ramp 3°C/min, Holding time of 2 hours and 50 minutes. d) B with Ramp 3°C/min, Holding time of 2 hours and 50 minutes. 44

Figure 3.1: Assembly for curing Prepreg: a) without core (used for the samples of this research), b) with honeycomb core. 52

Figure 3.2: a) VBO technique using an oven and its controller b) Final cured prepreg product after using the VBO technique..... 52

Figure 3.3. The extension technique for the prepreg composite bars using the Instron device¹⁴. 54

Figure 3.4: Rate of enhancement in mechanical properties by increasing the holding time after the curing process. In orders: A) Type A at initial point (Ramp at 2°C/min, Temp at 121°C, Holding time of 2 hours 50 minutes), B) Type B at initial point, C) Type A at optimum point (Ramp at 3°C/min, Temp 121 °C, Holding time of 2 hours 50 minutes), D) Type B at optimum point, E) Type A with higher holding time (Ramp at 3°C/min, Temp at 121°C, Holding time of 7 hours), F) Type B with higher holding time..... 57

Figure 3.5: Optimization phase analysis part II: a) Desirability plot and contour in type A prepreg (Optimum point number 1), b) Desirability plot and contour in type B prepreg (Optimum point number 11th), c) Storage modulus plot and contour in type A prepreg (Optimum point number 1), d) Storage modulus plot and contour in type B prepreg (Optimum point number 11th), e) Loss modulus plot and contour in type A prepreg (Optimum point number 1), f) Loss modulus plot and contour in type B prepreg (Optimum point number 11th), g) Stiffness plot and contour in type A prepreg (Optimum point number 1), h) Stiffness plot and contour in type B prepreg (Optimum point number 11th), i) Tan δ plot and contour in type A prepreg (Optimum point number 1), j) Tan δ plot and contour in type B prepreg (Optimum point number 11th). 63

Figure 3.6: Optical Microscopic structure of both A and B prepregs in different conditions: a) A with Ramp 2°C/min, Holding time of 2 hours and 50 minutes. b) B with Ramp 2°C/min, Holding time of 2 hours and 50 minutes. c) A with Ramp 3°C/min, Holding time of 3 hours and 39 minutes. d) B with Ramp 3°C/min, Holding time of 3 hours and 39 minutes. e) B with

Ramp 2°C/min, Holding time of 7 hours. f) B with Ramp 3°C/min, Holding time of 7 hours.
 65

Figure 3.7: The TGA overlapping results before and after the curing process a) A sample, ramp 2°C/min, holding time 2 hours and 50 minutes, b) A sample, ramp 3°C/min, holding time 2 hours and 50 minutes, c) A sample, ramp 3°C/min, holding time 3 hours and 39 minutes, d) B sample, ramp 2°C/min, holding time 2 hours and 50 minutes, e) B sample, ramp 3°C/min, holding time 2 hours and 50 minutes, f) B sample, ramp 3°C/min, holding time 3 hours and 39 minutes. 72

Figure 3.8: a) A sample Ramp 2°C/min, temperature 121°C, holding time 2 hours and 50 minutes, b) A sample Ramp 3°C/min, temperature 121°C, holding time 2 hours and 50 minutes, c) A sample Ramp 3°C/min, temperature 121°C, holding time of 3 hours and 39 minutes, d) B sample Ramp 2°C/min, temperature 121°C, holding time 2 hours and 50 minutes, e) B sample Ramp 3°C/min, temperature of 121°C, holding time 2 hours and 50 minutes, f) B sample Ramp 3°C/min, temperature 121°C, holding time 2 hours and 39 minutes. 76

Figure 3.9: Stress-strain curves for prepregs having both optimum and initial curing conditions with ramping rate of 2 and 3°C/min and holding time after the curing process value of 2 hours and 50 minutes and 3 hours and 39 minutes for both type A and B prepregs. 77

Figure 3.10: a) Tensile strength and percentage of the resin loss bar chart for both prepregs considering initial and optimum conditions using Instron, b) Tensile strength zoomed in to accurately compare two prepregs at same conditions using Instron. 78

Figure 3.11: Elongation at break point for both A and B prepregs. 80

Figure 3.12: a) Young’s modulus bar chart for both prepregs considering initial and optimum conditions using Instron, b) Young’s modulus zoomed in, to accurately compare two prepregs at same conditions using Instron. 82

Figure 3.13: Toughness modulus for both type A and B prepregs using the surface area under the stress vs the strain plot. 83

Figure 3.14: Hardness for both A and B type of prepregs using the Buehler MicroMet 5100 series hardness device. 84

Figure 3.15: Indentation mark on the surface of the samples using Buehler MicroMet 5100 series as hardness device a) A sample, ramp 2°C/min, holding time 2 hours and 50 minutes, b) A sample, ramp 3°C/min, holding time 2 hours and 50 minutes, c) A sample, ramp 3°C/min, holding time 3 hours and 39 minutes, d) B sample, ramp 2°C/min, holding time 2 hours and 50 minutes, e) B sample, ramp 3°C/min, holding time 2 hours and 50 minutes, f) B sample, ramp 3°C/min, holding time 3 hours and 39 minutes. 86

List of Abbreviations, Symbols and Nomenclature

Abbreviations

ANOVA	Analysis of Variance
NH ₂	Amino groups
BPA	Bisphenol A
CCD	Central composite design
CFRPs	Carbon fiber- reinforced polymers
DGEBA	Diglycidyl ether of bisphenol A
DSC	Differential Scanning Calorimetry
DMA	Dynamic Mechanical Analysis
DOE	Design of experiment
DOF	Degree of Freedom
DPH	Diamond Pyramid Hardness
EPM104	Epoxy resin
HV	Vickers Pyramid Number
MWCNT	Multi- Walled Carbon Nanotubes
OH	Hydroxyl groups
OoA	Out of autoclave
PID	Proportional Integral Derivative Controller (Three term controller)
S100	Dyhard Curing agent

Tg	Glass Transition Temperature
TGA	Thermal Gravimetry Analysis
UR500	Dyhard Epoxy resin
UD	Unidirectional
UV	Ultraviolet Light
VBO	Vacuum Bagging Only Method

Symbols

A	Area
A	Distance from the center of the experiment
-COOH	Carboxyl groups
°C	Degree Centigrade
C _p	Number of repetitions at central point
Cm ²	Square Centimeter
dL	Differential of the length (Integrator)
2D	Two Dimensional
3D	Three Dimensional
E	Young's Modulus
F	Force
F-Value	Fisher's test value
h	Hour
K	The factor numbers

k	Number of variables
L_0	Single length
L	Final length after applying force
δL	Length difference
m	Meter
m^2	Square Meter
min	Minute
mm	Millimeter
MPa	Mega Pascal
MN/m^2	Mega Newton per Square meter
N	Newton
Pa	Pascal
P-Value	Probability Value
PSI	Pound-force per square inch
R^2	Correlation Coefficient
Adj- R^2	Adjusted correlation coefficient
x_i	A coded value of the variable
X_i	Actual value of the variable
X_0	Actual value of X_i at the central point
δX	Change of the variable
X_1	Ramp

X_2	Temperature
X_3	Holding time after curing
X_4	Type of prepreg
Y	Predicted response variable
β_0	Constant term
β_i	Coefficients of the linear parameters
β_{ii}	Coefficients of the quadratic parameters
β_{ij}	Coefficients of the interaction parameters
σ	Tensile Stress
σ_{el}	Stress of the elastic portion of the sample
σ_y	Stress at the nonlinear portion of the stress-strain curve
ε	Tensile Strain
ε_f	The tensile strain at breakage
ε_{pl}	Plastic strain
ε_t	Total Strain
Γ	Peak Factor

Chapter 1

1 Literature Review and experimental analysis and methods

1.1 Into the marine world and boat industry

Fiber reinforced polymer composite materials are being widely used in the aerospace and automotive industries (Figure 1.1). In the past several years, many marine industries have been using these advanced polymer composites, such as the supporting company of this thesis, Hudson Boats Works.



Figure 1.1: Numerous usages of polymer composite materials from the automotive to marine industry².

In recent years, marine industries have shifted towards using carbon fiber reinforced with epoxy resins compared to the glass fibers previously used. This is due to the high tensile strength, high modulus, lower weight, good corrosion resistance and great damping properties of these carbon fiber based composites³⁻⁴.

One of the most recent projects of the Hudson team is the SHARK series, which utilizes composite materials by adopting aerospace technology and creating a new construction methodology consisting of carbon fibers reinforced with epoxy resins and sandwiched

between honeycomb layers. This structure was demonstrated to be 4 times more impact resistant and 50% stiffer than the previous structures made by the company (Figure 1.2)⁵.



Figure 1.2: The SHARK production being viewed from different angles⁵

1.2 Epoxy Resin

Polymeric materials are widely used in numerous industrial applications due to their unique properties such as thermomechanical, chemical and electrical properties and easy processability⁶⁻⁷. One of the most challenging environments for polymers is marine applications, which require high UV and salt resistance. Epoxy resins are one of the main barrier coating materials for use in marine applications due to their resistance to corrosion, high tensile strength and modulus as well as easy processing, good thermal resistance, chemical resistance and dimensional stability⁷⁻⁸.

Epoxy resins were first discovered in 1909, being defined as thermoset pre-polymers having more than one epoxide group and low molecular weight. Since this time, epoxy resins have been used in a variety of engineering applications from packing materials, coatings, semi-conductors in electrical equipment, insulation and adhesives being used in the automotive and aerospace industries⁹.

Epoxies can be hardened using numerous curing or accelerating agents which both speed up the curing procedure and are important to the polymers resulting mechanical properties. The curing process is dependent on the proportion of the epoxy resin, curing agent and the accelerator type being used⁸⁻⁹.

Epoxies can provide good protection to metals due to the hydrophilic nature of their chemical groups in the cured structure, hence they are often used for metal coatings due to the presence of the carboxyl groups (-COOH), hydroxyl groups (OH) and amino groups (NH₂) which add in unpaired electrons⁸.

From the curing process, epoxies experience enhanced mechanical properties and low shrinkage as well as a long shelf-life and perfect damage tolerance¹⁰. Due to the crosslinking feature of cured epoxies, they are quite brittle, prone to crack initiation and growth⁸. The lack of toughness can affect the performance of these materials for various applications. In order to minimize these issues, coupling the epoxy resin to the carbon fiber in the prepreg format and adding a honeycomb structure can improve these properties as well as having the possibility of using some commercial additives¹¹.

The epoxide functional group, also known as the oxirane or ethoxy group, is the representation unit of the epoxy polymer. The commercial epoxy resin used for both types of the prepregs used in this dissertation was the oligomers of the diglycidyl ether of bisphenol A (DGEBA) as shown in Figure 1.3.

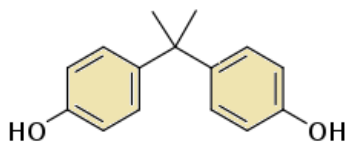


Figure 1.3: The chemical structure of the Bisphenol A (BPA)¹.

The epoxy oligomers, when reacting with the hardener, become cured and turn into the final thermosetting polymer as shown in (Figure 1.4).¹² Amine-based hardeners are the most common these days, while anhydrides and amides are also used¹⁰.

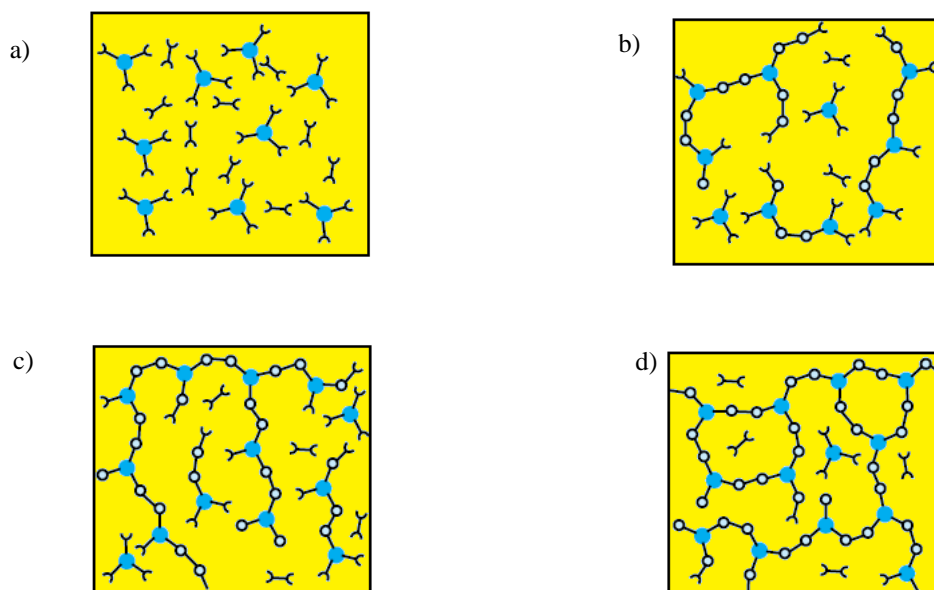


Figure 1.4: Curing Stages of the Epoxy resin: a) Epoxy resin uncured, b) Epoxy resin partially cured but still fusible, c) Epoxy resin becoming infusible (gel point) around 60% cured, d) Epoxy resin (fully-cured, infusible).

Among the various epoxy resin candidates, bisphenol A type resins are the most widely used. They can provide excellent mechanical properties and adhesion due to the formation of the crosslinked network structure through the chemical reaction in the epoxy rings (Figure 1.4).

The properties of epoxy resins can be predetermined by the chemical structure of the resin and its hardener and the network achieved from them by the curing process. Despite their several advantages, the resins also suffer from brittleness, poor strength and a lack of toughness. In different applications, the prepreg composites of carbon fiber and epoxy resin are mostly used while having sandwich composites with a honeycomb layer of Nomex. The process of preparing epoxy resins from the curing agent and the accelerator using commercial products is shown in (Figure 1.5).

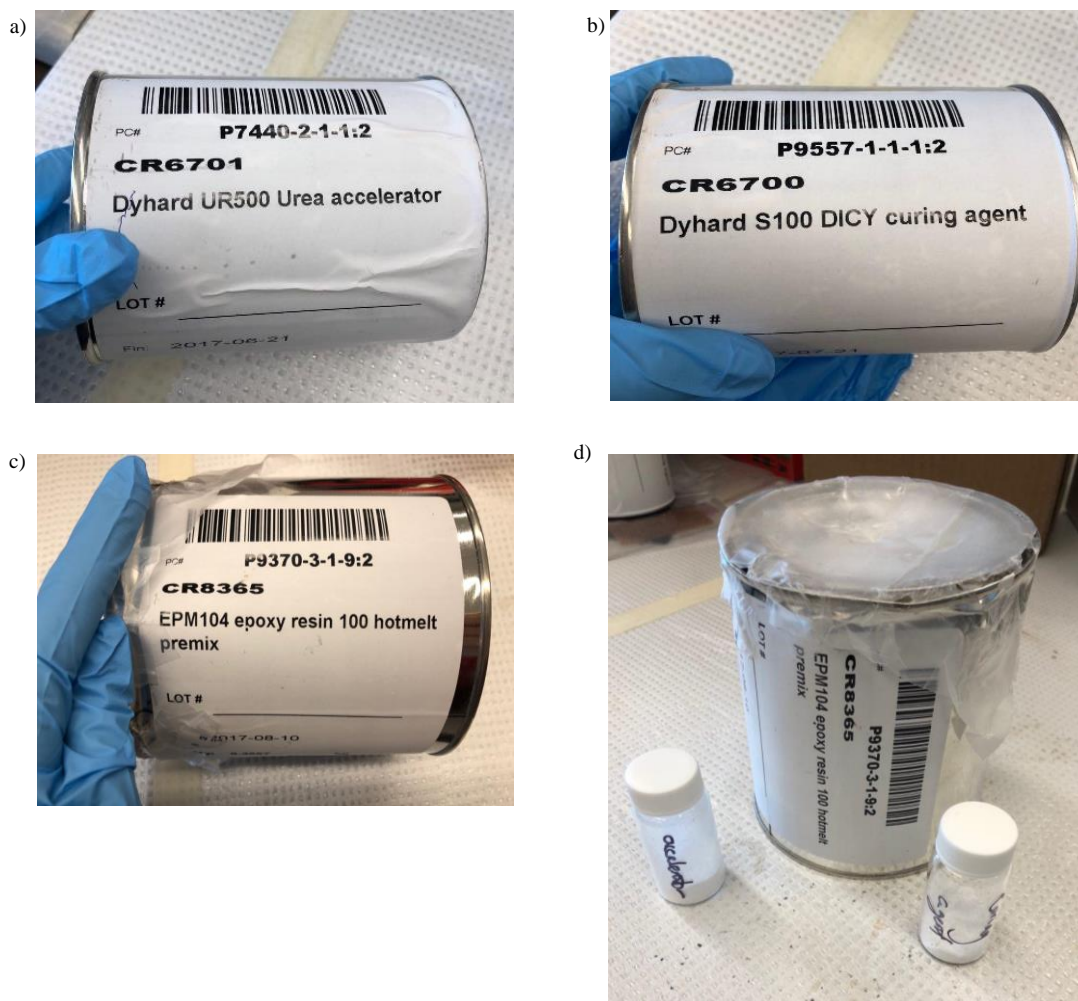


Figure 1.5: a) Dyhard UR500 epoxy resin accelerator, b) Dyhard S100 curing agent, c) EPM104 epoxy resin, d) the overview of the three commercial components together.

The lack of mechanical properties of epoxy resins such as resistance against stress and crack propagation and high brittleness make these materials of interest for composite formation^{6, 13}. The need for having lighter weight materials is also vital in the aerospace and automotive industries¹³, which is also a tremendous benefit in other fields, such as for use in marine racing hulls as in this dissertation.

1.3 Carbon fiber

Carbon fibers have been of tremendous interest to the scientific and industrial communities, particularly when using a thermosetting resin for mechanical reinforcement. The use of

carbon fibers provides a higher strength to weight performance, better fatigue strength and potentially greater options for freedom in design¹⁴.

To help reduce the weight of the epoxy materials, carbon fiber- reinforced polymers (CFRPs) can be used. In this research, CFRP were used, which contain carbon fibers embedded in an epoxy resin thermosetting matrix¹⁵. This combination is known to provide excellent mechanical properties and chemical stability, making these materials a good replacement for metals that would suffer from corrosion or larger thermal expansion¹⁶. Of additional interest is that carbon fibers are lower priced compared to glass or exotic nanomaterials³. Note that the fiber- reinforcement phase includes carbon fibers as the reinforcement step and the thermosetting epoxy as the binding material³. Therefore, carbon fiber- epoxy resin composites are used in the form of pre-impregnated materials called prepregs¹⁷.

Carbon fiber prepregs are commonly used in a variety of industries, such as by Hudson Boat Works for making marine racing hulls. Carbon fiber prepregs have been used in industrial epoxy resins since the early 1980's as non-critical secondary structures for aircraft manufacturing. Their use has been dramatically increasing, with prepregs being used nowadays not only in aircraft primary structures, but in a variety of other industries including automotive, wind energy, sports goods and especially the marine industry. They are formulated in a resin matrix which is reinforced with fibers of carbon (Figure 1.6).

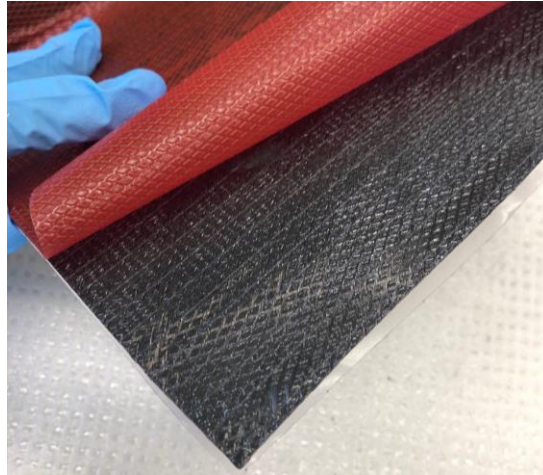


Figure 1.6: Sample of the unidirectional commercial prepreg being used for this research.

Note that in the CFRP combination, the reinforcement polymers must deliver two main advantages for enhancing the matrix material: providing high strength and also having low ductility⁸. According to the literature, reinforcements are deliberately used for polymers to make them stronger, lighter, less expensive and electrically conductive at the same time¹⁸. The type of fiber filler used for this thesis is carbon fibers working as the reinforcement material (Figure 1.7).



Figure 1.7: The woven carbon fiber fabrics as the reinforcement materials, fillers, before the curing process.

Such samples have been shown to contain voids and pinholes on the surface of the materials¹⁹, which was a challenge found by our supporting company (Figure 1.8), to be addressed in this work.

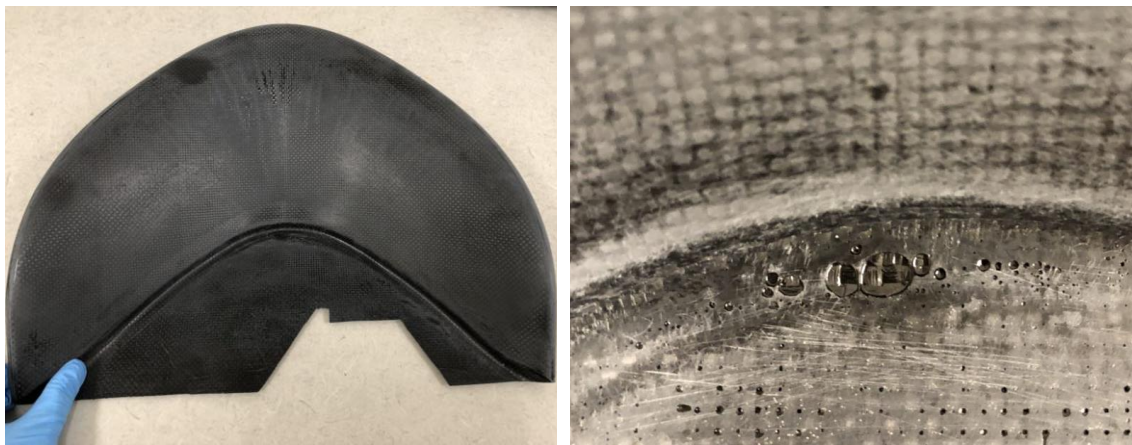


Figure 1.8: Types of the numerous pinholes and voids the supplied prepregs were suffering from in the seat section of the rowing halls.

1.4 Nomex honeycomb

For the past few decades, sandwich composites have been utilized in the aerospace and high-speed railway industries. Nowadays, they are of great importance in the marine industry due to their lightweight, high strength and stiffness¹⁶. Nomex honeycomb is the standard non-metallic composite structure used for its lighter weight as shown in (Figure 1.9). Fabricators mainly use such sandwich cores for their high strength to weight ratios²⁰. In this research, commercial grade honeycomb made with aramid fiber paper (DuPont Nomex) which is coated with phenolic resin was used, as this material is known to have great resiliency, low density and low pricing²¹. Note that the expanded cell structure leads the honeycomb to be highly flexible, which is a key property for use in tight radius curves such as boat ends and seats. In addition, using Nomex honeycomb provides high fire resistance and thermal insulation as well as great bonding with the epoxy resin which helps to reduce peel.

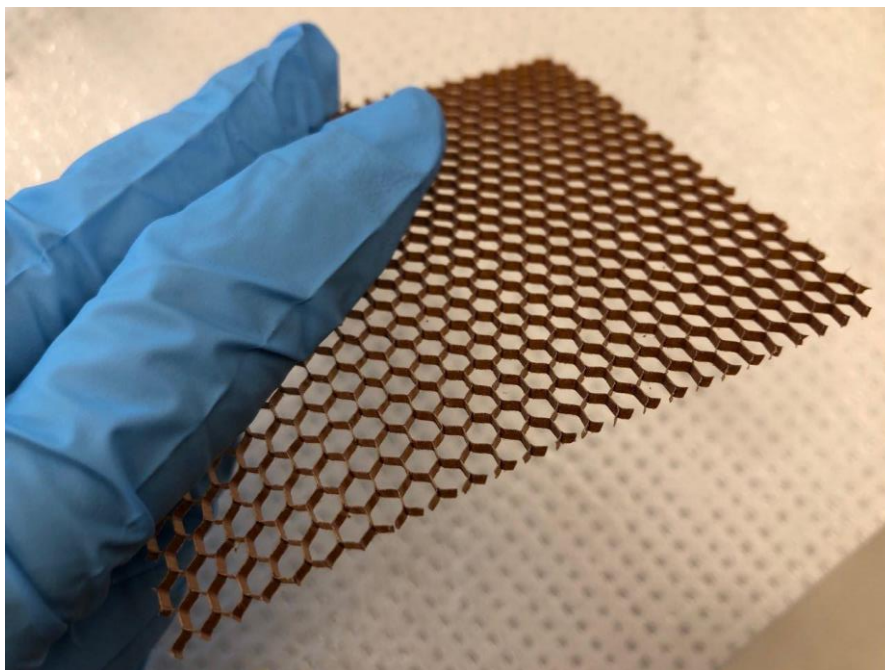


Figure 1.9: The Nomex honeycomb texture used for this dissertation.

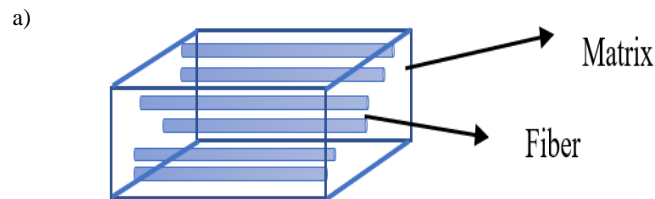
According to the literature, a sandwich construction contains a thin high strength prepreg skins (carbon fiber-epoxy resin) bonded to the honeycomb, foam or balsa core. In this thesis, the bonded layer to the prepreg skin is Nomex honeycomb. Such a sandwich construction can be called a “self-adhesive” prepreg, which does not need additional adhesive layers. These systems allow the production of light weight structures while reducing fabrication costs. Such assemblies are suitable for aerospace technologies due to their low weight, high stiffness, durability and the reduced production costs¹⁴.

An additional advantage of the sandwich technology is that the shearing stresses are supported by the honeycomb layer while the tensile and compression stresses are maintained by the skins (carbon fiber- epoxy resin prepregs). The prepreg layers are also stable through the entire length and the structure will experience rigidity in several directions when utilizing a sandwich construction²¹.

In this research, the honeycomb sandwich composites were fabricated using carbon fiber-epoxy resin prepregs and Nomex honeycomb core, due to requirement for the lowest possible weight structure.

1.5 Matrix

The term matrix is used for the polymeric component supporting the fibers and bonding them together in a composite structure. In the matrix construction, any applied forces are distributed to the fibers while the fibers are maintained in their position and orientation. The maximum service temperature and environmental resistance of the preregs can be controlled using the matrix as shown in (Figure 1.10) ¹⁴. One of the key criteria when choosing a suitable prepreg matrix is knowing the maximum service temperature of the selected preregs, which for our case is 150 °C. Using higher temperatures than this can result in having burnt preregs with lower mechanical properties.



b)



c)

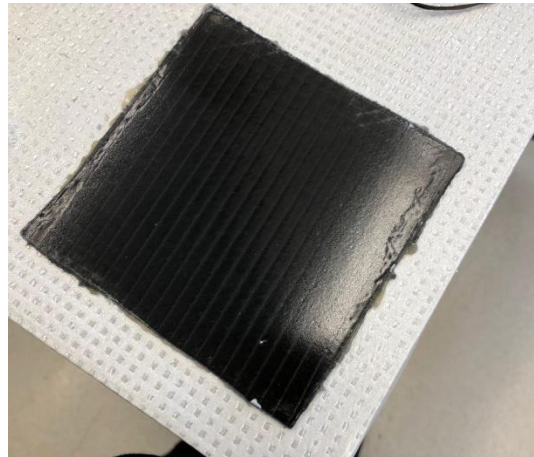


Figure 1.10: a) The visual components of a matrix, b) the matrix components using carbon fiber, epoxy resin and Nomex honeycomb, and c) the cured matrix being used for the experiment, measuring the thermomechanical properties.

1.6 Composites

Generally, composites are made from polymers or the combination of polymers and other types of materials such as glass, ceramics, clay or carbon. Hence, composite materials include two or more components resulting in improved physical and chemical properties over those of the individual components. Composites have been used in numerous applications over the years in a variety of industries from medical and sporting goods to automotive and marine. Composites help boost the mechanical performance of the virgin materials; enhancing stiffness and strength, as well as enhancing other properties such as providing better thermomechanical, electrical and chemical properties, while potentially providing weight savings over metals¹⁴.

Consequently, unidirectional composites (UD), as used for this research, have major mechanical properties in one direction and are called anisotropic while, the isotropic materials (most metals) experience equal properties in all directions¹⁴. For having optimum mechanical properties, components made from fiber-reinforced composites can be produced having the advantages of both UD composites and of true isotropic metals (Figure 1.11).

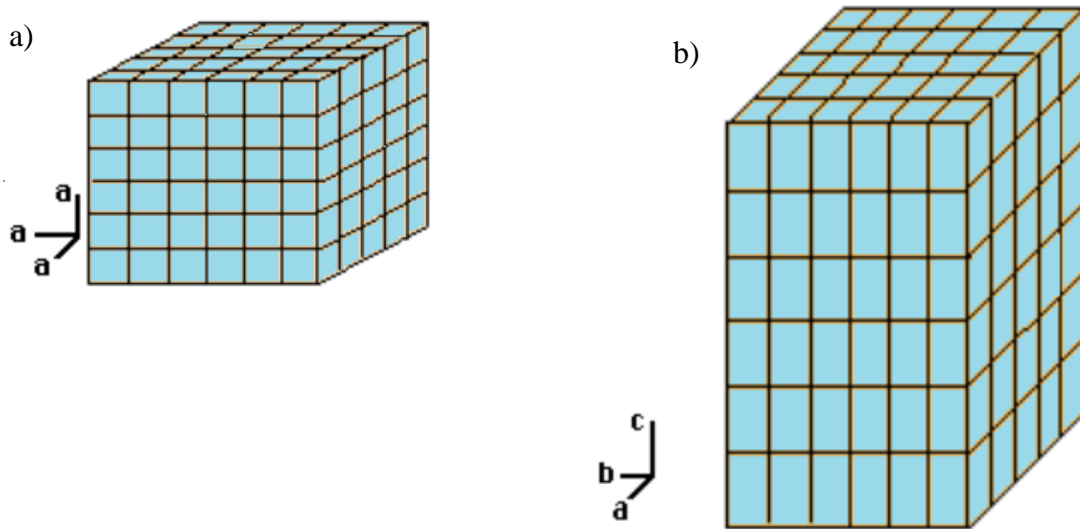


Figure 1.11: Schematic definition of both a) Isotropic and, b) Anisotropic structure of materials.

1.7 Vacuum oven curing system

The curing process in an epoxy matrix can be represented by reactive sites of the epoxy pre-polymers formed during the polymerization and cross-linking process²². For this research project, we used the post curing step to provide better cross linking in the epoxy phase and as a result to obtain more homogeneous composites with better mechanical properties²³.

The glass transition temperature (T_g), which highlights the physical phase change in the matrix properties, is used as an indication of the maximum service temperature in the prepregs. Vacuum oven curing can be used to help boost the thermomechanical properties of a composite while also enhancing the T_g value, resulting in the stabilization of the maximum service temperature in the carbon fiber- epoxy resin matrix²⁴. In this technique, an oven apparatus is utilized, rather than working with an autoclave, and the composite layers are under constant vacuum during the curing process.

1.7.1 Prepregs and the Vacuum Bagging Only method (VBO)

Both autoclave or out of autoclave (OoA) techniques are generally being replaced by the vacuum bagging oven curing method (VBO)²⁵. The vacuum bagging method is one of the vacuum oven curing systems that can create a mechanical pressure on stacks of prepregs during their curing cycle²⁶. While former techniques mostly involve complicated temperature or pressure control, the vacuum bagging oven curing system is a straightforward method using only resin impregnation into the fiber. This may result in less void formation, while producing complicated structures involving little joining, machining and production of the uniquely shaped components. Note that using prepregs, the fiber content would be high (around 65%) and the content of the voids is typically 0.5% in the out of autoclave prepreg procedure²⁷.

Conventionally, the prepreg layers are firstly formed in a laminate structure, then they are enclosed in a vacuum bag assembly and are placed in an autoclave (pressurized oven). Having the temperature raised in the autoclave, the desired vacuum is then drawn in the bag and the vessel is pressurized. However, today the new generation of the OoA prepregs which have been introduced indicate that it is possible to produce autoclave- quality pieces for high performance applications using the VBO technique²⁵.

The capacity to use higher performance, higher viscosity resins and combine modifiers, as well as having the ability to control fiber alignment and fiber volume fraction are key factors that make prepregs commonly used compared to other OoA methods such as the infusion or resin transfer molding technique²⁶.

The vacuum bagging-only technique also helps decrease the purchase and operating costs and provides the manufacturer the possibility for using lower cost cure set-ups including traditional ovens, heating blankets and heated tooling. They are also considered environmentally friendly due to the lower energy consumption requirements utilized during the curing process. One of the other advantages is that the lower cure pressure during the curing process can eliminate defects such as honeycomb core crush made by the autoclave curing method. This can allow the use of lighter and less expensive cores in different thickness and diameters²⁶.

While the process of curing using the VBO technique can help reduce void formation, the porosity of the surface can be increased due to the increased value of the resin viscosity²⁶.

Note that the mechanical properties of the composites, mainly the compression strength and the interlaminar shear strength, can be reduced if the void content persists as the applied force would be in the direction of the cracks or their interactions²⁸.

Today, the industry is shifting towards faster, more efficient and environmentally friendly methods using the VBO technique. Using the prepreg materials can help the process of enabling this change. For numerous high value applications from aerospace to the marine industry, the lower cost tooling is enabled by the installation of parallel production lines in which one autoclave can be replaced by several oven-based curing environments. In the VBO method, the unnecessary ovens can be eliminated by lower cost tooling or heating tools during the absence of the atmospheric pressure²⁸.

It is expected that the VBO prepreg materials can help provide rapid, efficient and sustainable processing as one of the viable steps towards enhanced composites as examined in this dissertation.

1.8 The relationship of DOE method and the materials (Chapter II)

In this project, design of experiment (DOE) techniques were utilized to help provide a better comprehension and optimization of the experimental system under examination. The following method was used to improve the DOE model's behavior and efficiency for the response surface, as shown in Figure 1.12.



Figure 1.12: a) Response surface with no curvature, b) Response surface with curvature

29.

According to the literature, having the ability to use the squared (or quadratic) terms allows us to model the curvature in the response. This is one of the differences between a response surface equation and a factorial design.

This technique is beneficial for the following reasons³⁰:

- Better mapping of any region of a response surface. Also, the different ways of affecting a response of interest by changing in variables helps model a response surface.
- Determining the levels of variables that does the optimization for a response ($-\alpha$, -1 , $+1$, $+\alpha$).
- Determining the best operating conditions to meet specific criteria.

Out of the two main types of response surface designs, (i.e. Central Composite method and Box-Behnken design); the central composite was used for our design of experiment methods in this dissertation²⁹.

1.8.1 Central composite design

One of the most commonly used response surface designs is the central composite design. It is a factorial or fractional factorial design with center points, improved with a group of axial points (also called star points) that help one to estimate curvature. It is the newest of the design of experiment method, which can cover both min and max points as well as the optimum points in the design²⁹.

There are numerous reasons behind the usage of this technique, namely³⁰:

- Estimating first-order and second-order terms efficiently.
- Adding center and axial points to a previous factorial design to model a response variable with curvature.

Note that the central composite design is the specific method used for the optimization procedure during the DOE technique. It can be useful in sequential experiments by adding axial and center points, or building on previous factorial experiments as well³⁰.

1.8.2 Reaching the optimization phase using the central composite design

Using the mentioned design for determining the optimized conditions, four quadratic mathematical model equations are utilized for predicting the production parameters for both optimization processes³¹. One of the objectives of the central composite design is to optimize the levels of the variables to determine the best response. It contains a full or fractional factorial point, a supplementary point at a distance of α ($\alpha=2(k-p)/4$) calculated from the center, and finally a central point³¹. The total number of experiments can be found by Equation (1.1):

$$N = k^2 + 2k + c_p \quad (1.1)$$

where k is the factor number, and c_p is the number of repetitions of experiment at the central point. All factors can be tested at four different levels ($-\alpha, -1, +1, +\alpha$). For statistical calculations, the actual variables and the coded variables are related according to the following Equation(1.2):

$$x_i = \frac{X_i - X_0}{\delta X} \quad (1.2)$$

where x_i is a coded value of the variable, X_i is the actual value of the variable, X_0 is the actual value of X_i at the center point, and δX is the step change of the variable. The four variables chosen for this work were: Ramp (X_1), temperature (X_2), holding time after the curing (X_3) and type of prepreg (X_4).

This methodology allows the response variables to be fitted by a quadratic equation (1.3) that can describe the process:

$$Y = \beta_0 + \sum_{i=1}^k \beta_i X_i + \sum_{i=1}^k \beta_{ii} X_i^2 + \sum_{i < j} \beta_{ij} X_i X_j \quad (1.3)$$

where Y , k , β_0 , β_i , β_{ii} , and β_{ij} are the predicted response variable, number of variables, constant term, coefficients of the linear parameters, coefficients of the quadratic parameters and coefficients of the interaction parameters, respectively.

1.8.3 Analysis of variance (ANOVA) for the statistical analysis technique

According to the literature, a statistical method that sections the total variation in a set of data into component parts is called analysis of variance (ANOVA)³⁰. Some common definitions for generating an ANOVA table are as follows:

- By dividing the sum of the squares of each variation source by their degrees of freedom, the mean square values are calculated.
- For determining the statistical significance, a 95% confidence level ($\alpha = 1.68$) was used in all analyses.
- For evaluating the results, various descriptive statistics such as the p-value, F-value, and the degree of freedom (DOF) are used.
- By Fisher's F-test and values of the "probability > F", the (R^2) of each coefficient in model equations have been determined.
- For predicting the level of accuracy in the response function, a small probability value ($p < 0.001$) is shown, indicating that the model was highly significant.
- Aiming the coefficients of determination R^2 (correlation coefficient) and adjusted coefficients of determination $\text{adj-}R^2$, the goodness-of-fit for the model was also evaluated.

1.8.4 The relationship of the mechanical properties on behavior of the preregs after the curing process (Chapter III)

It is expected that increasing the porosity on the surface of the preregs will affect the tensile strength and generally the mechanical properties of the preregs. While most of the literature has focused on changing the curing parameters in order to reach better

thermomechanical properties, the effects of the pinholes and void distribution on the composite laminates needs to be monitored. These are candidate factors which will affect the performance of the composites and consequently, the thermomechanical properties of the prepregs.

In this research, the maximum tensile strength, the stress at that point, the extension at the breaking point, the yield before breaking, the maximum load bearable by the samples and the Young's modulus were derived using an Instron device.

1.8.5 Tensile properties of the composite prepregs

The percentage of strain value can be calculated using Equation (1.4).

$$\text{Strain}(\%) = \frac{\text{Extension}}{\text{Original length}} \times 100 \quad (1.4)$$

The mechanical properties of a polymer involve its behavior under stress and such properties help differentiate polymeric materials from small molecules³². Below is the brief definition for each expression that will be used to define the mechanical properties of these prepregs:

1.8.5.1 Stress

According to the literature, the force F applied normal to the face of an element of material which is spread through the surface and balanced by the equal and opposite force on the other side to maintain it in equilibrium, is called the tensile stress Equation (1.5).

$$\sigma = \frac{F}{A} \quad (1.5)$$

From the above equation, σ (MPa) shows the tensile stress, F carries the force (N) and A (m^2) is the area of each element³².

1.8.5.2 Strain

Strain is the response of materials to an applied stress. A tensile stress σ is applied to the surface of a sample and will cause the element to stretch³². If the element originally has a

length L_0 (m), which stretches by $\delta L = L - L_0$, the tensile strain which is unitless, follows Equation (1.6):

$$\varepsilon = \frac{\delta L}{L_0} \quad (1.6)$$

1.8.5.3 Stress- Strain curves and moduli

Figure 1.13 provides typical stress-strain curves for polymers in different stages. Referring to the curves, the initial part which shows the elastic portion of the sample σ_{el} is approximately linear (Hooke's law) and also it is elastic, meaning the material will return to its original shape when the stress is removed. The stress value would be measured using MPa or MN/m² as its units. It is important that stresses above the elastic limit cause permanent deformation and according to the material type, it can experience ductile behavior or brittle fracture.

Within the linear portion of the plot in the elastic region, strain is proportional to stress according to Equation (1.7):

$$\sigma = E\varepsilon \quad (1.7)$$

The constant of proportionality, E , is called Young's modulus. With the material taken to failure, the yield properties and ductility can also be measured using the tensile test.

For polymers, σ_y is the stress at which the stress-strain curve is non-linear, mostly a strain of 1% (Figure 1.13). The behavior of the sample beyond the yield point depends on the temperature relative to the glass transition temperature T_g . Typically, below the T_g point, most polymers are brittle. As the material approaches the T_g point, the plasticity in it would become possible³².

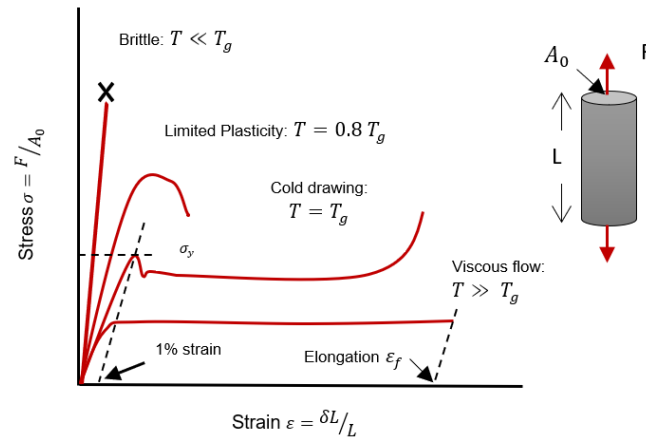


Figure 1.13: Stress-Strain Curves for a polymer.

For thermoplastic materials, around the T_g point they exhibit so-called cold drawing, which is the large plastic extension at a constant stress that can happen when the molecules are pulled into alignment in the direction of strain. This is followed by hardening and fracture when alignment is complete. Note that at higher temperatures, thermoplastic materials become more viscous and can be molded while thermosets develop a rubbery and decomposed texture. Not to mention that we are working with carbon fiber-epoxy resin prepregs which are a good example of thermoset materials.³²

1.8.5.4 Plastic Strain

ϵ_{pl} is the permanent strain resulting from plasticity, therefore, it is the total strain ϵ_{tot} minus the recoverable elastic portion as shown by Equation (1.8):

$$\epsilon_{pl} = \epsilon_{tot} - \frac{\sigma}{E} \quad (1.8)$$

The amount of the plastic strain that the material can tolerate is called the ductility factor. In standard tensile tests, the ductility factor can be measured by the elongation ϵ_f (the tensile strain at breakage) which is generally measured as a %. ϵ_f . It is not a true material property as it depends on the sample's dimensions, but it can be used as a measure of the ability of the material to be deformed³².

1.8.5.5 Tensile Strength

Tensile strength is the essential **stress to break a sample**. In our case it is expressed in MPa, and each MPa would be equal to 145 psi. For the polymers in their stretched mode, the tensile strength is an important property. Our prepreg carbon fibers for instance, must have good tensile strength as shown in Figure 1.14³³.

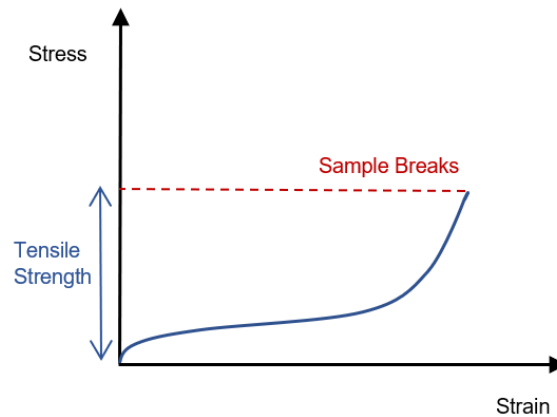


Figure 1.14: Tensile strength at break point for polymers using the stress-strain curve.

1.8.5.6 Elongation percentage to Break

The **strain on a sample at breakage** can give us the amount of elongation, which is usually expressed in percentage (%). It can also be called the ultimate elongation³³. Mostly fibers have a low elongation at breakage and elastomers have a high elongation at breakage (Figure 1.15).

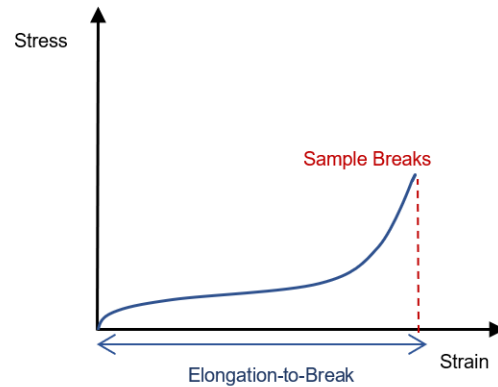


Figure 1.15: The amount of elongation at break point using the stress-strain curve.

1.8.5.7 Young's Modulus

The ratio of stress to strain provides us with the Young's modulus. It is also called the modulus of elasticity or the tensile modulus depending on the device used. It is basically **the slope of a stress-strain curve**³³. Note that the stress-strain curves are normally not straight-line plots, meaning the modulus will vary with the amount of strain. The initial slope is used as the modulus for our case as shown in (Figure 1.16).

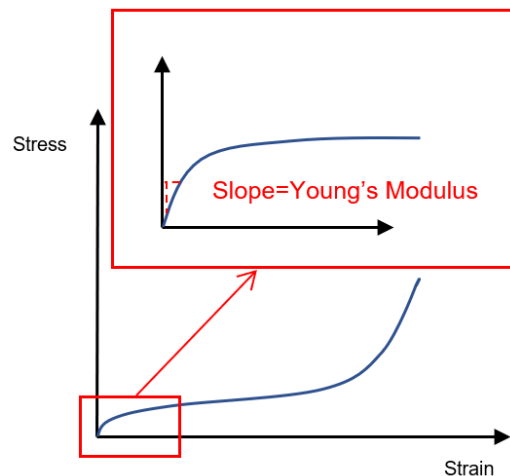


Figure 1.16: The Young's modulus using the stress-strain curve.

Note that rigid materials, such as metals, have a high modulus and in general, fibers have high Young's modulus values, elastomers have low values, and plastics lie somewhere in between. Overall, the Young's modulus is a mechanical property that measures the stiffness of a solid material and shows the relationship between the stress and strain mostly by using the linear elasticity region of a uniaxial deformation, Equation (1.9)

$$E = \frac{\delta}{\varepsilon} \quad (1.9)$$

1.8.5.8 Modulus of toughness

The toughness modulus of a material is the **area under the stress-strain curve**. The stress is related to the tensile force on the material and the strain is due to its length. The area under the curve is proportional to the integral of the force over the distance that the polymer stretches before its breaking point, as described by Equation (1.10).

$$Area \propto \int F(L)dL \quad (1.10)$$

According to the above relationship, this integral is the amount of work (energy) required to break the sample. Note that, **the modulus of toughness is a measure of the energy one sample can absorb before it breaks**³³. In order to derive the modulus of toughness value for each material, the force vs the elongation plot as shown in (Figure 1.17) is used.

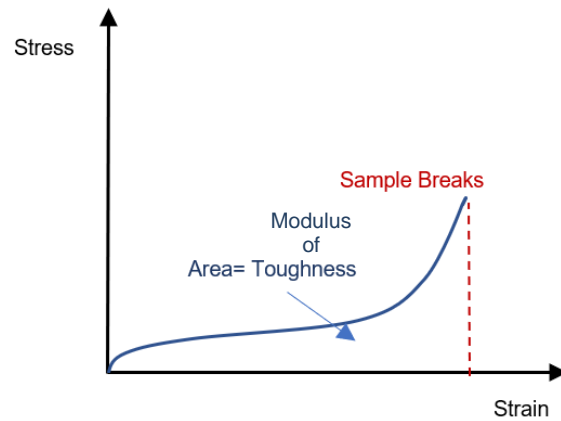


Figure 1.17: The toughness modulus area for polymers using the stress-strain curve.

1.8.5.9 Hardness

Among the various hardness tests, the Vickers test is the easier one to be used as most of the calculations are not dependent on the size of the indenter, and regardless of the amount of hardness, the indenter can be used for all materials (Figure 1.18). Hardness is not a fundamental physical property and can be considered more as a characteristic factor of a material³⁴. Using a fixed force and a given indenter, the material is harder when having a smaller indentation³⁴.

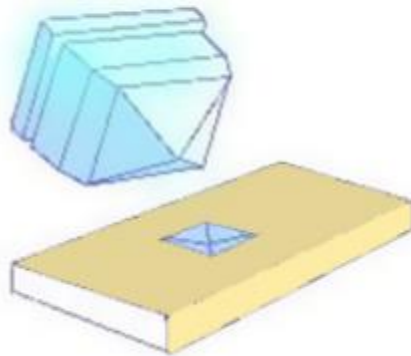


Figure 1.18: A typical diamond structure that the indenters would leave on the surface of the samples during the hardness test.

As with all measures of hardness, the rule is having a material that can resist plastic deformation from a standard source. Note that the common units are known as the **Vickers Pyramid Number (HV)** or **Diamond Pyramid Hardness (DPH)**. Not to mention that the hardness values can be converted into pascals (Pa) as well.

The microhardness test is one of the other names for this method, as it is mostly suitable for small pieces, thin units and case depth surfaces. The testing apparatus is built to be used on any surface such as metals, ceramics and composites. Below is one of the versions of the hardness device which can be seen having different elements as shown in (Figure 1.19):

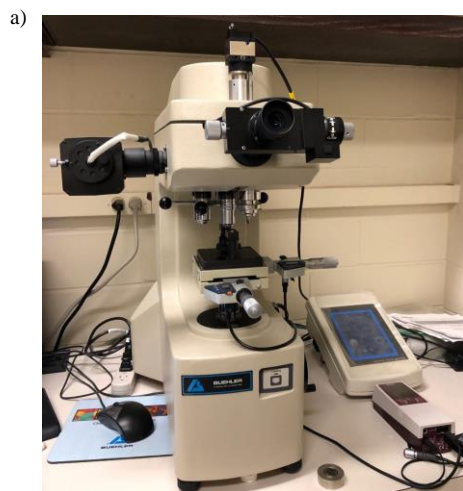


Figure 1.19: a) Buehler MicroMet 5100 series device for hardness testing. b) The mounted sample being used for the hardness test using the paraffin wax.

Hardness was measured using a Buehler MicroMet 5100 series device as shown in Figure 1.19(a). A paraffin wax material was used so that the samples would be maintained steady during the process of hardness testing Figure 1.19(b).

1.8.6 Statistical analysis using the Holm-Sidak method (t-test)

The t-test is a type of inferential statistic to determine if there is a significant difference between the means of two groups. With this method, we assume that the dependent variable fits a normal distribution. Normally, the t-test method can be used to study the differences between two population averages. In other words, this method is mostly used when we need to compare two means. It is important that the scores be calculated on an interval or ratio measurement scale. In a way, we can conclude that using the t-test method shows the number of standard units that the means of the two groups are apart³⁵⁻³⁶. The significance of the p-value results are described using the notations provided in Equation (1.11)³⁷.

$P \leq 0.05$	Significant result being shown by *	
$P \leq 0.01$	Significant result being shown by **	
$P \leq 0.001$	Significant result being shown by ***	(1.11)
NS	Not significant result	

Chapter 3 of this dissertation will cover these aspects thoroughly.

1.9 Scope of the research

The thermoset epoxy resin undergoes a curing reaction that leads the prepreg to reach a solid structure which is highly durable, temperature resistant, stiff and extremely lightweight³⁸. These fiber-reinforced resins are cured under a variety of heat and pressure conditions to form components. To manufacturers, performance and cost are two important parameters that influence the selection of the prepregs and curing conditions for the various

applications of interest. In this work, a simulated lab scale curing process was developed for enhancing carbon fiber-epoxy resin prepreg thermomechanical properties.

The following were identified as the main objectives of this project:

- I. Optimizing the carbon fiber- epoxy resin matrix composites to improve the thermomechanical properties.
- II. Comparing the mechanical properties of two commercial prepreg matrixes using both initial and optimum conditions for the curing cycles.

Improving the thermomechanical properties of the prepregs and shortening the curing cycle of them are two main goals behind this master thesis.

1.10 References

1. Hexcel HexPly® Prepreg Selector Tool. .
2. Hasnine, M., *Durability of Carbon Fiber/Vinylester composites subjected to marine environments and electrochemical interactions*. Florida Atlantic University: 2010.
3. Tavares, S. S.; Caillet-Bois, N.; Michaud, V.; Månson, J.-A., Vacuum-bag processing of sandwich structures: Role of honeycomb pressure level on skin–core adhesion and skin quality. *Composites Science and Technology* **2010**, *70* (5), 797-803.
4. Works.H.B. Prepregs in marine industries
5. Kausar, A., Rafique, I., Anwar, Z. and Muhammad, B., Perspectives of epoxy/graphene oxide composite: Significant features and technical applications. *Polymer-Plastics Technology and Engineering* **2016**, *55*(7), 704-722.
6. Kausar, A., Rafique, I. and Muhammad, B., Aerospace application of polymer nanocomposite with carbon nanotube, graphite, graphene oxide, and nanoclay. . *Polymer-Plastics Technology and Engineering* **2017**, *56*(13), 1438-1456.
7. Mahmood, I. A.; Shamukh, M. Z., Characteristics and properties of epoxy/polysulfide blend matrix reinforced by short carbon and glass fibers. *Al-Nahrain Journal for Engineering Sciences* **2017**, *20* (1), 80-87.
8. Lionetto, F., Moscatello, A. and Maffezzoli, A. , Effect of binder powders added to carbon fiber reinforcements on the chemoreology of an epoxy resin for composites. *Composites Part B: Engineering* **2017**, *112*, 243-250.

9. Saba, N., Jawaid, M., Alothman, O.Y., Paridah, M.T. and Hassan, A., Recent advances in epoxy resin, natural fiber-reinforced epoxy composites and their applications. . *Journal of Reinforced Plastics and Composites* **2016**, 35(6), 447-470.
10. Norhakim, N., Ahmad, S.H., Chia, C.H. and Huang, N.M., Mechanical and thermal properties of graphene oxide filled epoxy nanocomposites. . *Sains Malaysiana* **2014**, 43(4), 603-609.
11. Wikipedidia Bisphenol A.
12. Solvay. Virantage, PESU Epoxy Tougheners for Prepreg Manufacturing 2015.
13. Haeri, S.; Asghari, M.; Ramezanzadeh, B., Enhancement of the mechanical properties of an epoxy composite through inclusion of graphene oxide nanosheets functionalized with silica nanoparticles through one and two steps sol-gel routes. *Progress in Organic Coatings* **2017**, 111, 1-12.
14. Hexcel *Hexply prepreg technology*; <http://www.hexcel.com/resources/selector-guides>, 2017.
15. Kima, C., Choa, C.H., Sona, I., Leeb, H., Woo, J., Hanb, J.G.K. and Leea, J.H., Effect of microscale oil penetration on mechanical and chemical properties of carbon fiber-reinforced epoxy composites. *Journal of Industrial and Engineering Chemistry* **2017**, 7.
16. Chen, C., Li, Y., Gu, Y., Li, M. and Zhang, Z., Improvement in skin–core adhesion of multiwalled carbon nanotubes modified carbon fiber prepreg/Nomex honeycomb sandwich composites. . *Journal of Reinforced Plastics and Composites* **2017**, 36(8), 608-618.
17. Chang, T., Zhan, L., Tan, W. and Li, S., Void content and interfacial properties of composite laminates under different autoclave cure pressure. *Composite Interfaces* **2017**, 24(5), 529-540.
18. Osswald, T., Understanding polymer processing process and governing equations. *Hanser Publishers, Munich* **2015**.
19. works, H. B., <https://www.hudsonboatworks.com/> **2017**.
20. Composites, C. Thermomechanical properties of composites
21. Fiberglass, *Fibreglast.com* **2018**.

22. Odom, M. G., Sweeney, C.B., Parviz, D., Sill, L.P., Saed, M.A. and Green, M.J., Rapid curing and additive manufacturing of thermoset systems using scanning microwave heating of carbon nanotube/epoxy composites. . *Carbon* **2017**, *120*, 447-453.
23. Domun, N., Hadavinia, H., Zhang, T., Sainsbury, T., Liaghat, G.H. and Vahid, S., Improving the fracture toughness and the strength of epoxy using nanomaterials—a review of the current status. . *Nanoscale* **2015**, *7(23)*, 10294-10329
24. Liu, T., Zhao, Z., Tjiu, W.W., Lv, J. and Wei, C., Preparation and characterization of epoxy nanocomposites containing surface-modified graphene oxide. *Journal of Applied Polymer Science* **2014**, *131(9)*.
25. Centea, T.; Grunenfelder, L. K.; Nutt, S. R., A review of out-of-autoclave prepregs—Material properties, process phenomena, and manufacturing considerations. *Composites Part A: Applied Science and Manufacturing* **2015**, *70*, 132-154.
26. Grunenfelder, L.; Dills, A.; Centea, T.; Nutt, S., Effect of prepreg format on defect control in out-of-autoclave processing. *Composites Part A: Applied Science and Manufacturing* **2017**, *93*, 88-99.
27. Islam, A. I.; Kelkar, A. D., Prospects and challenges of nanomaterial engineered prepregs for improving interlaminar properties of laminated composites—a review. *MRS Communications* **2017**, *7 (2)*, 102-108.
28. Tavares, S. S., Caillet-Bois, N., Michaud, V. and Månson, J.A., Vacuum-bag processing of sandwich structures: Role of honeycomb pressure level on skin–core adhesion and skin quality. *Composites Science and Technology* **2010**, *70(5)*, 797-803.
29. minitab.com, what are response surface designs, central composite designs? *Minitab articles* 2018.
30. Sarrai, A.; Hanini, S.; Merzouk, N.; Tassalit, D.; Szabó, T.; Hernádi, K.; Nagy, L., Using central composite experimental design to optimize the degradation of tylosin from aqueous solution by photo-fenton reaction. *Materials* **2016**, *9 (6)*, 428.
31. Ahmadi, S., Manteghian, M., Kazemian, H., Rohani, S. and Darian, J.T., Synthesis of silver nano catalyst by gel-casting using response surface methodology. *Powder technology* **2012**, *163-170*, 228.
32. Ashby, M. F., Shercliff, H. and Cebon, D., *Materials: engineering, science, processing and design*. Butterworth-Heinemann.: 2014.

33. uscupstate Polymer Chemistry in mechanical properties.
34. Ametek vickers testing basics.
35. investopedia t- test technique.
36. StatsDirect, P Values (Calculated Probability) and Hypothesis Testing. *StatsDirect* **2018**.
37. Mumin, M. A.; Akhter, K. F.; Oyeneeye, O. O.; Xu, W. Z.; Charpentier, P. A., Supercritical fluid assisted dispersion of nano-silica encapsulated CdS/ZnS quantum dots in poly (ethylene-co-vinyl acetate) for solar harvesting films. *ACS Applied Nano Materials* **2018**, *1* (7), 3186-3195.
38. Hexcel *Hexply Prepreg Technology*.; Hexcel.com, 2017.

Chapter 2

2 Optimizing the carbon fiber- epoxy resin matrix composites to improve the thermomechanical properties

2.1 Abstract

The goals for this chapter were to develop an efficient curing process for carbon fiber composite prepregs in epoxy resins for use in marine rowing racing boats. Enhancing the manufacturing curing process can potentially improve the company's competitive advantage in having high performance and low weight racing hulls. An oven and software system were setup to mimic the current industrial heating rates used by the company to understand the curing process by using a vacuum bagging technique. To help optimize the curing process, a Design of Experiment (DOE) approach using a central composite design was undertaken. Later, the results of the two types of B prepreg materials were examined using a solvent casting method (vacuum-ramping technique) and a solvent free method (conventional curing without vacuum-ramping technique). The results showed that both types of B prepreg samples gave similar results to type A samples, although the A samples gave more consistent results with less property variation. Weaker adhesion between the epoxy resin and carbon fiber were found with the B samples, but they gave stronger bonding to the honeycomb core. Further, the resin system used in the type B prepreg gave a lower onset temperature and had a significantly higher curing enthalpy. The curing rate of the B prepreg using the currently utilized processing temperature (121 °C) is approximately two times that of the A prepreg. The results from the curing testing using DMA analysis showed a decrease in the curing time of up to 50% by optimizing the curing process conditions. Both types of prepregs (A and B samples) were found to give enhanced mechanical properties at the optimum condition of ramp 3°C/min, temperature 121 °C and a holding time of 2 hours and 50 minutes. Note that A samples had better performance overall while the B samples gave better stiffness results due to their difference in chemistry, carbon fiber and epoxy resin content. By this optimization the amount of void-free and pinhole-free composite surfaces was improved as examined by microscopy.

Keywords

Carbon fiber- epoxy resin, Composite prepregs, Conventional Curing, Curing enthalpy, Design of experiment (DOE), Dynamic mechanical analysis (DMA), Ramp curing, Vacuum bagging technique (VBO),

2.2 Introduction

Improving the mechanical properties of composites is a major challenge in today's world. Enhancing the mechanical properties in carbon fiber- epoxy composites for rowing racing shells is a major challenge in the marine industry¹. The conventional method of fiber-matrix composites used for marine racing hulls can result in numerous defects and lower mechanical properties due to the large amount of resin soaked into the fibers; therefore, the Vacuum Bagging only technique (VBO) has been shown to increase the performance of the curing process². Accordingly, VBO in out of the autoclave technique is using constant vacuum portion to heat and cure the composites.

The main barrier coating materials that are used in the marine industry are epoxy resins as the reinforcement phase; due to their high tensile strength and modulus as well as easy processing, good thermal resistance, chemical resistance and dimensional stability³. Epoxy resins are defined as prepolymers having epoxide functional groups and low molecular weight⁴. As an important thermosetting resin, they can be hardened using numerous curing agents with both the curing process as well as the role of accelerators during the polymerization and cross-linking process². The unique features of the curing process are dependent on the chemical composition of the epoxy resin, the curing agents and the accelerators used⁴. The usage of carbon fibers have been shown to boost the mechanical performance of the epoxy composites, providing excellent stiffness and strength, good thermomechanical, electrical and chemical properties, while providing enhanced weight savings over metals³. Due to the lower price of carbon fibers compared to the glass or polymer fibers, these composites are suited for the automobile, aerospace industry as well as the marine industry and sports; therefore, they are focused on carbon fibers as fillers to enhance the thermomechanical properties and provide a smooth surface⁵.

Carbon fiber-reinforced polymers (CFRP) that contain the carbon fibers embedded in the epoxy resin thermosetting matrix need excessive resin applied to their surface for the

process of curing. This has led to using carbon fiber preregs as a common method for reinforcing fabrics which have been pre-impregnated with resin and a curing agent, which are both easier to use and have shown enhanced mechanical properties⁶. The preregs can be layered into a mold without any additional resin for the curing process⁷.

Our aim in this work was to both understand and improve the currently used industrial manufacturing process and to help lower the defect rates. This will help us understand the role of the resin and material suppliers better towards producing more consistent high-performance racing shells. To do so, a Design of Experiment (DOE) technique was utilized to examine the curing process at the lab scale to find which conditions enhance the thermomechanical properties of the preregs by producing void-free and pinhole-free surfaces. Moreover, our goal was also to understand the influence of the carbon fiber reinforced with the epoxy resin preregs from two different suppliers, type A and B, towards producing both enhanced and more consistent high-performance racing hulls. To do so, working on the innovative formulation of epoxy resin and reinforcing materials as well as modifying the optimum conditions of curing at the lab scale were examined thoroughly.

2.3 Experimental objectives

2.3.1 Sample preparation

The vacuum bagging only technique (VBO) was used for preparing the samples both with and without a Nomex honeycomb core. For assembling these commercial preregs, three layers of preregs with 90° between the layers was used under the constant vacuum as shown in (Figure 2.1).

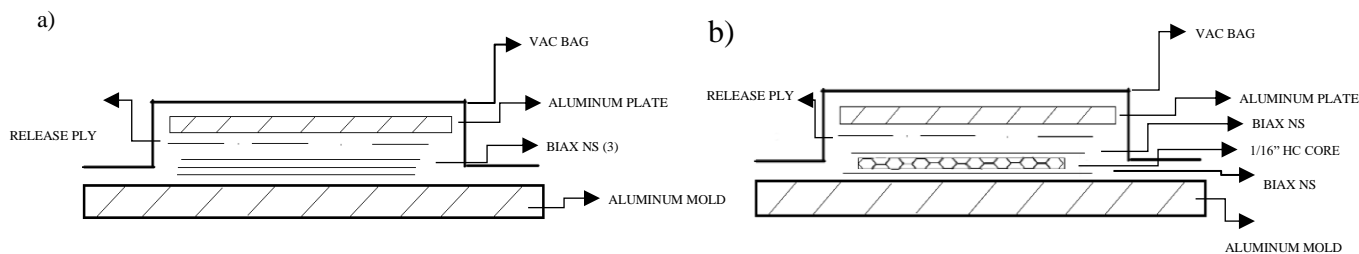


Figure 2.1: Assembly for curing Prepreg, a) without core, b) with honeycomb core.

Consequently, with the VBO molding process using the oven curing cycle, type A preregs were cured as shown in Figure 2.2. A vacuum oven (Thermo/Lindberg/Blue M VO914C) was used for the curing process which was modified by adding in an OMEGA CN7800 controller.

1)



2)



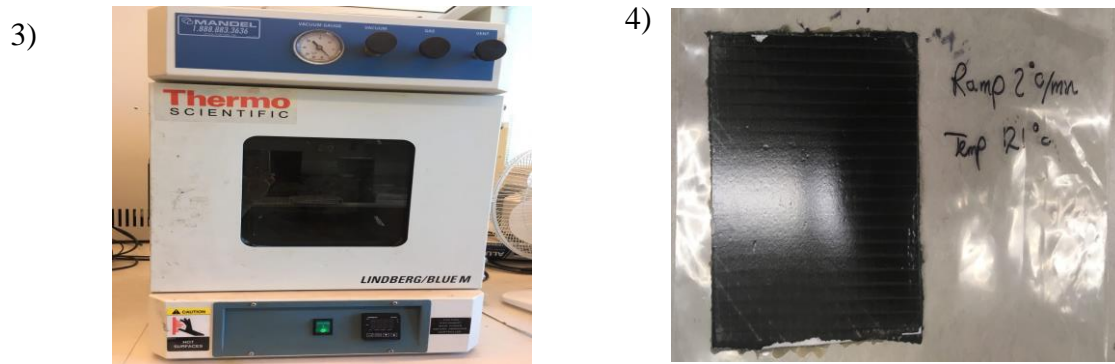


Figure 2.2: Conventional curing technique using oven 1) The Vacuum Bagging process (VBO), 2) Installation of the direct vacuum line inside the oven, 3) Installation of the controller for the oven, 4) Final cured prepreg product after using the VBO technique.

The procedure was repeated with type B sheets supplied by Hudson, meaning three layers of type B prepreps were used for each sample preparation and a pair of aluminum plates were employed to hold these layers together during the curing process under vacuum. Using the VBO technique, first the vacuum was released at the end of each curing cycle resulting in air bubble formation. Therefore, the samples were maintained under 11 psi constantly using a vacuum line inside the oven during the curing process and also for the holding time after the curing process¹.

2.3.2 Methodology

2.3.2.1 Curing procedure of prepreps in lab scale

For the curing procedure of both type A and B prepreps in the lab scale; firstly, the system was tested without sample to validate its performance. To model a 2°C/min ramp, the Proportional Integral Derivative Controller (PID) technique was used for all onset, current and peak temperatures. As PID is mainly useful for holding the temperature at a target point, using ramp 1°C/min which ramping indicates increment of temperature and holding it afterwards, was not beneficial for this condition. Later, the ramp and soak method were tested for various curing rates and times. Different ramp conditions were examined, starting from room temperature (24 °C) to peak temperature of the samples (150 °C) examining ramps of 2 °C/min, 3 °C/min, 4 °C/min and 5 °C/min.

2.3.2.2 The response surface design of analysis

Three layers of both type A and B samples with 90° as their angle of orientation were used as shown in Figure 2.3. Cured samples were cut into 12.81mm*35.70mm width and length. Dynamic Mechanical Analysis (DMA) was used to monitor the curing parameters. Cured batches of preregs were prepared in the lab using a central composite design by changing 4 factors according to the Design of experiment method (DOE).

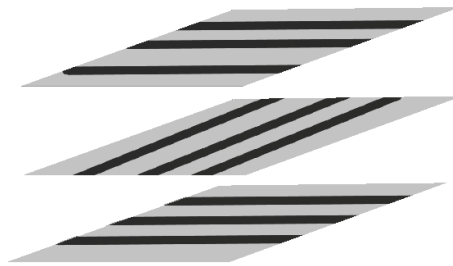


Figure 2.3: Orientation of the unidirectional carbon fibers for each layer of the prepreg composite matrix construction for both type A and B samples.

2.3.2.3 Optimization condition using the central composite design

A central composite design (CCD) was used to optimize the production parameters influencing the mechanical properties and the curing process of the examined preregs. The studied parameters are: ramping rate, curing temperature, holding time after curing and type of preregs. The type of prepreg is a categorical factor as only two types (A and B) were examined. In the studied optimization processes, full factorial designs were used in only one block and the factor ranges were in terms of alphas as shown in Table 2.1. The minimum and maximum ramping rates and holding time after curing were derived in order to have $2.5^\circ\text{C}/\text{min}$ and 2 hours and 50 minutes as their central values respectively. Order of the temperatures of 92°C and 150°C were chosen to demonstrate the extreme ends during the curing process of the preregs, uncured composites and burnt samples. Note that 121°C was representing the onset curing temperature of the VBO process.

Table 2.1: Levels of variables for central composite experimental design.

Variables	low axial ($-\alpha=-1.68$)	Center (0)	Low factorial (-1)	High factorial (+1)	High axial ($+\alpha=+1.68$)
X_1 : Ramp (°C/min)	1	2.5	1.81	4.19	5
X_2 : Temperature (°C)	92	121	103.76	138.24	150
X_3 : holding time (Hour)	1	2.50	1.61	3.39	4

These parameters were found to have a direct influence on the storage modulus, loss modulus, stiffness and $\tan \delta$. Design Expert 7.0.0 was used for the experimental design and for regression analysis of the data.

If categorical factors are added, CCD will be duplicated for every combination of the categorical factor levels. As a result for the response surface development, 40 runs were carried out using four independent parameters to optimize the mechanical properties of our samples as shown in Table 2.2.

Table 2.2: Design runs using central composite design.

Run	Ramp (°C/min)	Temperature (°C)	Holding time (Hour)	Types of prepreg
1	3	121	2.5	B
2	3	121	2.5	A
3	3	150	2.5	A
4	3	121	2.5	B
5	1.81	138	3.39	A
6	1.81	104	1.61	B
7	3	121	2.5	A
8	4.19	138	3.39	A
9	3	121	4	A
10	3	121	2.5	A
11	3	92	2.5	A
12	4.19	138	1.61	B
13	4.19	104	3.39	A

14	4.19	104	1.61	A
15	3	121	2.5	A
16	1.81	104	3.39	B
17	3	121	1	B
18	1.81	138	1.61	A
19	3	121	2.5	B
20	1.81	138	1.61	B
21	4.19	104	3.39	B
22	3	150	2.5	B
23	1.81	104	1.61	A
24	3	121	2.5	B
25	3	121	1	A
26	3	121	2.5	A
27	3	121	2.5	B
28	4.19	138	1.61	A
29	5	121	2.5	B
30	1.81	138	3.39	B
31	3	121	4	B
32	1	121	2.5	A
33	3	92	2.5	B
34	3	121	2.5	B
35	1.81	104	3.39	A
36	3	121	2.5	A
37	5	121	2.5	A
38	1	121	2.5	B
39	4.19	138	3.39	B
40	4.19	104	1.61	B

Note that Analysis of Variation (ANOVA), which sections the total variation in a set of data into component parts, was used to check the confidence levels of the experiment and the significance of its models⁸.

Consequently, A and B samples were examined using a Nikon Eclipse L150 optical microscope for the occurrence of possible voids and pinholes. Optical microscopy was also used to compare both commercial matrix composites in their initial condition and their optimization phase.

2.3.2.4 Dynamic Mechanical Analysis (DMA)

To measure the mechanical properties of the carbon fiber epoxy systems, dynamic mechanical testing was performed using a Dynamic Mechanical Analysis (DMA) TA Q800 system with a single cantilever clamp according to ASTM D4065-12⁹. All 36 sample bars were subjected to vibration at 1Hz and an amplitude of 15 μm . The oven temperature ramps were from room temperature to 200°C using a ramp rate of 3 °C/min, while the force was measured using an applied 1 Hz frequency on one side of the sample while the other side was clamped and fixed shown in Figure 2.4 .

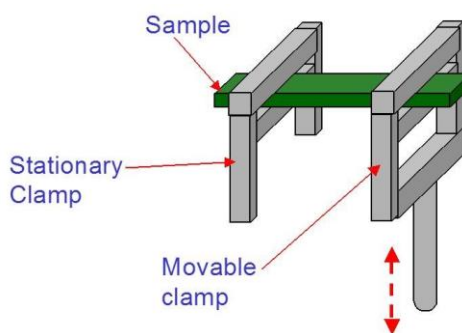


Figure 2.4: Testing mode using the DMA device for both prepreps⁹.

2.3.2.5 Thermal Gravimetric Analysis (TGA)

To determine the heat stability and relative epoxy resin/carbon fiber adhesion, 12-15 mg of the uncured prepreps were heated from room temperature to 700 °C at a ramping rate of 10°C/min in N₂ atmosphere, with a purge rate of 50mL/min using thermogravimetric analysis (TGA) on a TA Q600 system.

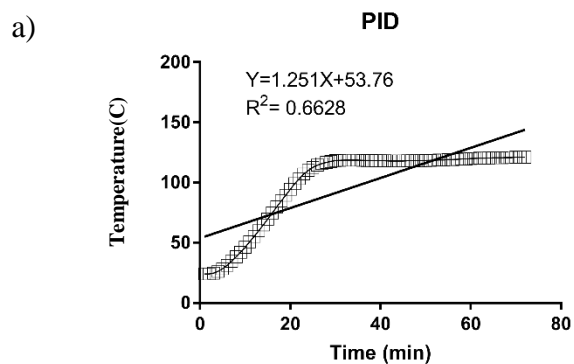
2.3.2.6 Differential Scanning Calorimetry (DSC)

The curing of resins was measured using differential scanning calorimetry (DSC) on a TA Q200 system. The uncured sample was subject to heat-cool-heat cycle at a ramping rate of 10°C/min for heating and 5°C/min for cooling. The upper and lower temperatures were set at 200°C and -20°C, respectively. To observe the curing enthalpy, the isothermal measurements were conducted at 121°C (current temperature used for industry production) and at designated temperature.

2.4 Results and discussion

2.4.1 Comparison of PID and Ramp and Soak curing technique

The first part of this work was to develop a laboratory sized heating system to mimic that used commercially for boat hull curing by using carbon fiber:epoxy prepregs. Working with both PID and the ramp and soak method, the results of R^2 derived from the process and the stability of the system were examined as shown in Figure 2.5. The ramp and soak technique was the candidate methodology used for this curing procedure and ramps of 2,3,4 and 5 °C/min were examined as shown in Figure 2.5. The slope of the diagram is the value for different ramp rates. Using a ramping rate of 5 °C/min showed fragile slope as the graph indicates; even though the R^2 for this condition sounds reasonable, having the ramp at 5 °C/min was deemed not practical for either the lab scale or potential industrial adoption.



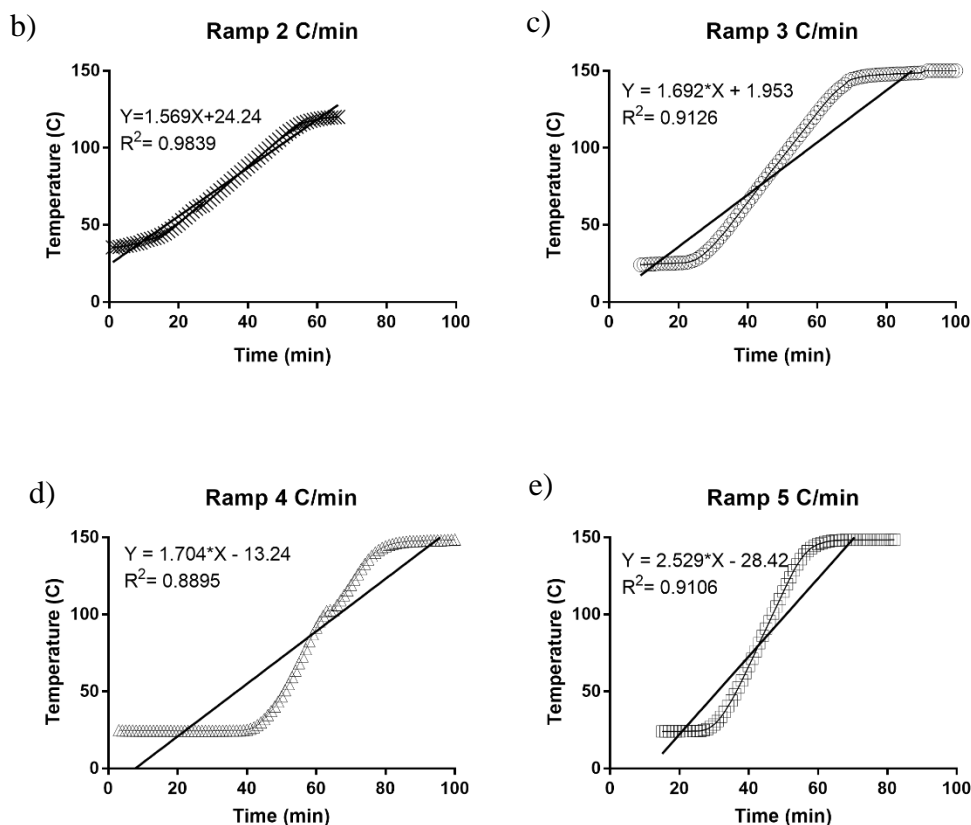


Figure 2.5: Curing conditions using: a) PID mode starting from the room temperature and increasing it manually, b-e) Ramp and Soak technique respectively using the values of 2, 3, 4 and 5 °C/min as the ramping factor starting from room temperature and increasing its value gradually with specific slope according to the ramp values.

2.4.2 The response surface design of analysis

2.4.2.1 Statistical Analysis using the analysis of variance (ANOVA)

In Table 2.3, the results of the analysis of variance (ANOVA) for testing the accuracy of the model and its residuals are summarized¹⁰. As Table 2.3 indicates, the Model F-value implies that the model is significant for each of the responses. Also, there is only a 0.01% chance that a "Model F-Value" this large could occur due to noise. Note that the values of "probability > F" that are less than 0.05 indicate that the model terms are significant¹¹. The large value of the correlation coefficient R^2 , mostly 0.95, indicates a high reliability of the

models in predicting the mechanical properties of the prepregs. This indicates that almost 95% of the response variability can be explained by the model.

Table 2.3: The results of ANOVA analysis of the developed models.

Response		Sum of squares	DOF	Mean square	F-value	p-value Prob>F	R-Squared	Adj R-Squared
Storage modulus	Model	83.57	13	6.43	38.35	<	0.95	0.93
	Residuals	4.36	26	0.17		0.0001		
Loss Modulus	Model	8.59E-004	13	6.61E-005	39.38	<	0.95	0.93
	Residuals	4.36E-005	26	1.68E-006		0.0001		
Stiffness	Model	1.75E+013	13	1.35E+012	38.31	<	0.95	0.93
	Residuals	9.13E+011	26	3.51E+010		0.0001		
Tan δ	Model	1.65E-005	13	1.27E-006	33.08	<	0.96	0.93
	Residuals	7.68E-007	20	3.84E-008		0.0001		

2.4.2.2 Elaboration on the equations for the central composite design models

Using four parameters as the variables in the central composite design, 40 experiments were run for this optimization process. Six replicates at the center point were determined as the experimental error for sufficiently enhancing the mechanical properties of the prepregs. The obtained results were entered into Design Expert 7.0.0 software and four quadratic models were selected to fit the results for the mechanical properties of the prepregs using the DMA device. (Equation (2.1)-(2.4))

$$\begin{aligned}
 \text{Storage Modulus} = & 15.76 + 0.11A + 0.70B + 0.60C + 0.98D + 0.57 AB \\
 & - 0.12 AC + 0.20 AD - 0.63 BC + 0.16 BD + 0.07 CD + 1.36E - 004 A^2 \\
 & - 0.50B^2 + 0.16 C^2
 \end{aligned} \tag{2.1}$$

$$\begin{aligned}
 \text{loss Modulus} = & 0.12 + 4.48E - 004 A - 2.81E - 003 B - 9.20E - 004 C \\
 & - 1.24E - 003 D + 1.53E - 003 AB - 3.38E - 003 AC - 1.69E - 004 AD
 \end{aligned} \tag{2.2}$$

$$-2.98E - 003 BC - 1.47E - 004 BD - 1.63E - 003 CD + 2.01E - 003 A^2 \\ - 9.27E - 005 B^2 + 1.52E - 004 C^2$$

$$\begin{aligned} Stiffness = & 7.61E + 006 - 2.23E + 005 A + 3.38E + 005 B + 2.93E \\ & + 005 C - 2.94E + 005 D + 82976.29 AB + 4.85E + 005 AC - 1.38E \\ & + 00 AD - 1.91E + 005 BC - 10510.19 BD - 1.54E + 005 CD - 1.92E \\ & + 005 A^2 - 1.46E + 005 B^2 - 77175.99 C^2 \end{aligned} \quad (2.3)$$

$$\begin{aligned} Tan\delta = & 7.16E - 003 - 2.10E - 004 A - 3.31E - 004 B - 1.82E - 004 C \\ & - 4.37E - 004 - 2.76E - 004 AB - 1.65E - 004 AC - 2.22E - 004 AD \\ & + 1.88E - 004 BC - 3.25E - 005 BD - 2.20E - 004 CD + 2.40E - 004 A^2 \\ & + 2.29E - 004 B^2 + 7.93E - 005 C^2 \end{aligned} \quad (2.4)$$

Using these models, all variables are in coded values, in which A is the ramp value, B is representing the temperature, C is the holding time after the curing process and D is the type of prepregs being used for this experiment. Also, AB , AC , AD , BC , BD , CD , A^2 , B^2 , C^2 and D^2 are the interactions of the main parameters together and with themselves¹².

2.4.2.3 Optimization phase

Three out of four factors were set as target values, meaning a ramp rate of 3°C/min, temperature at 121°C, holding time at 2 hours and 50 minutes and only the fourth parameter, prepreg type, were maintained in the ranges shown in Table 2.4. Our goal was to find an optimum point with the best performance in mechanical properties, including to maximize the storage modulus, stiffness and $Tan \delta$ and minimize the loss modulus at the same time.

Table 2.4: Constrains on the first optimization using the central composite design.

Name	Low limit	Upper limit	Lower weight	Upper weight	Importance
Ramp (°C/min)	2	3	1	1	5
Temperature (°C)	121	138	1	1	3
Holding time (Hour)	2	3.39	1	1	4
Types of prepregs	A	B	1	1	3
Storage modulus (GPa)	12.44	18.71	1	1	4
Loss modulus (GPa)	0.11	0.13	1	1	3
Stiffness (KN/m)	5.33E+006	8.63E+006	1	1	3
Tan δ	6E-3	8.8E-3	1	1	4

The storage modulus, which represents the energy being stored at the elastic portion of the samples, should be at the highest level while the loss modulus, which measures the energy dissipated as heat representing the viscous portion of the samples, should be at its lowest value¹.

Similarly, a polymer transformation from a hard-glassy material to a soft rubbery one meaning the ratio of loss and storage moduli, Tan δ value, should be at the highest value as well. Such factors along with the stiffness and toughness of the prepregs are the critical aspects that would enhance the mechanical properties of the samples and are the reasons why we chose such limits for our responses¹³.

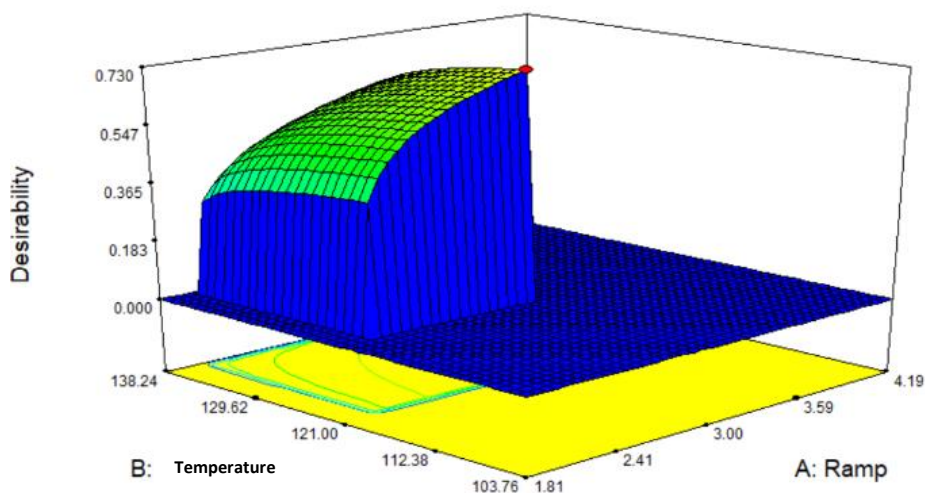
Following the response surface design utilized, 8 solutions were found considering the conditions for two combinations of categoric factor levels. Yet, only two of the conditions would be our practical solutions and will be used for the next steps of the experiment which are tensile and adhesion bonding tests, highlighted columns Table 2.5.

Table 2.5: Suitable solutions possible for central composite design optimum value for both types of A and B samples.

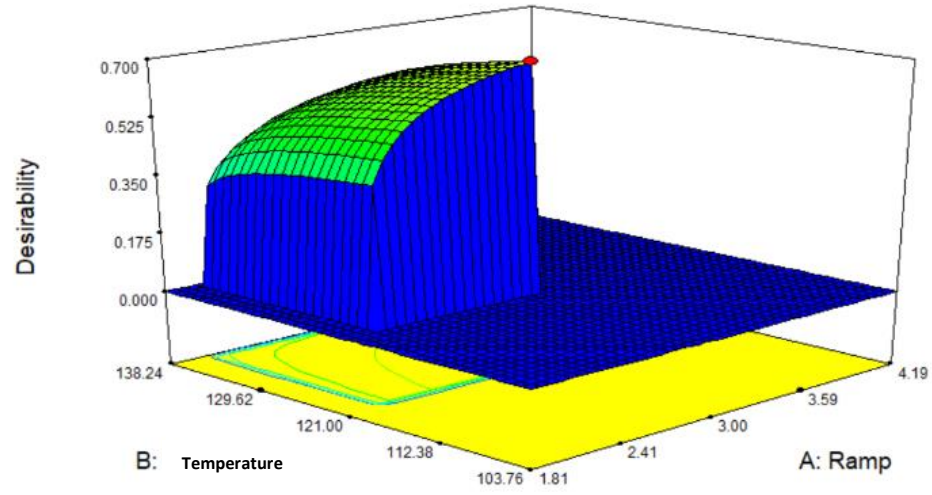
Num	Ramp (°C/min)	Temp (°C)	Holding time (Hour)	Types of prepregs	Storage Modulus (GPa)	Loss Modulus (GPa)	Stiffness (GN/m)	Tan Delta	Desirability
1	3	121	2.5	A	14.78	11.81E⁻²	7.91	7.6E⁻³	7.23E⁻¹
2	3	121	2.51	A	14.79	11.81E ⁻²	7.91	7.6E ⁻³	7.21E ⁻¹
3	3	121	2.52	A	14.80	11.81E ⁻²	7.92	7.6E ⁻³	7.21E ⁻¹
4	3	122	2.5	A	14.80	11.80E ⁻²	7.92	7.6E ⁻³	7.20E ⁻¹
5	3	121	2.5	B	16.73	11.56E⁻²	7.32	6.7E⁻³	6.94E⁻¹
6	3	121	2.5	B	16.75	11.55E ⁻²	7.32	6.7E ⁻³	6.93E ⁻¹
7	2.96	121	2.5	B	16.72	11.56E ⁻²	7.33	6.7E ⁻³	6.91E ⁻¹

The 3D surfaces and 2D contour plots for the examined CCD provides a graphical representation for the conditions of the reaction system. Using these plots, the response parameters of the two factors are shown, while all other factors are at fixed levels¹⁴. The results of the interactions between four independent variables and the two dependent variables are shown in (Figure 2.6), while two other dependent variables were kept constant. As shown in the plots, the first optimum point which is for the A prepreg shows a good improvement in the mechanical properties comparing to the B prepreg as the fifth(5th) optimum point Table 2.5. However, only in the stiffness part, type B shows better qualities but overall it would not change the fact that A prepregs are better candidates for industrial and lab scale usage in the curing process.

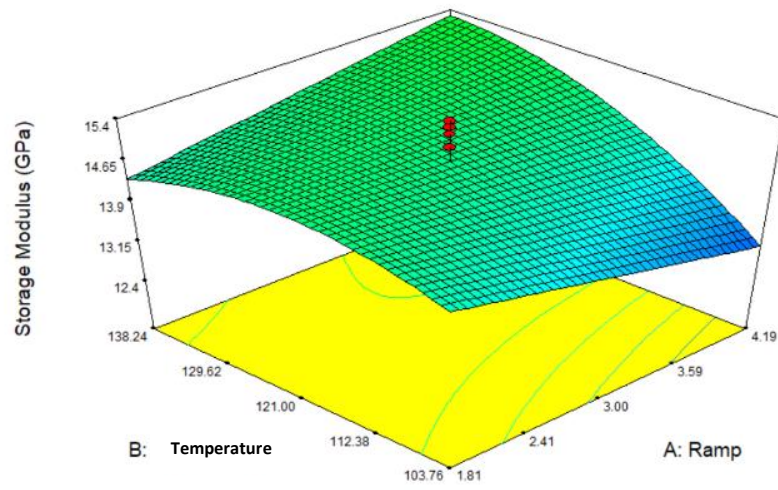
a)



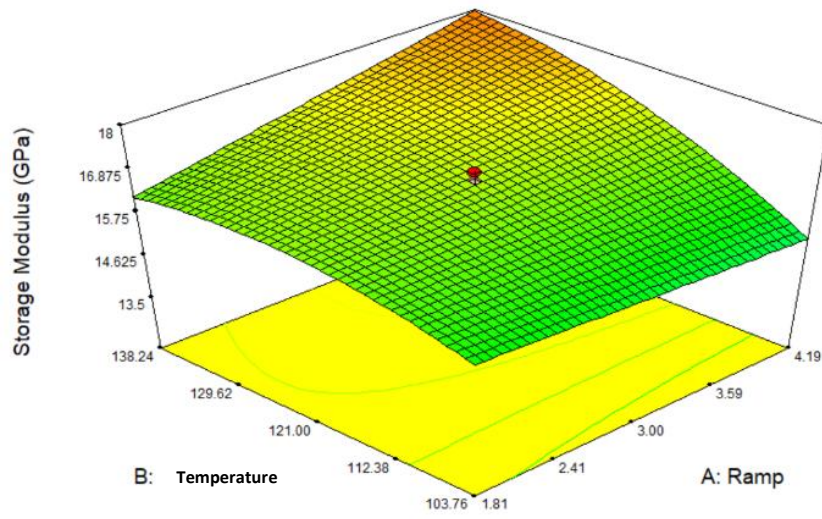
b)



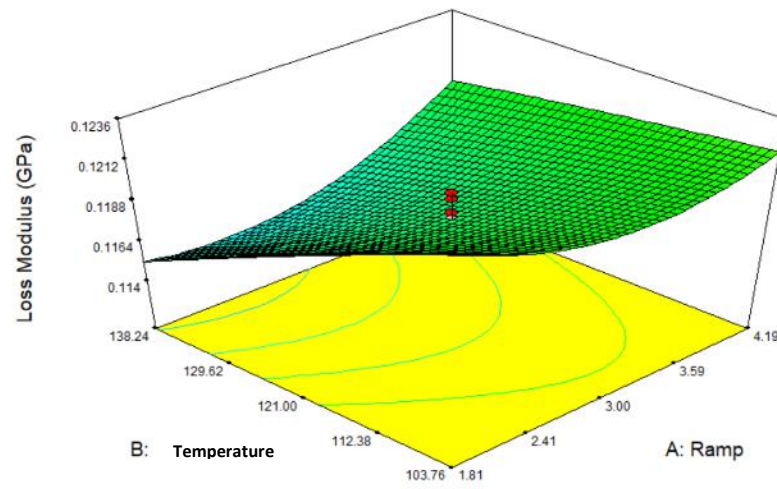
c)



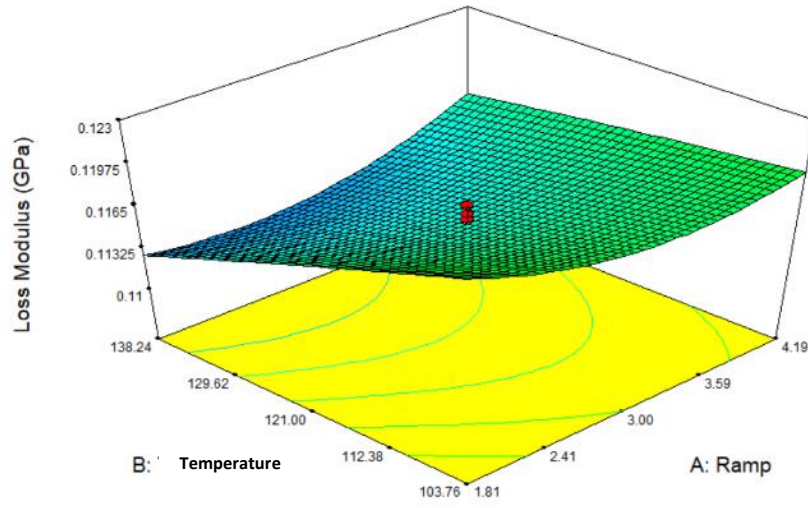
d)



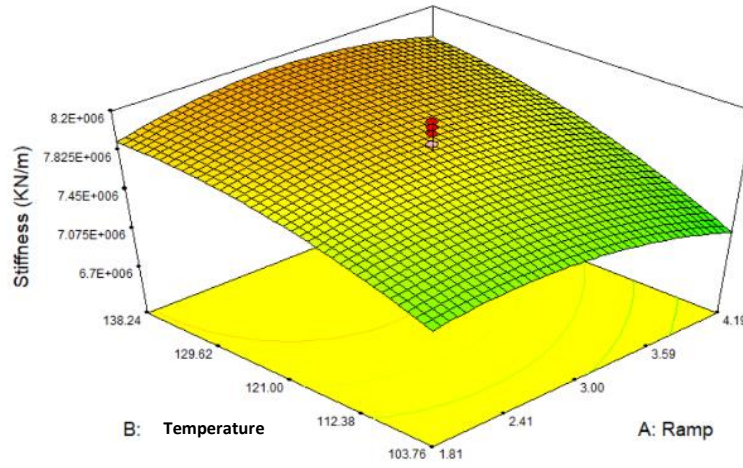
e)



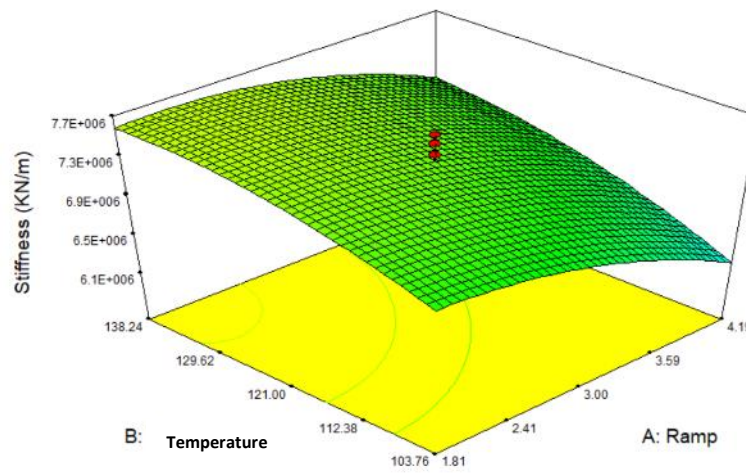
f)



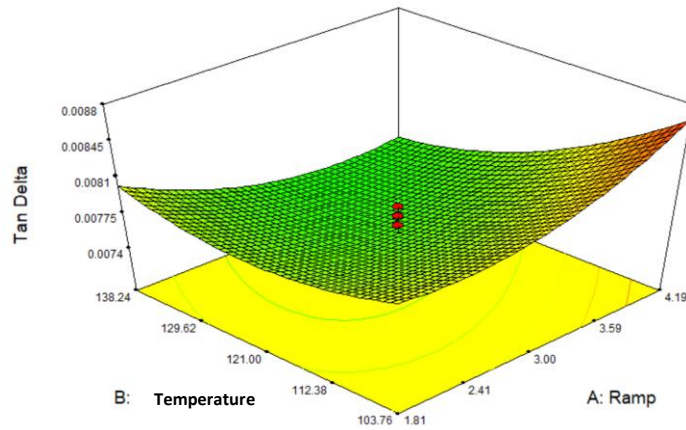
g)



h)



i)



j)

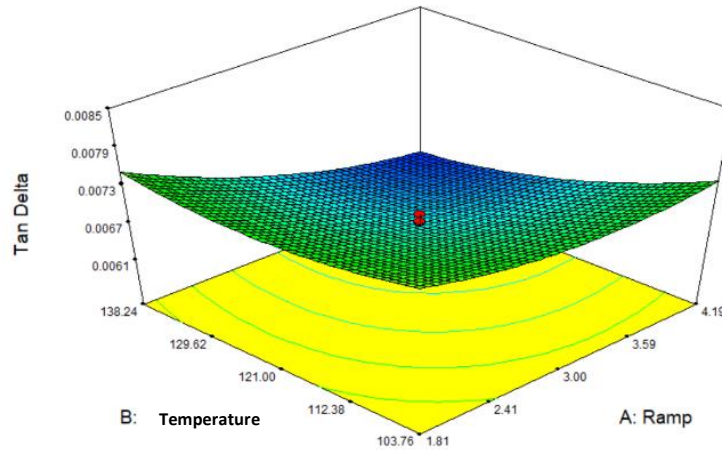
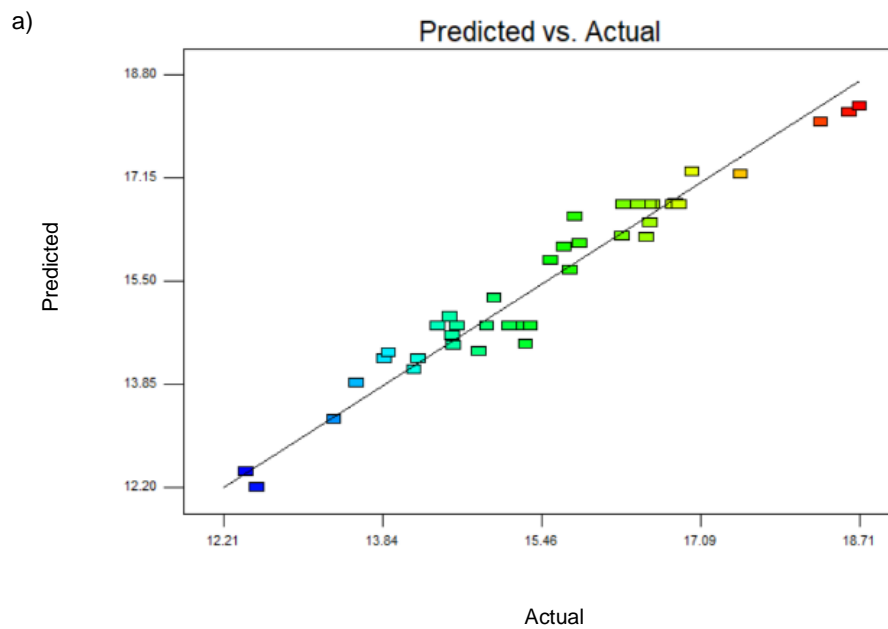
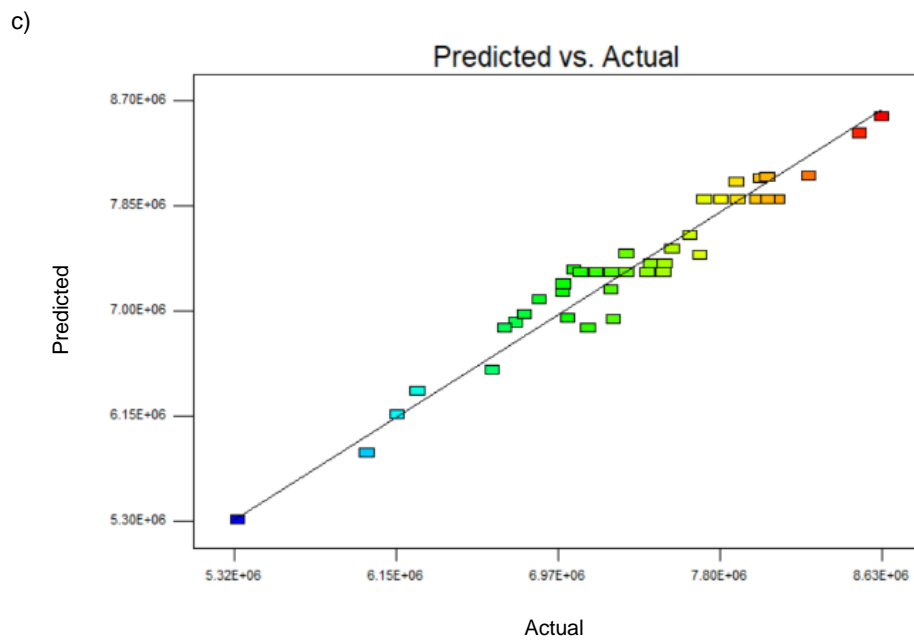
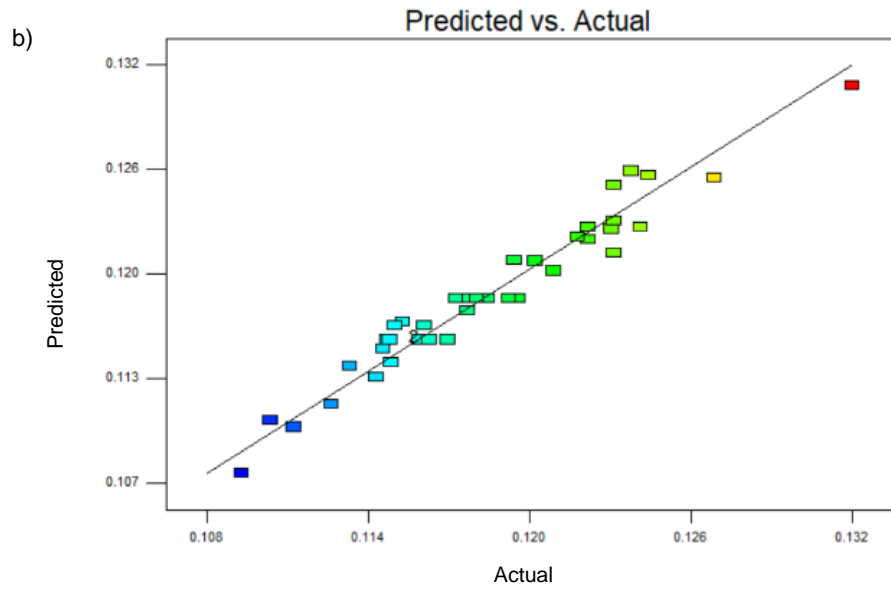


Figure 2.6: a) Desirability plot and contour in A prepreg (Optimum point number 1), b) Desirability plot and contour in B prepreg (Optimum point number 5), c) Storage modulus plot and contour in A prepreg (Optimum point number 1), d) Storage modulus plot and contour in B prepreg (Optimum point number 5), e) Loss modulus plot and contour in A prepreg (Optimum point number 1), f) Loss modulus plot and contour in B prepreg (Optimum point number 5), g) Stiffness plot and contour in A prepreg (Optimum point number 1), h) Stiffness plot and contour in B prepreg (Optimum point number 5), i) Tan δ plot and contour in A prepreg (Optimum point number 1), j) Tan δ plot and contour in B prepreg (Optimum point number 5).

2.4.2.4 The prediction of the optimum condition for having enhanced mechanical properties

For confirming the model's adequacy to reach the best mechanical properties (response function), a new design using the optimum levels was carried out (two highlighted conditions) as shown in (Figure 2.7)¹⁴⁻¹⁵. The results show that there is a good agreement between the predictive and experimental results at the optimum levels, providing a high validity to the model. Correspondingly, the R^2 mostly around 95% supports the models validity.





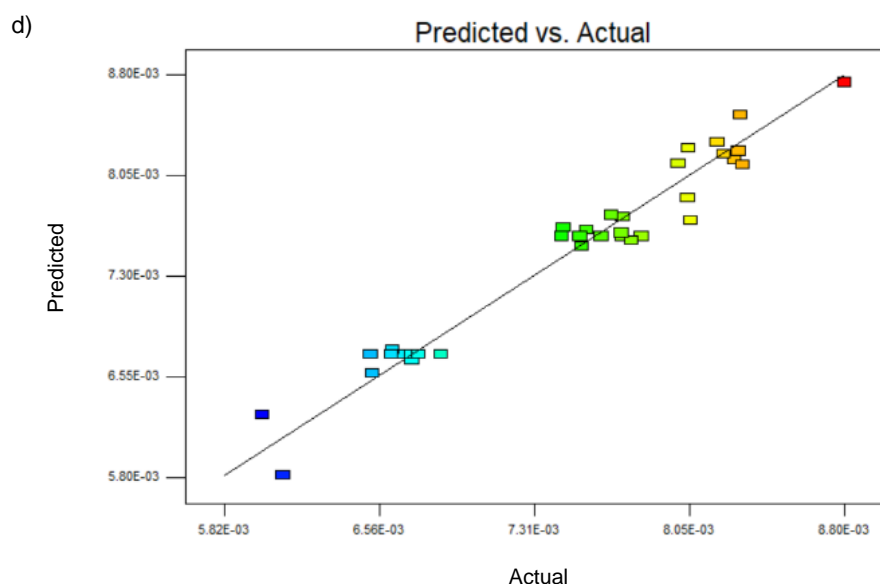


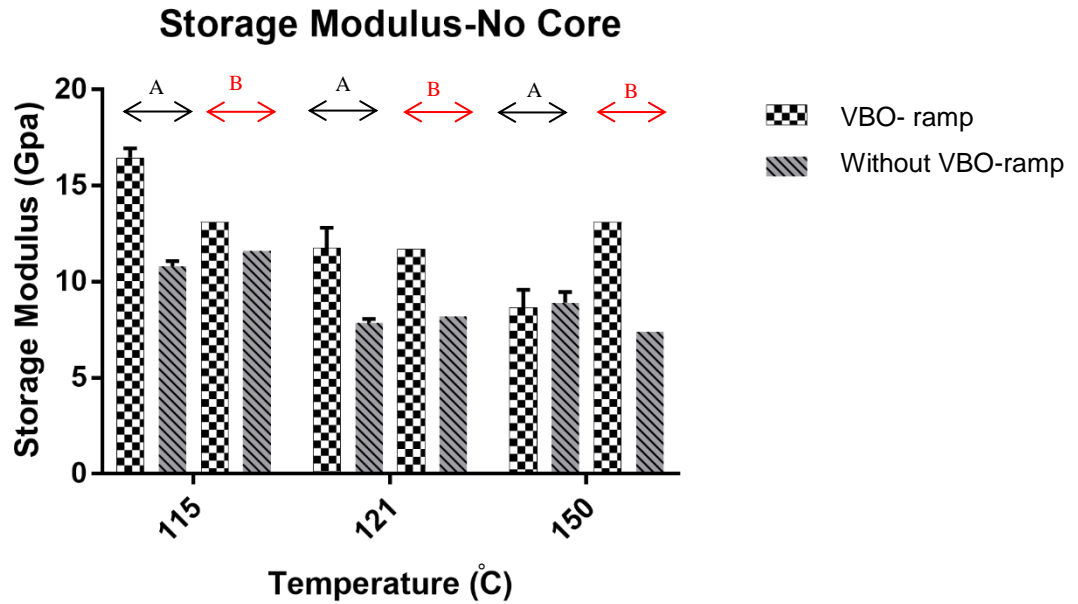
Figure 2.7: Predicted vs. actual values of a) Storage modulus, b) Loss modulus, c) Stiffness and d) $\tan \delta$ as four responses of this central composite design of experiment.

2.4.3 Checking basic mechanical properties for both two commercial prepreps

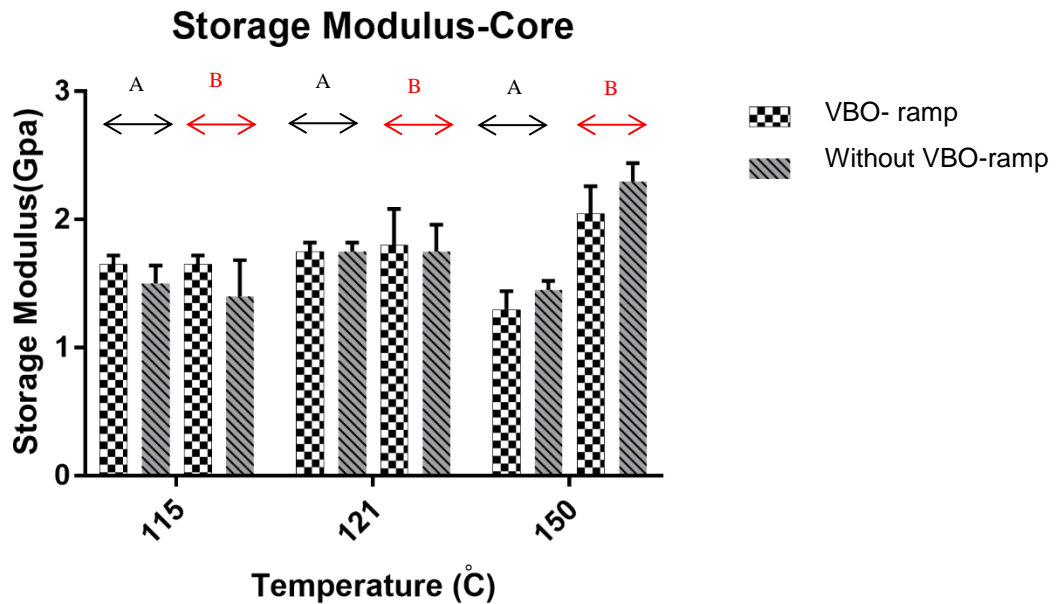
In this work the result of using different curing techniques and different curing temperatures were examined. Two types of commercial samples A and B were tested using the DMA device. Note that type A and B prepreps were cured using both the ramping technique (VBO-ramp technique) and the conventional oven curing method (without VBO-ramp). In the subgroup of B prepreg, two different types of *in solvent* and *hotmelt* were used. Therefore, different chemistry and curing techniques were utilized for the preparation of type B samples. *In solvent* prepreg was cured while having more epoxy resin content and a normal ramp curing method (VBO-ramp technique) while the *hotmelt* kind had to use the conventional oven curing method (without VBO-ramp). Comparing type A with these two B typed prepreps, it was understood that for the samples with no core, if they were cured by ramping to target temperature, the storage modulus of both B *in solvent* prepreg and B *hotmelt* prepreg indicated a better consistency at three different final

temperatures, whilst the A prepreg varies significantly, and the storage modulus decreased as the final temperature was increased (Figure 2.8).

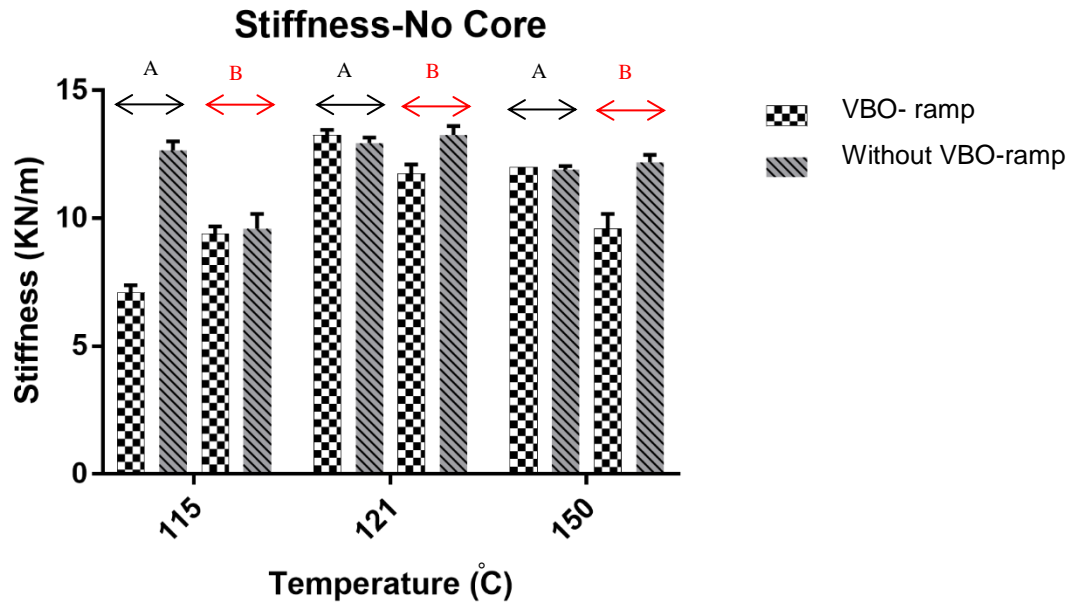
a)



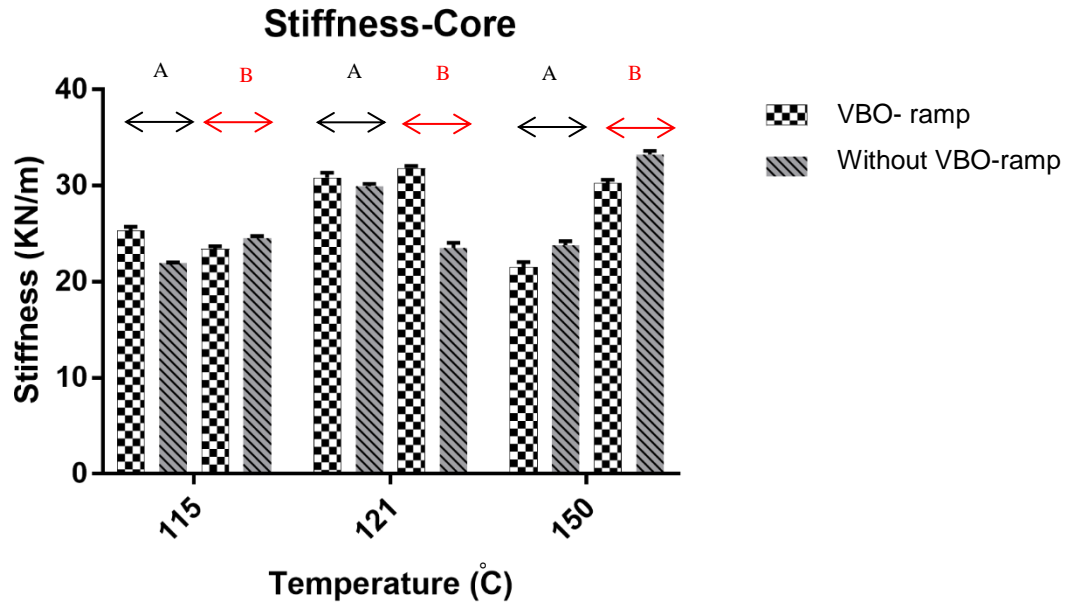
b)



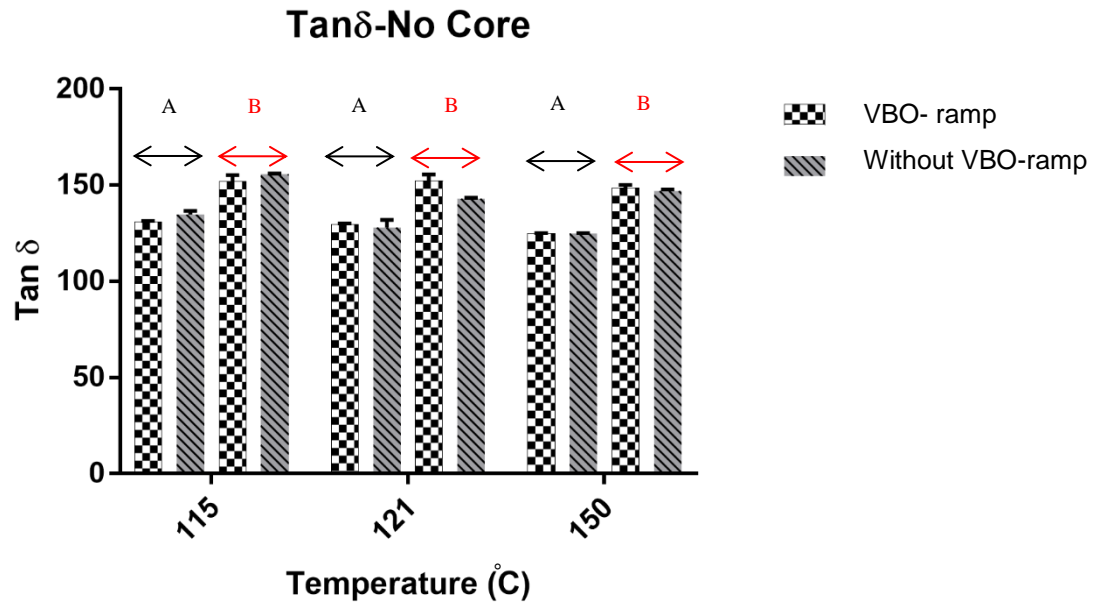
c)



d)



e)



f)

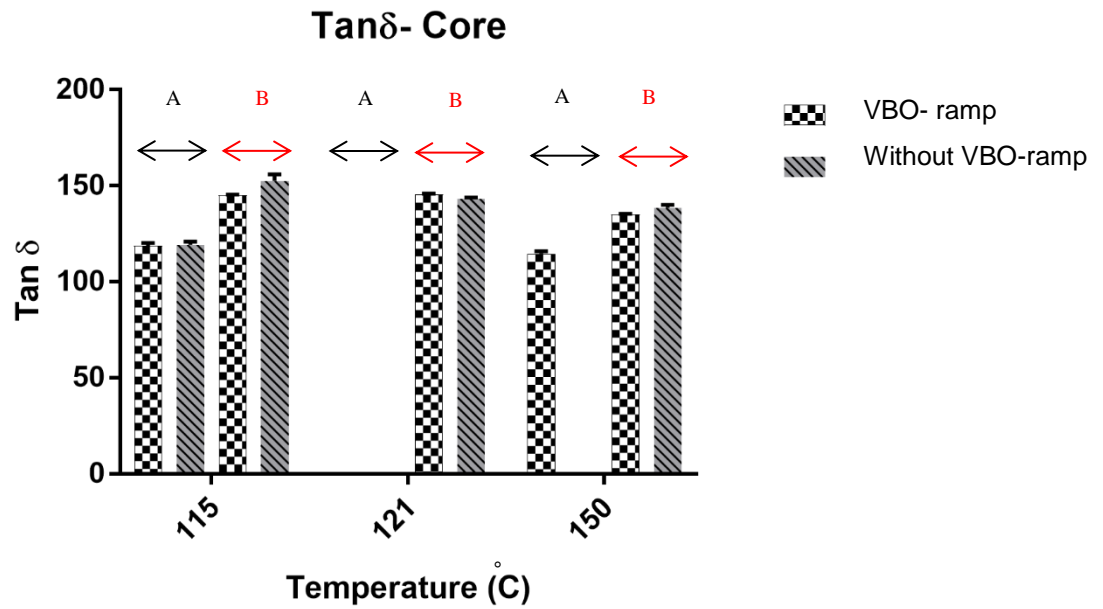


Figure 2.8: DMA results for A and B prepregs: a) Storage Modulus no- core, b) Storage modulus- with core, c) Stiffness-no core, d) Stiffness- with core, e) Tan δ - no core and f) Tan δ - no core.

During the curing process at constant temperature (without VBO-ramp), the *in solvent* type B prepregs and A samples showed a decrease in storage modulus while having an increase in temperature, compared to those cured by the ramping technique of VBO-ramp (a-Figure 2.8). The results show that the modulus of the cured B *hot melt* prepregs is insensitive to the curing temperature and examined curing method (either VBO-ramp or without VBO-ramp) (a-Figure 2.8).

Moreover, adding a Nomex honeycomb core between the two layers of B *in solvent* prepregs and A prepregs led to a lower and more consistent storage modulus, which appears insensitive to the curing method and temperature. The cored B *hot melt* prepregs show an increase in sensitivity with curing temperature, although they are not affected by the curing method (b-Figure 2.8).

Stiffness of the samples with and without core was also found to be insensitive to the curing method (c& d- Figure 2.8). However, adding the honeycomb core was found to double or triple the stiffness meaning increasing their maximum value from 15 KN/m up to 40 KN/m compared to the samples without a honeycomb core(d-Figure 2.8). At 121 °C (250°F), the current curing temperature used by the company, the A prepregs show a higher stiffness than either of the type B prepregs, whilst the latter has a higher stiffness at high curing temperatures (c& d- Figure 2.8). However as for the rowing hall applications the maximum stiffness is not the ideal condition therefore, it is better to work with the composites around their onset curing temperature value(121 °C)¹⁶.

Maximum $\tan \delta$ (T_g) was found to vary with the sample source, that is, type B samples showed a higher T_g (by 10-20 °C) than the A samples (e- Figure 2.8). This phenomenon follows the same trend compared to the DSC results of rapid dynamic curing (shown later). Both resin products showed that adding the honeycomb core decreased the $\tan \delta$ maximum peak temperature by about 10°C (f- Figure 2.8). The curing conditions were generally found to not affect the $\tan \delta$ peak temperature for either prepreg supplier. Compared to the literature this is one of the advantages of working with vacuum bagging only curing method (VBO)¹³.

In this study, we examined the peak factor to quantify the width of the $\tan \delta$ peak. The peak factor (I) is defined as the full width at half maximum of the $\tan \delta$ peak divided by its height (Figure 2.9)¹⁶. It was used to understand how these results relate to prepreg quality. More than one peak value usually indicates significant heterogeneity at a macro scale, so that wider peak values for $\tan \delta$ indicate a lower homogeneity in the material during the same scale¹¹.

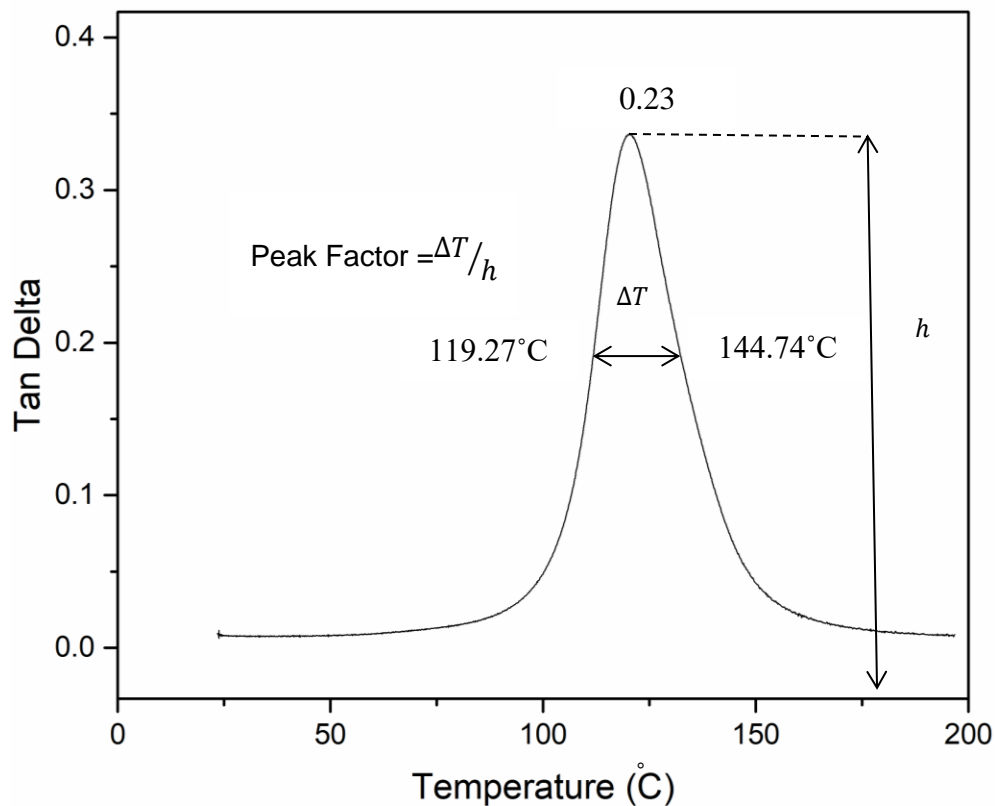


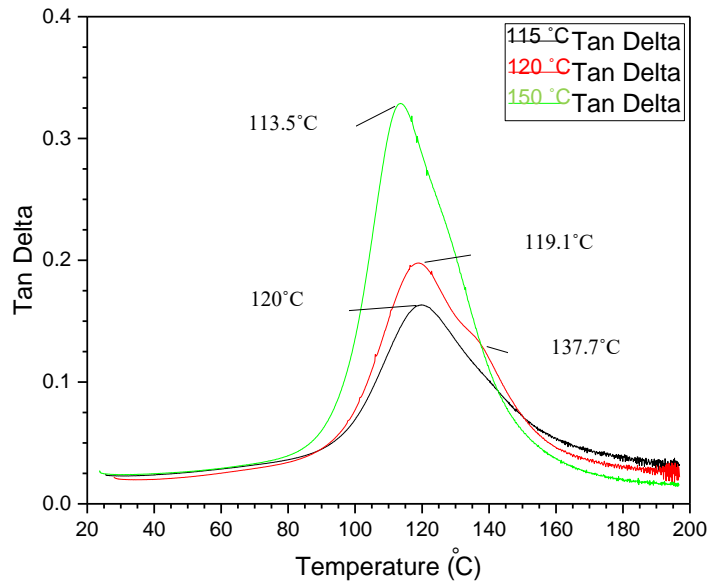
Figure 2.9: Typical $\tan \delta$ profile of cured prepreg without honeycomb core. Where ΔT is the temperature difference at $\frac{1}{2}h$, and h is the height of the $\tan \delta$ peak

The A samples without core showed a significant low peak factor (3 to 4 times) than their B counterparts (a& c- Figure 2.10). Thus, during the curing conditions used to prepare

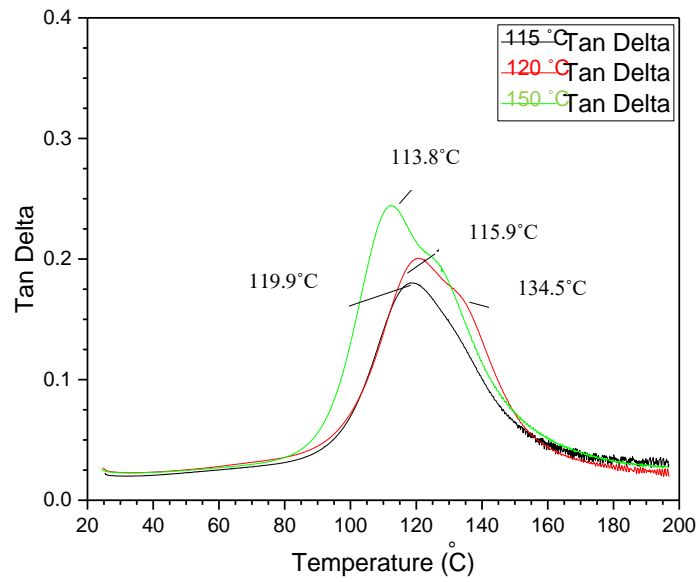
these samples, the A prepreg shows better homogeneity than the B prepreg. This may indicate a stronger resin-fiber adhesion for the A prepreg, which would lead to better quality and lower defect parts. Peak factor of cured prepreg from both companies seem to be consistent under different curing conditions, although higher curing temperatures (either VBO-ramp or without VBO-ramp methods) yield a low peak factor (Figure 2.10). For the two types of B prepreps, the *hot melt* seems to have a lower peak factor.

It is not surprising that adding the Nomex honeycomb core in-between the two prepreg layers caused a significant increase in the peak factor, since the honeycomb Nomex structure would lead to heterogeneity at the macro scale, which may cause voids and pinholes in addition to making the structure stronger (b& d-Figure 2.10). The shape of the Tan δ profile is deformed in the case of the type A-core samples shown in (b-Figure 2.10). In this extreme case, the Tan δ profile displayed two peaks, green and red plots, thus the definition of peak factor for this type of material wouldn't be applicable (b-Figure 2.10). For both B samples with core, although the Tan δ peak becomes relatively wide, the peak factor definition is still valid and could be calculated (d-Figure 2.10). It is important that although some A-core samples show double peaks, the overall profile of Tan δ is narrower than its B counterparts, comparing b& d-Figure 2.10. This indicates better homogeneity of the cured type A prepreps. It is reasonable to suggest that the bimodal Tan δ peaks are caused by the addition of the honeycomb core, whose mechanical properties should be consistent assuming there is no chemical reaction occurring inside the core during the DMA test. The bimodality is very likely to be the sign of weaker adhesion between the prepreg and the honeycomb as shown in (Figure 2.10).

a)



b)



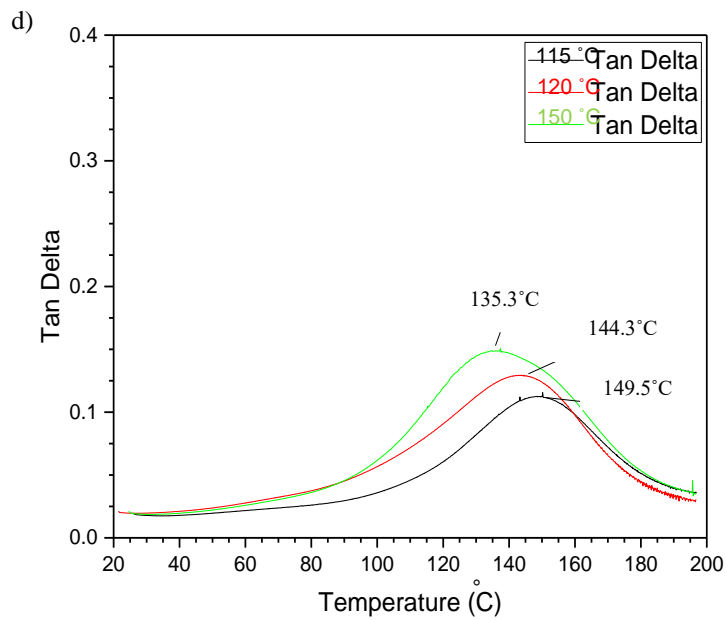
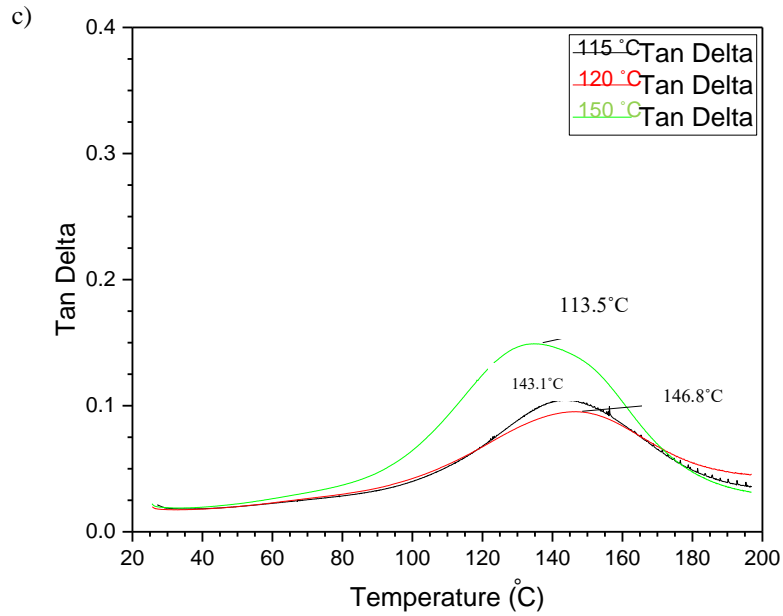


Figure 2.10: Tan δ profile of type A prepreg and B *in solvent* prepreg without and with honeycomb core a) A prepregs at 115, 121 and 150 °C temperature without core, b) A prepregs at 115, 121 and 150 °C temperature with core, c) B prepregs at 115, 121 and 150

°C temperature without core and d) B prepregs at 115, 121 and 150 °C temperature with core.

2.4.4 Comparison of both A and B prepregs

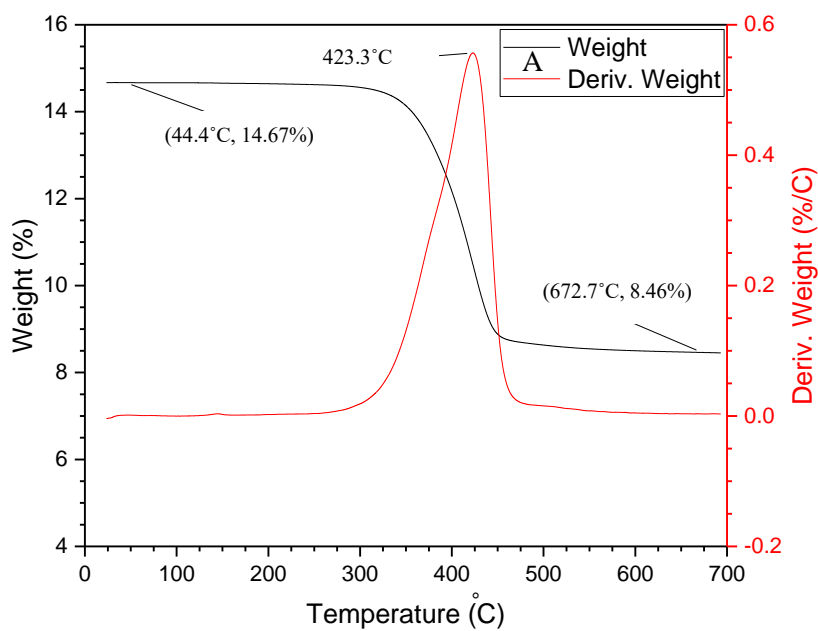
The two commercial prepregs were subjected to TGA analysis to understand their differences. Note that, only A samples and the uncured B *in solvent* prepregs were available for thermal analysis that for the rest of this dissertation they would be recalled as A and B prepregs. Neither product showed significant weight loss up to 245°C (99.7% for the A type and 99.3% for B prepregs). The A sample was found to have a higher onset temperature (360 °C versus 330 °C). This has relevance to the basic material properties and the homogeneity of the samples. Since the weight loss from both A and B prepregs (0.02% for A and 0.16% for B prepregs) is negligible at 121 °C (the current curing temperature in boat manufacturing) according to the TGA results, the pinholes/voids are less likely to be caused by evaporation of low boiling point components. It is possible that the shrinkage of resin during curing plays a key role to form voids inside and pinholes on the surface. The interfacial properties between the mold and prepreg can also be one of the possible reasons for surface defects which can be solved by either: a) a longer vacuum holding time or b) longer holding periods after the process of curing.

According to the weight loss profile shown in Figure 2.11, the A sample has better thermal stability, i.e. slower weight loss before the onset temperature. Also, in the last stage of the TGA analysis, the residue material (carbon fiber) used in A shows higher thermal stability than type B prepregs. Residue of B sample shows the tendency of continuous weight loss, while it is quite stable for type A. Compared to literature materials of both the epoxy-clay glass fiber composites and the epoxy-multi-walled carbon nanotubes(MWCNT) that are dealing with faster but less weight loss, the heat stability for A and B prepregs are more reliable¹⁷⁻¹⁸. This is less likely to affect the product quality since the boat will be primarily used at ambient temperature. It is also possible that the thermal decomposition behavior is caused by the carbon fiber quality used in the manufacturing process.

The calculation using the final remaining weight indicates that the resin content is approximately 40% and 35% by weight for both A and B prepregs, respectively using the

TGA technique. It is notable that the resin content measured by TGA testing can be lower than the other methods like DSC (shown later), since the residue carbon from pyrolysis of resin (while using nitrogen as purging gas) can potentially increase the remaining weight of the non-resin component.

The derivative of the weight loss shows that the B prepregs have more significant two-stage decomposition features than the A samples, which is also indicative of resin formulation differences.



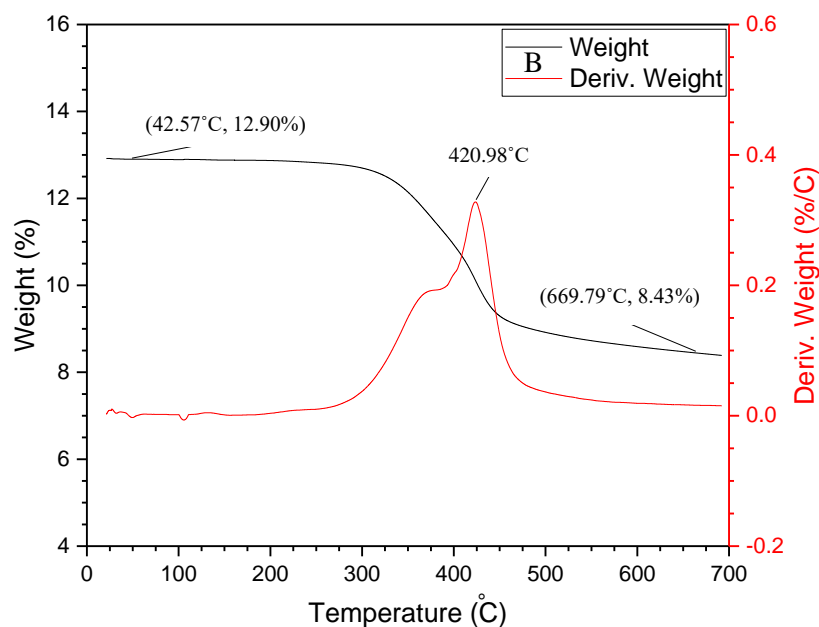


Figure 2.11: TGA analysis of type A (top) and B (bottom) prepreps.

2.4.5 Differential Scanning Calorimetry (DSC)

The isothermal test for both A and B prepreps at peak temperature was carried out by loading the samples into the preheated DSC chamber. Initial results using this approach were found not to work well for either of these two products. This is attributed to the rapid rate of curing near the peak temperature with the curing rate being too fast for the instrument to measure accurately. Also, loading the samples will cause the DSC chamber temperature to drop several degrees and the instrument needs some time to reach the set isothermal temperature in a controlled way which is called the on-hold period. During this time delay, the curing is almost finished thus acquiring the exact heat flow would be quite challenging as shown by (Figure 2.12).

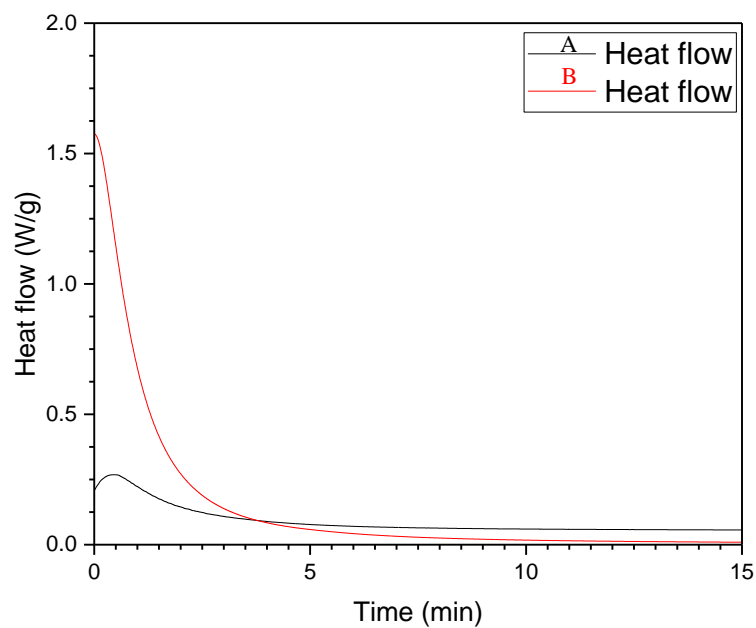
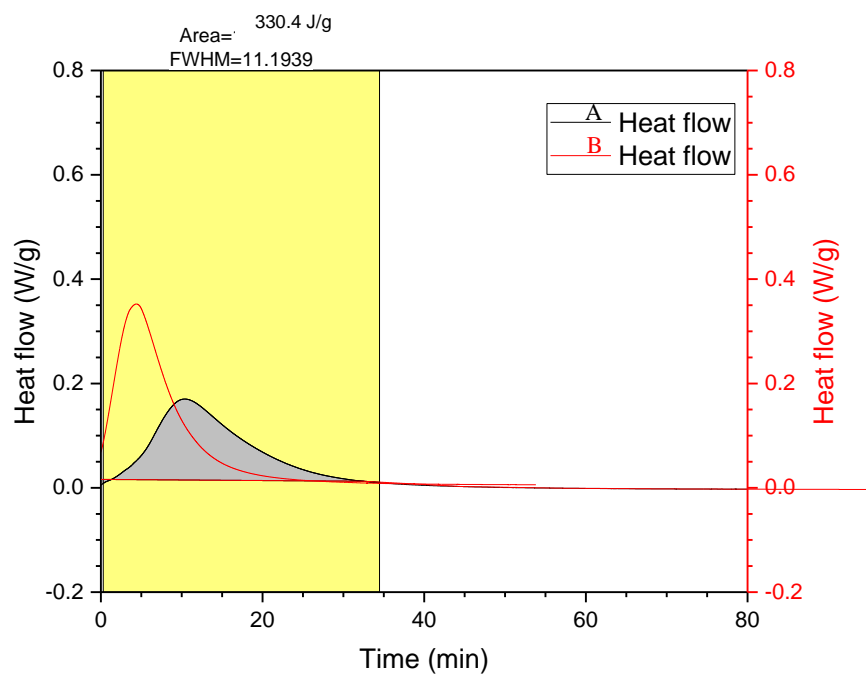


Figure 2.12: Heat flow of A and B prepregs isothermal at 121 °C (top, after weight adjustment) and peak temperature, 155 °C and 145 °C, respectively.

Later, another method was designed in which the sample was loaded at standby temperature (40 °C), then the instrument was programmed to quickly ramp to the target temperature using 10°C/min as the ramping rate. It was found that chamber reached the target temperature in about 1.2 min for both tests. The resulting DSC analysis shows that the onset curing temperatures for type A and B prepregs are 139 °C and 129 °C. Therefore, there are points where the reaction rate of the epoxy resin curing reaches the maximum for both prepregs using the first heat cycle. The lower the onset temperature, the more reactive the resin system would be for the B prepregs.

The curing enthalpy for A and B prepregs were calculated to be 275.6 J/g and 509.0 J/g based on the total mass of the prepreg. This was determined by integrating the heat flow of the first heating cycle based on the TGA residue weight at 690 °C. For this step, the resin weight was adjusted by the residue weight at 500 °C. Therefore, the curing enthalpy of B prepreg is 577.5 J/g as B shows some weight after 500 °C, after which the A weight appears stable until the end of the test (Figure 2.13).

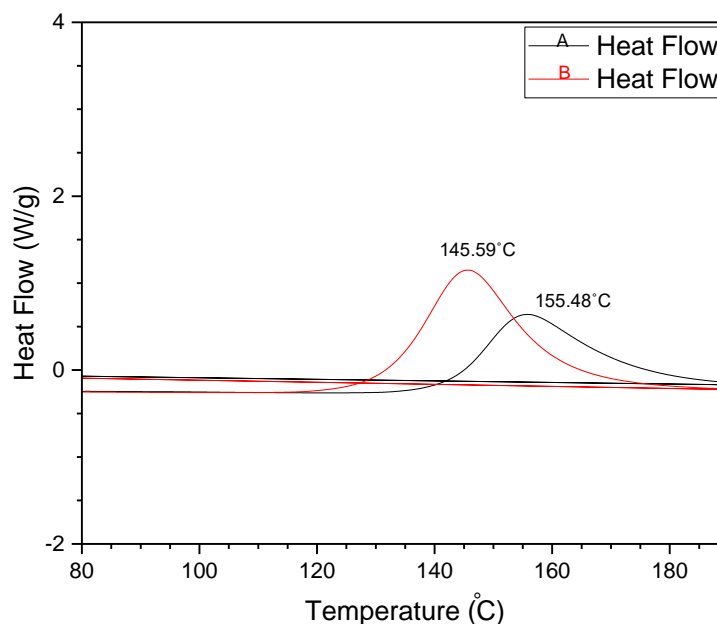


Figure 2.13: Curing enthalpy of A and B prepregs (after weight adjust according to TGA result).

The glass transition temperature (T_g) was also measured for the second heating cycle, where the T_g is 117.5 °C and 137.6 °C for A and B prepregs, respectively. As there is no significant heat flow in the second heating, it is reasonable to conclude that there is no further chemical reaction or primary transition occurring (Figure 2.14).

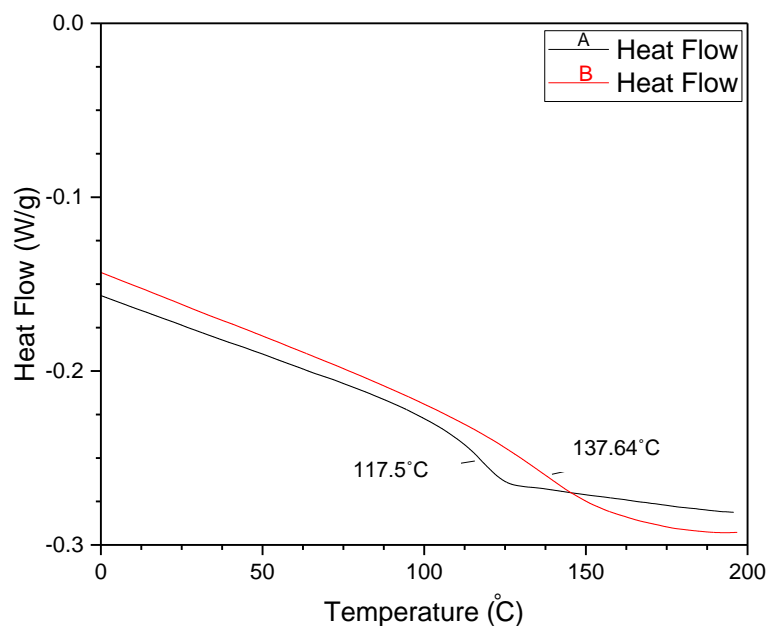


Figure 2.14: Glass transition temperature of A and B prepregs after dynamic curing.

Note that the heat flow and sample temperature profile shown in (Figure 2.15) and the curing enthalpy were calculated after the sample mass was adjusted to the resin content. The starting point of the integration was determined by the time when the heat flow turns to be positive (i.e. releasing heat from the sample). It is interesting that at the peak temperature, the curing speed is very similar and the curing enthalpy is 244.6 J/g and 408.6 J/g, for A and B prepregs, respectively.

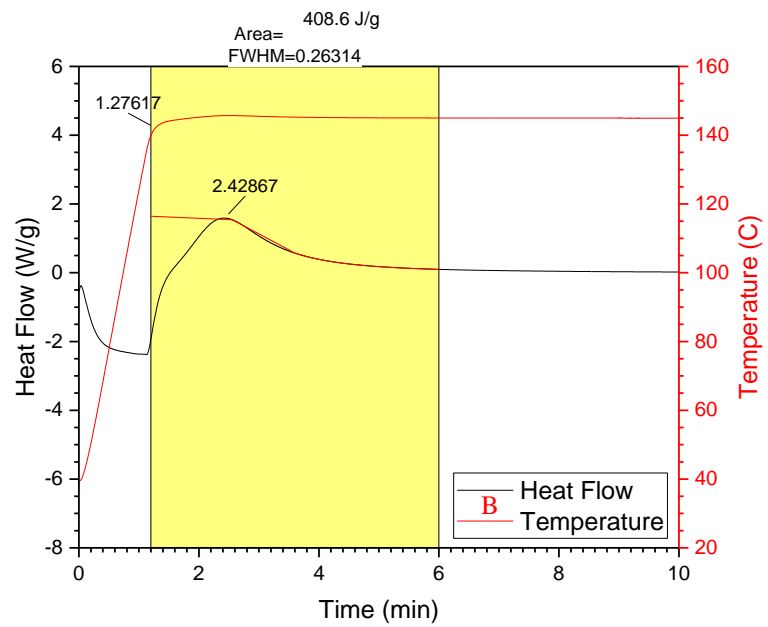
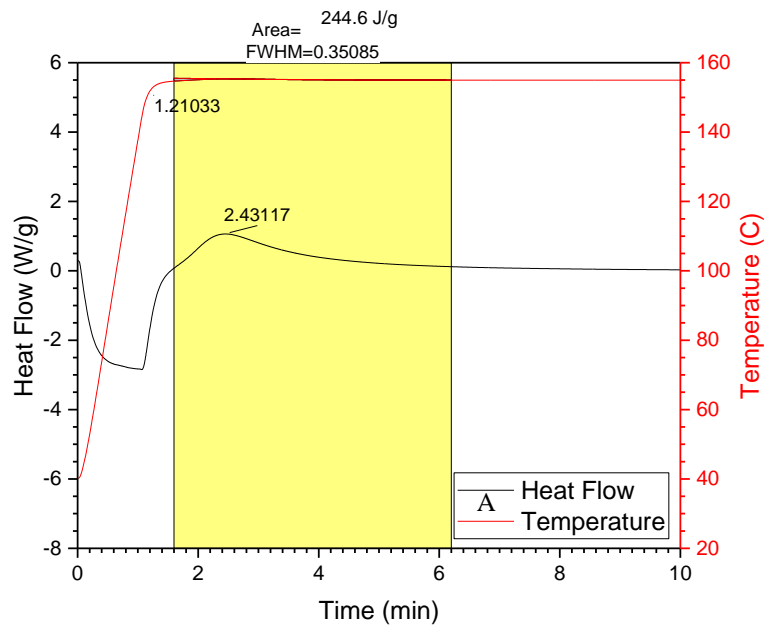


Figure 2.15: Curing profile for A (top) and B prepreps (bottom) at peak temperature using *temperature jump* method. Mass corrected to the resin content in prepreg.

2.4.6 DMA results for curing type B samples in lab scale

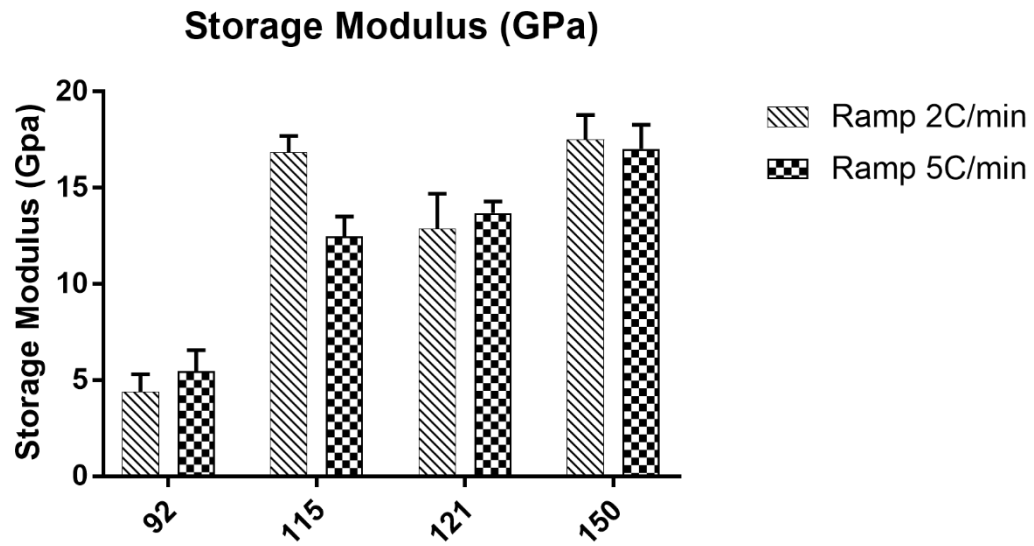
As predicted, by increasing the ramp during the curing process at each temperature, the T_g point increased as well. The loss modulus decreased as we have more stiff material in each step. Both the storage and loss modulus decreased at higher ramp rates as heating up the prepregs required less force for deformation (Figure 2.16). We were expecting the material to be less stiff/strength, as more energy is dissipated as heat, increasing the loss modulus¹⁹.

As the testing temperature increased, less energy is stored which would lead the polymeric molecules to slide past one another more quickly with increased force, leading to a rapid decline in storage modulus. As the storage modulus increase indicates, the stiffness and hardness are resistant to deformation due to the amount of energy being stored in the elastic portion of the composites. We were expecting that both the storage and loss moduli should decrease with increasing temperature, although only the loss modulus started to decrease which is the physical appearance of the T_g .

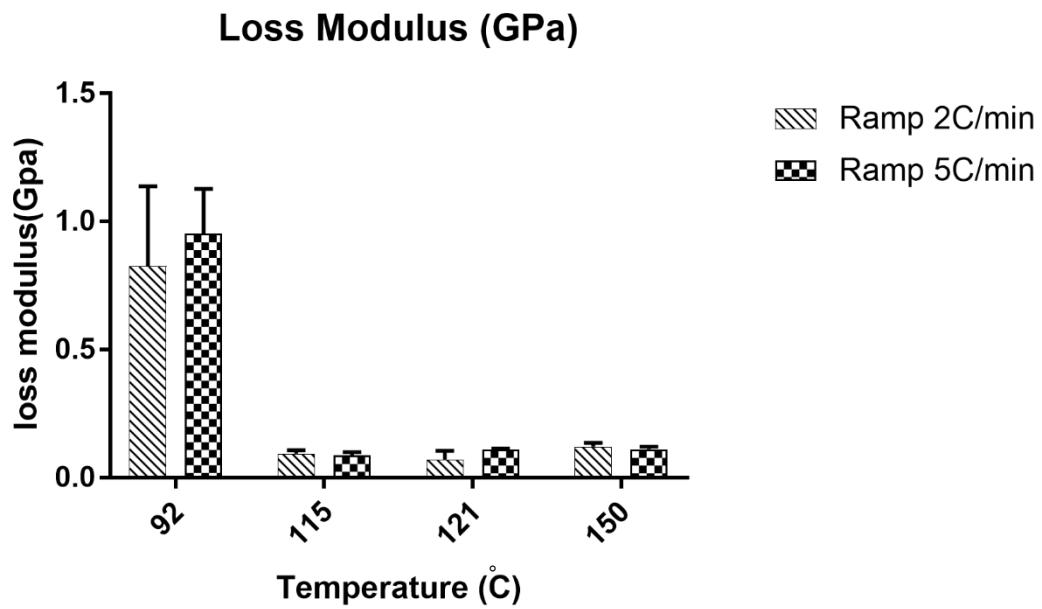
Therefore, the recorded trend indicates that using a 5 °C/min ramp increased the speed of the curing process, but not necessarily increased the T_g point or enhanced the thermomechanical properties of the material. A slower heating rate (2 °C/min) led to higher T_g values compared to faster heating at 5 °C/min²⁰. Also, the results were not as stiff and tough at 92 °C as we expected, because this temperature is far lower than the pre-curing condition of the B samples. Consequently, our given solution is choosing a lower but safer and more accurate ramp in the range of (2.5-3.5 °C/min).

By heating up the process, the polymeric chain mobility would be enhanced, and the curing reactions happen more rapidly. So, the T_g point using Tan δ curve at higher curing temperatures would be lower as expected²¹.

a)



b)



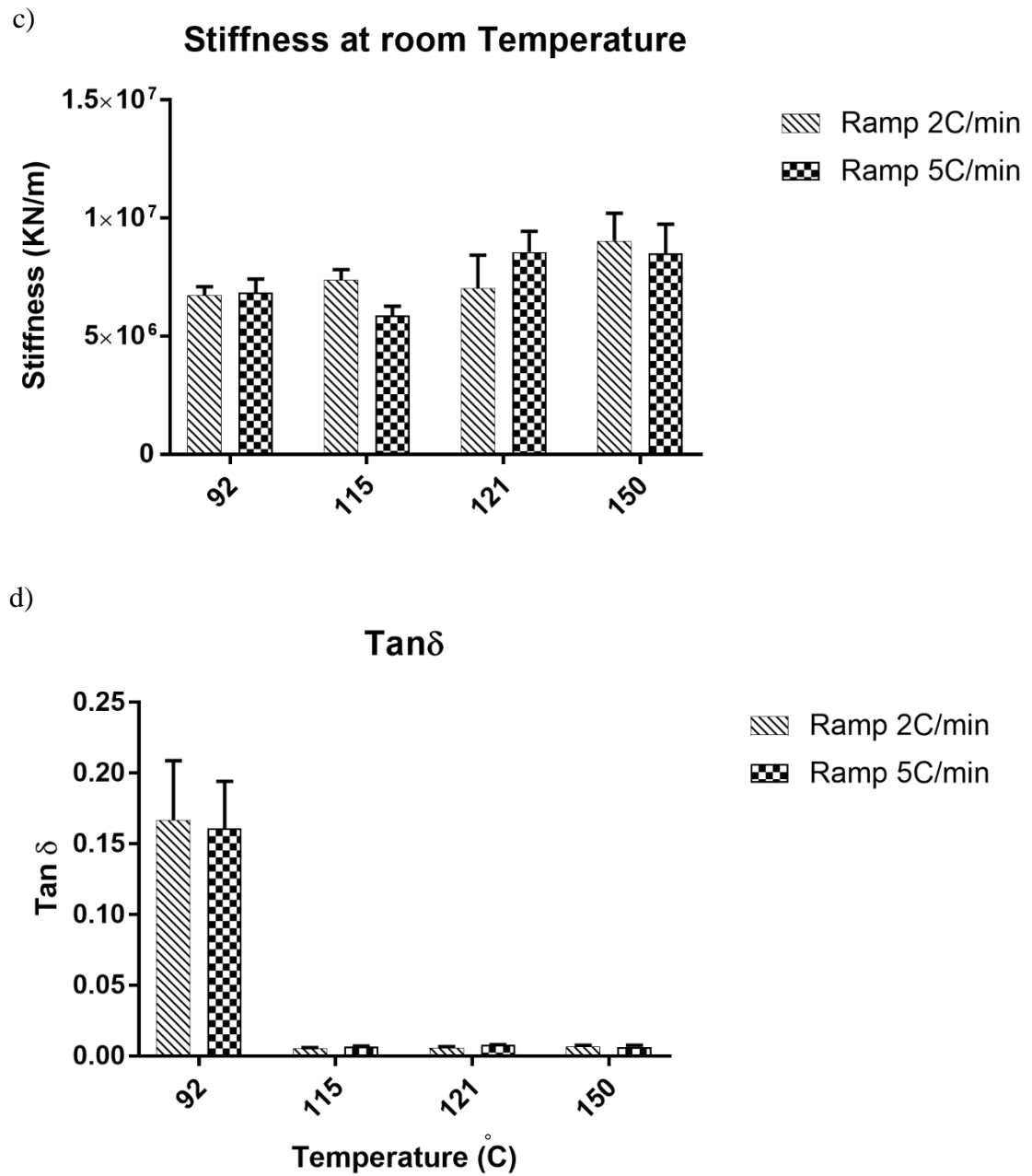


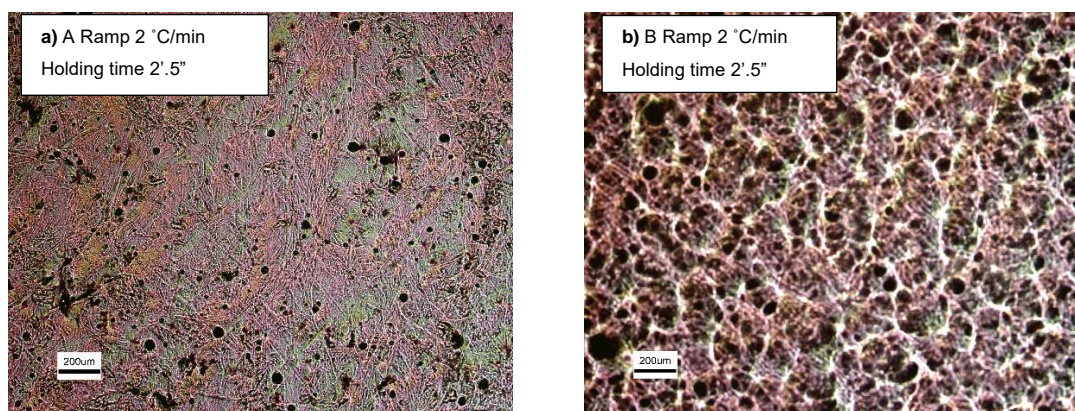
Figure 2.16: DMA results for type B preregs cured in lab scale. a) Storage Modulus, b) Loss modulus, c) Stiffness and d) Tan δ .

2.4.7 Optical Microscopic figures for both types of prepregs

The core free samples, regardless of their type, do not have regular surface defects such as pin holes. Weaker thermomechanical properties can occur along with the composition of fibers in one prepreg and as a result, can be a possible site for defect formation. The type B *hot melt* prepregs having a core were found to give more defects through the line of fiber configuration as in the interface, the adhesion bonding between honeycomb and carbon fiber is weaker compared to other tested prepregs, which may provide sites for voids and pinholes to occur. While testing the B *in solvent* prepregs with core they are less possibility for any voids and pinholes to occur along with the fiber line. As tested, A prepregs suffer from much larger defects, which act as voids and holes on the surface.

Our experiments suggest that the aluminum mold being used for sample preparation can cause different defects on the surface of the prepregs while curing. Therefore, the amount of releasing reagent being used, and the surface of each mold was monitored during each curing session.

Accordingly, the surface of both A and B prepregs were monitored. All the mentioned criteria were under controlled and as a result, the surface of each samples was examined considering all the DOE changeable parameters. Consequently, it is ideal to work with ramping rate $3^{\circ}\text{C}/\text{min}$ and holding time of 2 hours and 50 minutes preferably with type A as our candidate prepregs (Figure 2.17).



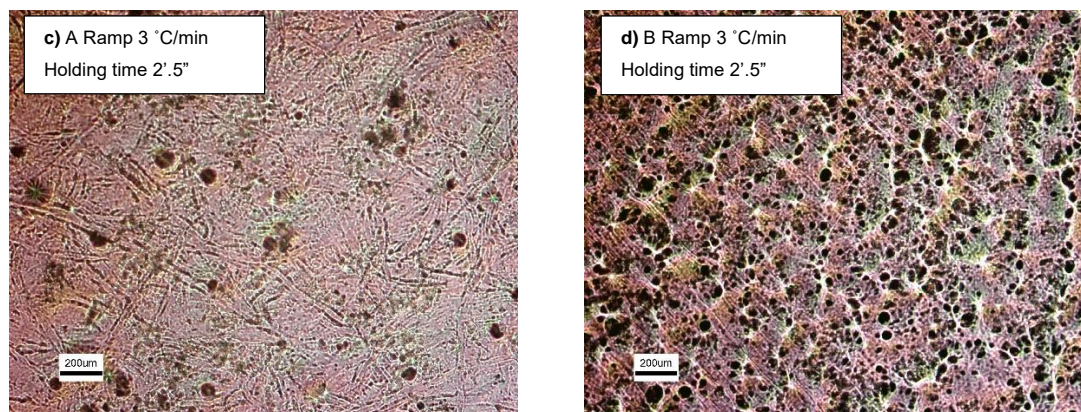


Figure 2.17: Optical Microscopic structure of both A and B preregs in different conditions: a) A with Ramp 2 °C/min, Holding time of 2 hours and 50 minutes. b) B with Ramp 2 °C/min, Holding time of 2 hours and 50 minutes. c) A with Ramp 3 °C/min, Holding time of 2 hours and 50 minutes. d) B with Ramp 3 °C/min, Holding time of 2 hours and 50 minutes.

Note that, as it is obvious in Figure 2.17, type B samples have severe voids and pinholes on the surface at lower ramps and start to have a uniform surface at higher ramps continuing to have negligible voids. Whereas, type A preregs would experience lower voids in general and most specifically, during the ramp of 3 °C/min and holding time of 2 hours and 50 minutes.

2.5 Summary

Both commercial preregs have pros and cons as mentioned earlier. As we increased the temperature the T_g point increased as well. At ramp 2 °C/min, by increasing the temperature both storage and loss modulus decreased. After the T_g point increased, using same samples at higher ramp (5 °C/min), the pattern is nearly the same with lower values. So, switching to a safer ramp (2.5– 3.5 °C/min) could be the best option so far.

To test this hypothesis later on, the central composite design as our design of experiment was being used. Having 4 parameters in the design for optimizing 4 responses resulted in running 40 tests. The evidence suggested that in order to have the best optimized conditions meaning maximized storage modulus, stiffness and $\tan \delta$ and minimized loss modulus our

parameters for the central composite design need to be at ramp 3°C/min, temperature 121 °C, holding time of 2 hours and 50 minutes after curing for both A and B prepregs Table 2.5.

All the contours and 3D plots for the statistical analysis section agree to the outcomes and according to the optical microscopic results, A samples have better uniformity and less holes by increasement of the ramp compared to B samples Figure 2.17.

At higher holding time the stiffness value for B samples are slightly more acceptable and practical compared to the values for A results shown in Figure 2.8& Figure 2.10. Using TGA and DSC devices, the type A sample shows better homogeneity (better adhesion between epoxy resin and carbon fiber) but weaker adhesion to Nomex honeycomb core, especially at current processing temperature (121 °C) or higher (150 °C), lowering the temperature seems slightly helpful but a tiny shoulder peak can be somewhat still noticeable.

All in all, it was understood that by increasing the ramp factor up to 3°C/min, type A prepregs have better thermomechanical performance and would experience less voids and pinholes on their surfaces. The probability of increasing the holding time after the curing process as one of the DOE variables would be covered within the rest of this dissertation. This could help to enhance the thermomechanical performance and lower the number of pinholes/ voids on the composite surfaces.

2.6 References

1. Centea, T., Grunenfelder, L.K. and Nutt, S.R.,, A review of out-of-autoclave prepregs–Material properties, process phenomena, and manufacturing considerations. . *Composites Part A: Applied Science and Manufacturing* **2015**, 70, 132-154.
2. Odom, M. G., Sweeney, C.B., Parviz, D., Sill, L.P., Saed, M.A. and Green, M.J., Rapid curing and additive manufacturing of thermoset systems using scanning microwave heating of carbon nanotube/epoxy composites. . *Carbon* **2017**, 120, 447-453.
3. Kausar, A., Rafique, I. and Muhammad, B., Aerospace application of polymer nanocomposite with carbon nanotube, graphite, graphene oxide, and nanoclay. . *Polymer-Plastics Technology and Engineering* **2017**, 56(13), 1438-1456.

4. Mahmood, I. A.; Shamukh, M. Z., Characteristics and properties of epoxy/polysulfide blend matrix reinforced by short carbon and glass fibers. *Al-Nahrain Journal for Engineering Sciences* **2017**, 20 (1), 80-87.
5. Liu, T.; Zhao, Z.; Tjiu, W. W.; Lv, J.; Wei, C., Preparation and characterization of epoxy nanocomposites containing surface-modified graphene oxide. *Journal of Applied Polymer Science* **2014**, 131 (9).
6. Chen, C., Li, Y., Gu, Y., Li, M. and Zhang, Z., Improvement in skin–core adhesion of multiwalled carbon nanotubes modified carbon fiber prepreg/Nomex honeycomb sandwich composites. *Journal of Reinforced Plastics and Composites* **2017**, 36(8), 608-618.
7. Hexcel *Hexply prepreg technology*; <http://www.hexcel.com/resources/selector-guides>, 2017.
8. Yong, A. X.; Sims, G. D.; Gnaniyah, S. J.; Ogin, S. L.; Smith, P. A., Heating rate effects on thermal analysis measurement of T_g in composite materials. *Advanced Manufacturing: Polymer & Composites Science* **2017**, 3 (2), 43-51.
9. ASTM, ASTM D, 4065-12: Standard practice for plastics: dynamic mechanical properties: determination and report of procedures. *ASTM International* **2001**.
10. software, D. E., T test experiment 2018
11. Mumin, M. A.; Akhter, K. F.; Oyeneye, O. O.; Xu, W. Z.; Charpentier, P. A., Supercritical fluid assisted dispersion of nano-silica encapsulated CdS/ZnS quantum dots in poly (ethylene-co-vinyl acetate) for solar harvesting films. *ACS Applied Nano Materials* **2018**, 1 (7), 3186-3195.
12. articles, M. what are response surface designs, central composite designs?
13. Grunenfelder, L.; Dills, A.; Centea, T.; Nutt, S., Effect of prepreg format on defect control in out-of-autoclave processing. *Composites Part A: Applied Science and Manufacturing* **2017**, 93, 88-99.
14. Sarrai, A.; Hanini, S.; Merzouk, N.; Tassalit, D.; Szabó, T.; Hernádi, K.; Nagy, L., Using central composite experimental design to optimize the degradation of tylosin from aqueous solution by photo-fenton reaction. *Materials* **2016**, 9 (6), 428.

15. Ahmadi, S.; Manteghian, M.; Kazemian, H.; Rohani, S.; Darian, J. T., Synthesis of silver nano catalyst by gel-casting using response surface methodology. *Powder technology* **2012**, 228, 163-170.
16. Zhou, Y., Hosur, M., Jeelani, S. and Mallick, P.K., Fabrication and characterization of carbon fiber reinforced clay/epoxy composite. *Journal of Materials Science* **2012**, 5002-5012.
17. Velmurugan, R.; Mohan, T., Epoxy-clay nanocomposites and hybrids: synthesis and characterization. *Journal of Reinforced Plastics and Composites* **2009**, 28 (1), 17-37.
18. Hosur, M.; Barua, R.; Zainuddin, S.; Kumar, A.; Trovillion, J.; Jeelani, S., Effect of processing techniques on the performance of Epoxy/MWCNT nanocomposites. *Journal of Applied Polymer Science* **2013**, 127 (6), 4211-4224.
19. Mravljak, M.; Sernek, M., The influence of curing temperature on rheological properties of epoxy adhesives. *Drvna industrija* **2011**, 62 (1), 19-25.
20. Michels, J., Sena-Cruz, J., Czaderski, C. and Motavalli, M.– In *Thermo-mechanical properties of commercially available epoxy resins for structural applications*, Third Conference on Smart Monitoring, Assessment and Rehabilitation: 2015, September.
21. Saba, N.; Jawaid, M.; Alothman, O. Y.; Paridah, M.; Hassan, A., Recent advances in epoxy resin, natural fiber-reinforced epoxy composites and their applications. *Journal of Reinforced Plastics and Composites* **2016**, 35 (6), 447-470.

Chapter 3

3 Improving and comparing the mechanical properties of two commercial prepregs by optimizing the carbon fiber- epoxy resin matrix composites

3.1 Abstract

By increasing the ramp factor up to 3°C/min, type A prepregs were found in the last Chapter to have better thermomechanical performance and less void and pinhole formation on their surfaces. In this chapter, the increase of holding time after the curing process as one of the DOE variables is examined as the second phase of the optimization. This could help to boost the thermomechanical performance and lower the number of pinholes/ voids on the composite surfaces.

Later, the mechanical properties of two commercial composite prepregs of interest were investigated for the manufacture rowing racing boats aiming carbon fiber- epoxy resin technology working with the two optimized conditions and the first initial condition that prepregs were cured in. The goals were to examine how to control the resin properties and curing temperature to improve adhesion, modulus of toughness and tensional strength. Developing an efficient curing process was required to enhance the curing characteristics and improve the mechanical properties. The initial curing conditions were examined following the two optimized steps for specific mechanical testing using an Instron device.

The results for the toughness modulus values suggest that among both type A and B prepregs, type B prepregs would have higher values. By increasing the ramp factor to 3°C/min, the toughness modulus decreased by 2% for both composites. The hardness test was also used to indicate that we were able to decrease voids and pinholes by switching the conditions from ramp 2°C/min and holding time of 2 hours and 50 to ramp 3°C/min while having the same holding time. Consequently, reaching the condition of ramp 3°C/min and holding time of 3 hours and 39 minutes made the prepregs more porous and burnt texture simultaneously.

Keywords

Adhesion bonding, Carbon fiber- epoxy resin, Composite prepregs, DMA, Instron, Ramp curing process, Modulus of toughness, Tensional strength, TGA.

3.2 Introduction

Improving the mechanical properties of composites is of tremendous interest in today's world. A composite material is a combination of two or more materials whose properties are different yet superior to the basic components¹. Carbon fibers are known to improve the mechanical performance of the composite, providing excellent stiffness and strength, as well as good thermomechanical, electrical and chemical properties, while having a tremendous weight savings over metals².

Due to the lower price of the carbon fibers compared to the other polymer fibers, these carbon fiber composites have been found suitable in automobile, aerospace industries as well as marine industry and sports applications³. Using the autoclave method and applying pressure during the process of the curing results in numerous defects and voids due to the excessive pressure force on the surface of samples within the curing process⁴. Therefore, the need for light weight composites has used both autoclave and out of autoclave (OoA) techniques be replaced by vacuum bagging only (VBO) using the oven curing method¹. While the autoclave technique involves complicated temperature or pressure control, the vacuum bagging oven curing method uses only resin impregnation into the carbon fibers which can result in less voids, producing complicated structures and overall production of the near neat shape components.

The main barrier coating materials that are suitable for the corrosive marine conditions are epoxy resins, which also provide reinforcement due to their high tensile strength and modulus as well as easy processing, good thermal resistance, chemical resistance and dimensional stability⁵⁻⁶.

Being firstly discovered in 1909, epoxy resins are defined as prepolymers having more than one epoxide group and low molecular weight⁷. As an important thermosetting resin, it can be hardened using numerous curing agents while the consumption of accelerators for making the process faster to some extent. The unique features within the process would be dependent on the exact proportion of the epoxy resin, the curing agents and the accelerators being used⁶⁻⁷.

Carbon fiber- reinforced polymers (CFRP), contain carbon fibers embedded in the epoxy resin thermosetting matrix. As a result, the prepreg is ready to lay up into the mold without any additional resin for the curing process ⁸.

According to the literature, the usage of carbon fibers helps boost the mechanical performance of the composites, providing excellent stiffness and strength, as well as good thermomechanical, electrical and chemical properties, while providing weight savings over metals ⁹ Due to the lower price of the carbon fibers compared to the glass or polymer fibers, such composites are ideally suited to the automobile, aerospace industry as well as marine industry and sports applications ¹⁰.

The interfacial properties between the mold and prepreg can also be one of the possible reasons for surface defects which can be solved by either: a) a longer vacuum holding times or b) longer holding periods after the process of curing. Comparing the mechanical properties of the prepregs would help in better understanding of their functions and in producing more defect- free surfaces.

In this research, the carbon fiber- reinforced polymer (CFRP), contain the carbon fiber embedded in the epoxy resin thermosetting matrix. As a result, the prepreg is ready to lay up into the mold without any additional resin for the curing process.

The possibility of having the second optimization phase for improving the mechanical properties of the prepregs and lowering the number of pinholes and voids was examined in this chapter. Considering the three critical conditions for curing prepregs as their commercial curing conditions, their mechanical performances were tested. Accompanying the initial curing condition of the prepregs (ramp 2°C/min, temperature of 121°C and holding time of 2 hours and 50 minutes), two optimized curing conditions using the design of the experiment (DOE) method were considered as three curing conditions were examined for this section of the thesis. For the optimized phases ramp 3°C/min, temperature of 121°C and accordingly holding times of 2 hours and 50 minutes and 3 hours and 39 minutes were used testing the mechanical properties using Instron machine and Hardness tests. Following the optical microscopy procedure, it became inevitable that increasing the ramp to 3°C/min and working with the holding time of 2 hours and 50

minutes resulted in cured- unburnt samples with the best mechanical property performances mostly for type A prepregs.

Enhancing the mechanical properties in carbon fiber-epoxy composites is a major challenge. Therefore, two commercial prepregs were compared with each other, in their specific curing conditions and glass transition points (T_g), using their initial and optimized circumstances to have the best enhanced mechanical properties and the lowest defect possible on their surfaces. For this research, type A and B prepregs were commercially available, providing unidirectional carbon fibers and bisphenol A thermosetting epoxy resins. A variety of mechanical tests from tensile to hardness and modulus of toughness tests are examined in order to help understand the role of resin and material supplier towards producing consistent high-performance racing shells. To do so, working with the lab scale cured prepregs of type A and B, the mechanical performances of each composites for reaching the voids-free and pinholes-free surfaces, while having the best mechanical function are provided.

Using the three curing circumstances and preparing a new batch of samples for monitoring their mechanical properties were the main aim of this chapter. The maximum tensile strength, the stress at that point, the extension at breaking point, the yield before breaking, the maximum load bearable by the samples, Young's modulus and hardness values were derived using an Instron and hardness devices to determine the performance of the prepregs.

3.3 Experimental objectives

In this chapter, our role in enhancing the mechanical properties of the carbon fiber reinforced with epoxy resin prepregs from different suppliers, type A and B, towards producing high-performance racing hulls is under examination.

3.3.1 Sample preparation

The vacuum bagging only (VBO) technique was used for preparing the samples. Note that, for this experiment, among the two types of preparation techniques, no Nomex honeycomb

core was used. Moreover, for assembling these commercial prepregs, our supplier VBO method was used, in the lab scale as shown in (Figure 3.1).

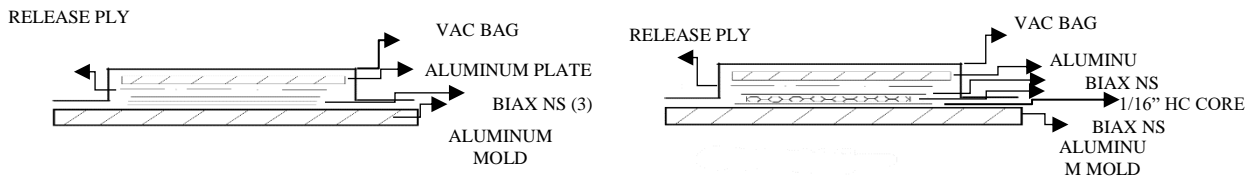


Figure 3.1: Assembly for curing Prepreg: a) without core (used for the samples of this research), b) with honeycomb core.

Consequently, with the VBO molding process using the oven curing cycle, both A and B prepregs were cured. Thermo/Lindberg/Blue M VO914C Laboratory Vacuum Oven was used for the curing process which can work at the temperature up to 200 °C. Later, the OMEGA CN7800 controller was installed for the oven helping the device to work by the ramp and soak mode (Figure 3.2).

a)



b)

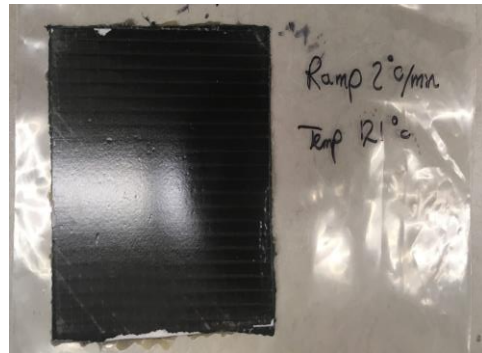


Figure 3.2: a) VBO technique using an oven and its controller b) Final cured prepreg product after using the VBO technique.

The procedure was then repeated using initial and two optimized curing conditions, meaning three layers of prepregs, specific type, were used for each sample preparation. A pair of (15*15 cm²) aluminum plates were employed to hold the samples together. To avoid the occurrence of air bubbles between the layers of the prepregs, the samples were maintained under constant 11 psi central vacuum line inside the oven to minimize air bubble formation⁴.

3.3.2 Methodology

3.3.2.1 Optimization condition using the central composite design phase II

The second phase of the optimization deals with higher holding time after the curing process compared to the first optimization phase. In other words, this section uses the same DOE variables with 40 runs for both A and B preregs while dealing with different limitations for the variables.

Consequently, the A and B samples were examined using a Nikon Eclipse L150 optical microscope for the occurrence of possible voids and pinholes focusing on the maximized holding time after the curing process. Optical microscopy was also used to compare both commercial matrix composites in their initial condition and their extreme holding time after the curing process condition.

3.3.2.2 Dynamic Mechanical Analysis (DMA)

To measure the mechanical properties of the carbon fiber epoxy systems, dynamic mechanical testing was performed using a Dynamic Mechanical Analysis (DMA) TA Q800 system with a single cantilever clamp according to ASTM D4065-12¹¹. All 36 sample bars were subjected to vibration at 1Hz with amplitude of 15 μm . The oven temperature ramps were from room temperature to 200°C using a ramp rate of 3 °C/min, while the force was measured using the applied 1 Hz frequency on one end while the other end of the samples are clamped and fixed.

3.3.2.3 Tensile tests using the Instron device

An Instron 5943 device was used for testing the tensile mechanical properties of the preregs. After running the DOE experiment meaning 4 parameters of ramp, temperature, holding time after the curing process and type of preregs and dealing with 4 response values of storage modulus, loss modulus, stiffness and $\text{Tan}\delta$, the optimization stage for the curing process three curing conditions were used for testing the tensile properties. By using the ASTM D3039/D3039M – 14 method for the tensile testing of the preregs, 5 samples were used for running each condition¹². Three layers of solid preregs with 90° as an angle

were layered on top of each other and after the curing process, a thin flat strip of material having a constant rectangular cross section was mounted in the grips of the mechanical testing machine (Instron), with the force loaded in tension. Correspondingly, the ultimate strength of the material was determined from the maximum force carried before failure¹³.

For all 30 samples tested using the tensile method, the same dimensions were used for each sample, i.e. length, width and thickness of each samples were 100.66mm, 6.04mm and 0.70 mm respectively.

This tensile testing used the strain control technique in which, greater extension means we are pulling the system quicker and in our case the extension value was 2.698 (mm/min) shown in Figure 3.3 . This is due to the samples being rigid, therefore in deformation rate control we don't have to pull them fast and can work with moderate speed.

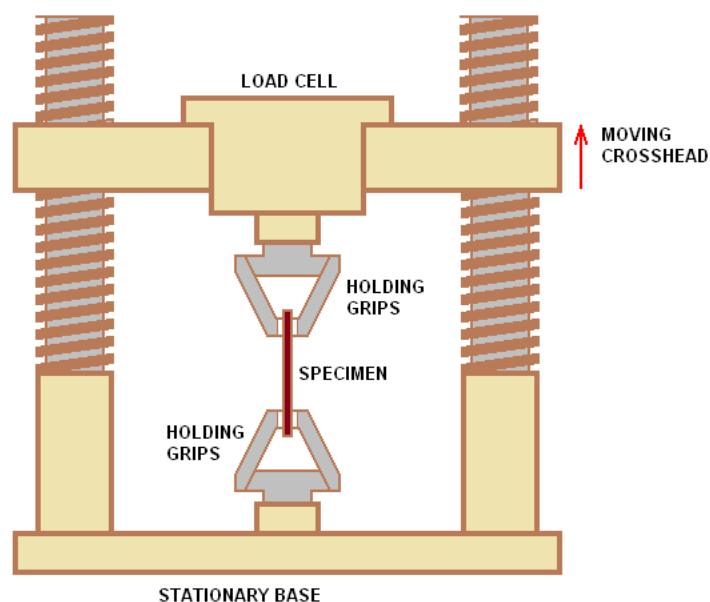


Figure 3.3. The extension technique for the prepreg composite bars using the Instron device¹⁴.

3.3.2.4 Thermal Gravimetric Analysis (TGA)

To determine the heat stability and relative epoxy resin/carbon fiber adhesion, the un-cured prepreg was heated to 700 °C at a ramping rate of 10°C/min in N₂ atmosphere, with a purge rate of 50mL/min using Thermogravimetric analysis (TGA) on TA Q600 system. For

assuring the resin and carbon fiber content, the second TGA batch was run using the same method.

3.3.2.5 Hardness technique

According to the E384 11E1ASTM method^{13, 15}, 3 samples were obtained using each curing condition and testing was performed on each surface 5X using different areas from the samples with a Buehler MicroMet 5100. Each part had to be mounted using a paraffin wax material so that they would be steady during the process of the hardness test.

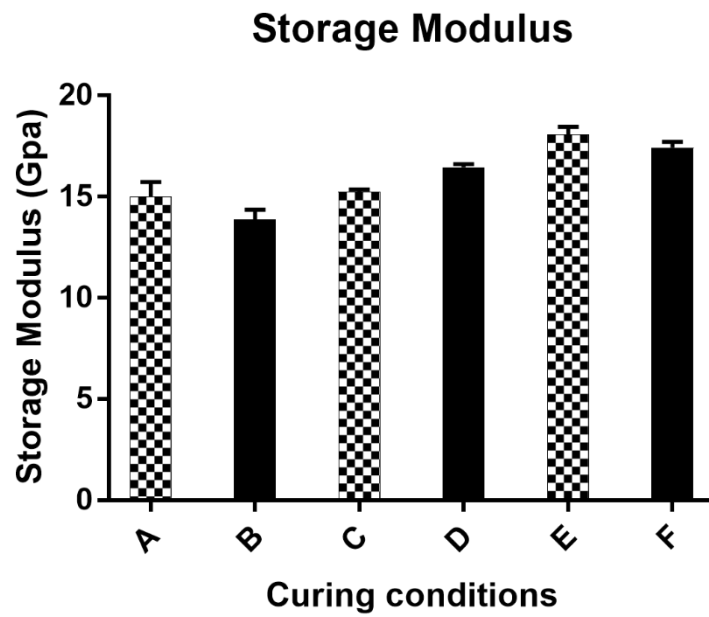
A square base pyramid shaped diamond was used for testing the hardness in the Vickers scale. Typically loads are very light, ranging from 10gm to 1kgf and for our case 50 gf was used as the proper load while having a magnification of 50x.

3.4 Results and discussion

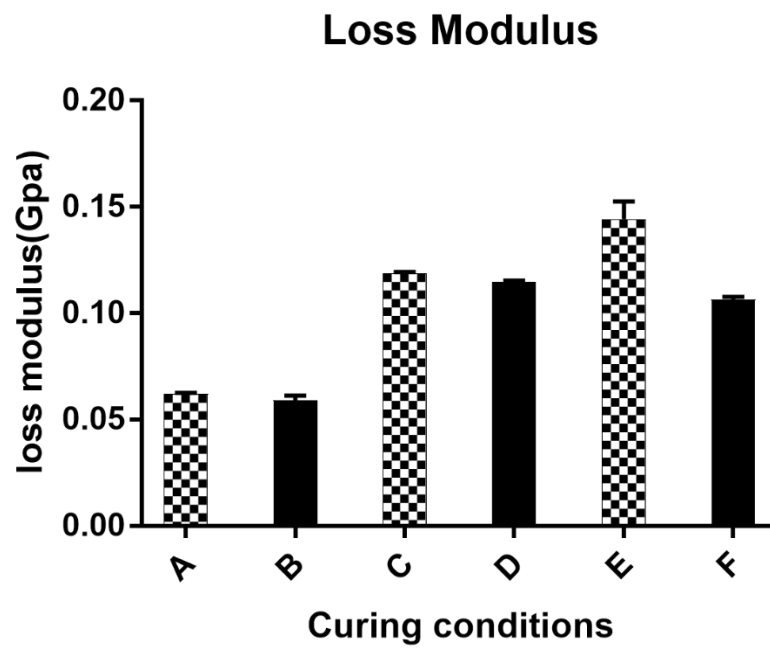
3.4.1 The Central composite design (CCD) as the DOE technique for the optimization condition

Using the CCD and maximizing the holding time after the curing process was found to enhance the mechanical properties of prepregs. Comparison of optimization phases and the initial curing condition are shown in Figure 3.4¹⁶.

a)



b)



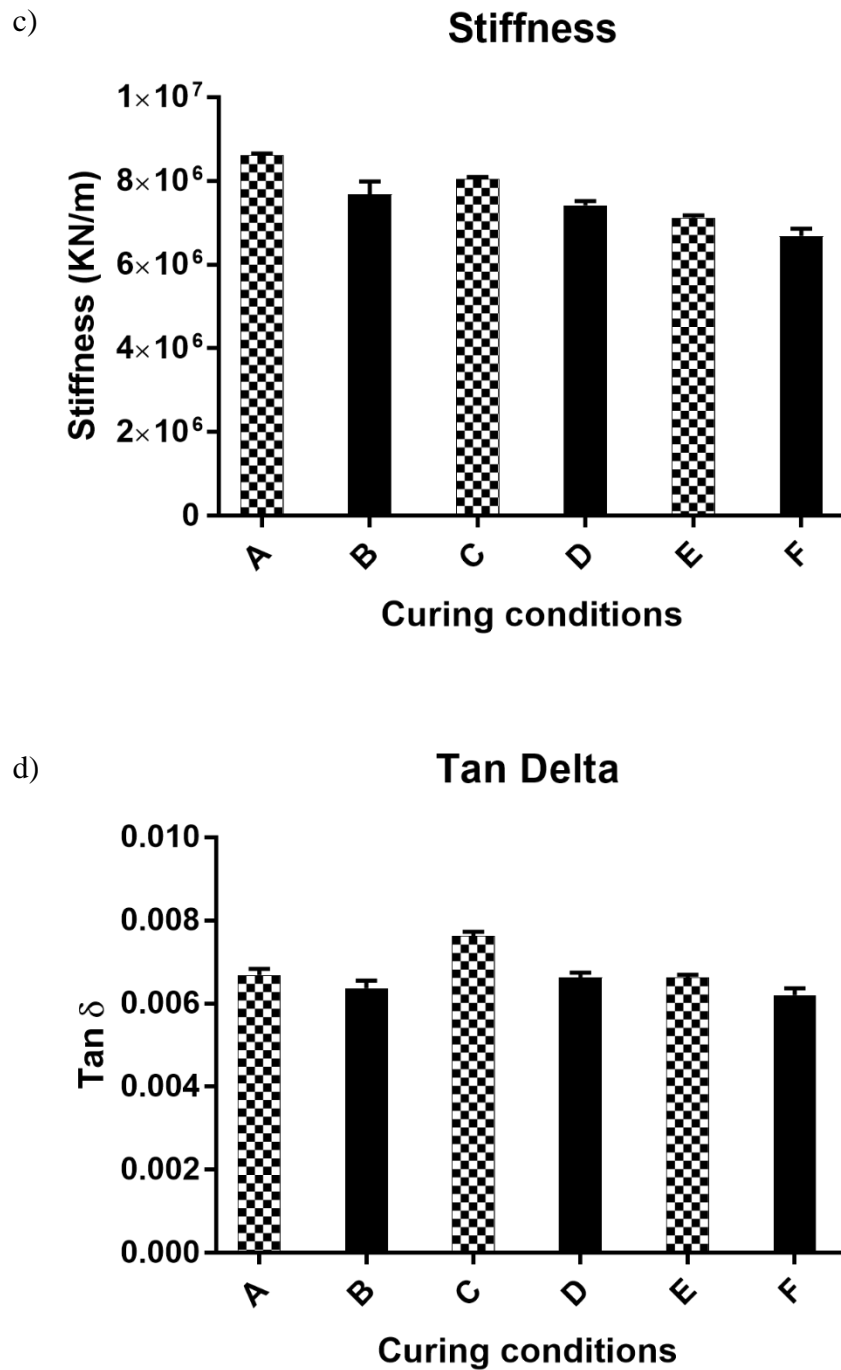


Figure 3.4: Rate of enhancement in mechanical properties by increasing the holding time after the curing process. In orders: A) Type A at initial point (Ramp at 2°C/min, Temp at 121°C, Holding time of 2 hours 50 minutes), B) Type B at initial point, C) Type A at optimum point (Ramp at 3°C/min, Temp 121 °C, Holding time of 2 hours 50 minutes), D)

Type B at optimum point, E) Type A with higher holding time (Ramp at 3°C/min, Temp at 121°C, Holding time of 7 hours), F) Type B with higher holding time.

As a result, the optimization was performed first using only the conditions that the industrial supplier wanted in their target values or in other words, optimal values. Later it was understood that by fixing all the factors in their target positions and maximizing the holding time after curing, the desirability of the optimum points for A samples would increase from 0.72 to 0.76. For the B samples, the desirability only slight decreased from 0.69 to 0.66.

3.4.1.1 The optimization phase part II

After running experimental 40 runs using the central composite method, the data was processed for the second phase of optimization. By increasing the holding period after the curing process as one of the parameters of the DOE design, the responses for the DMA device and mechanical properties were significantly enhanced ¹⁶.

The second phase of the DOE used the same four quadratic models that were fit to enhance the mechanical properties of the prepregs. First, three out of the four factors were set as target values while maximizing the holding time after the curing process, meaning we set the ramp at 3°C/min, temperature at 121°C. Both types of prepregs were maintained. Our goal was to find an optimum point with the best performance in mechanical properties which is having the maximized storage modulus, stiffness and Tan δ and minimized loss modulus at the same time Table 3.1 .

Table 3.1: Constraints on the second phase optimization using the central composite design.

Name	Low limit	Upper limit	Lower weight	Upper weight	Importance
Ramp (°C/min)	2	3	1	1	5
Temperature (°C)	121	138	1	1	3
Holding time (Hour)	2	3.39	1	1	5
Types of prepregs	A	B	1	1	3

Storage modulus (GPa)	12.44	18.71	1	1	4
Loss modulus (GPa)	0.11	0.13	1	1	3
Stiffness (KN/m)	5.33E+006	8.63E+006	1	1	3
Tan δ	6E-3	8.8E-3	1	1	4

It is obvious that the storage modulus, as the energy being stored at the elastic portion of the samples, should be at the highest level. However, the loss modulus, which represents the energy dissipated as heat in the viscous portion of the samples, should be at its lowest value⁴. Similarly, a polymer transformation from a hard-glassy material to a soft rubbery one, Tan δ value, should be at the highest value. These factors, along with the stiffness and toughness modulus of the preregs, are the critical aspects that would enhance the mechanical properties of the samples and are the reasons why we chose such limits for our responses⁴.

As a result, three of the responses (storage modulus, stiffness and Tan δ) should be maximized and the loss modulus should be minimized¹. Following the response surface design being used for the second time, 19 solutions were found considering the conditions for two combinations of categorical factor levels. However, only two of the conditions would be our practical solutions and will be used again for the tensile and adhesion bonding tests for further analysis Table 3.2.

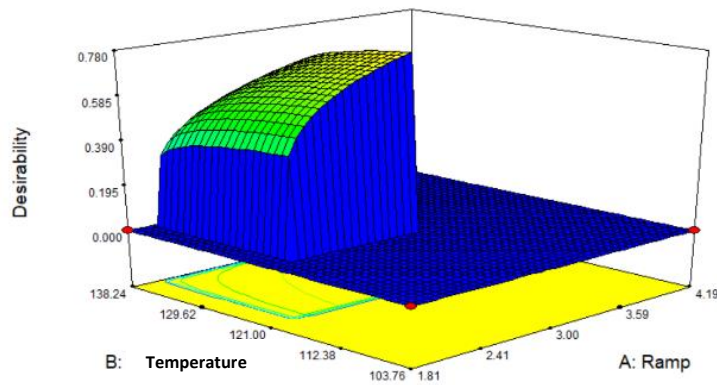
Table 3.2: Propriate solutions possible for central composite design optimum value for both types of A and B samples in the second phase optimization.

Num	Ramp (°C/min)	Temp (°C)	Holding time (Hour)	Types of preregs	Storage Modulus (GPa)	Loss Modulus (GPa)	Stiffness (GN/m)	Tan δ	Desirability
1	3	121	3.39	A	15.46	11.89E⁻²	8.26	7.7E⁻³	7.74E⁻¹
2	3	121	3.39	A	15.46	11.88E ⁻²	8.28	7.7E ⁻³	7.72E ⁻¹
3	3	121	3.37	A	15.44	11.89E ⁻²	8.27	7.7E ⁻³	7.7E ⁻¹
4	3	121	3.35	A	15.42	11.89E ⁻²	8.26	7.7E ⁻³	7.67E ⁻¹
5	3	124	3.39	A	15.43	11.8E ⁻²	8.30	7.7E ⁻³	7.63E ⁻¹
6	3	125	3.39	A	15.42	11.77E ⁻²	8.30	7.7E ⁻³	7.59E ⁻¹
7	3	121	3.26	A	15.34	11.88E ⁻²	8.23	7.7E ⁻³	7.53E ⁻¹
8	2.87	121	3.39	A	15.48	11.93E ⁻²	8.23	7.7E ⁻³	7.53E ⁻¹

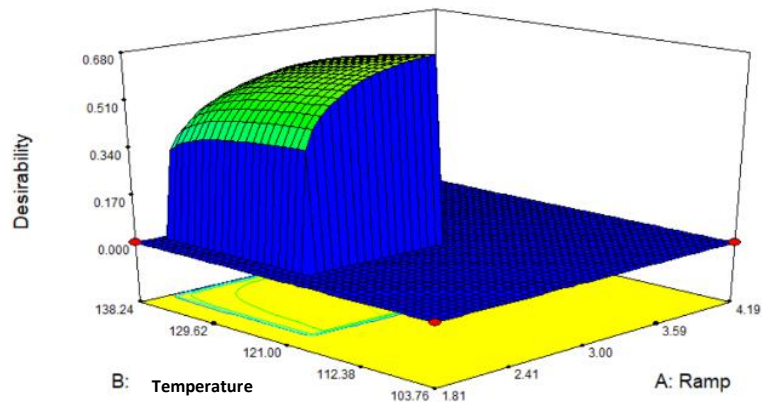
9	3	129	3.39	A	15.32	11.64E ⁻²	8.32	7.7E ⁻³	7.35E ⁻¹
10	3	130	3.39	A	15.29	11.61E ⁻²	8.32	7.7E ⁻³	7.28E ⁻¹
11	3	121	3.39	B	17.56	11.32E⁻²	7.38	6.4E⁻³	6.74E⁻¹
12	2.96	121	3.39	B	17.56	11.33E ⁻²	7.37	6.4E ⁻³	6.74E ⁻¹
13	3	121	3.36	B	17.53	11.33E ⁻²	7.39	6.4E ⁻³	6.73E ⁻¹
14	3	121	3.39	B	17.57	11.31E ⁻²	7.38	6.4E ⁻³	6.72E ⁻¹
15	2.9	121	3.38	B	17.53	11.35E ⁻²	7.37	6.5E ⁻³	6.70E ⁻¹
16	2.87	121	3.39	B	17.54	11.36E ⁻²	7.36	6.5E ⁻³	6.7E ⁻¹
17	3	121	3.21	B	17.37	11.37E ⁻²	7.38	6.5E ⁻³	6.64E ⁻¹
18	3	121	2.97	B	17.13	11.43E ⁻²	7.37	6.5E ⁻³	6.45E ⁻¹
19	3	121	2.90	B	17.06	11.45E ⁻²	7.36	6.6E ⁻³	6.38E ⁻¹

The 3D surfaces and 2D contour plots for the second optimum phase of this central composite design are also available. The results of the interactions between four independent variables and the two dependent variables are shown in (Figure 3.5), while two other dependent variables were kept constant¹⁷.

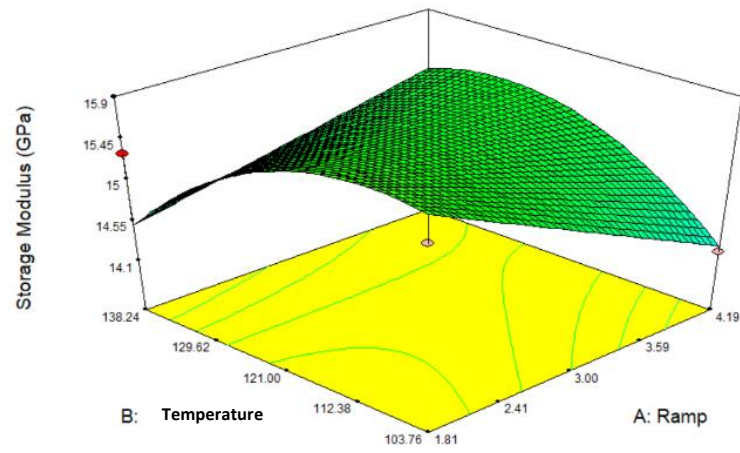
a)



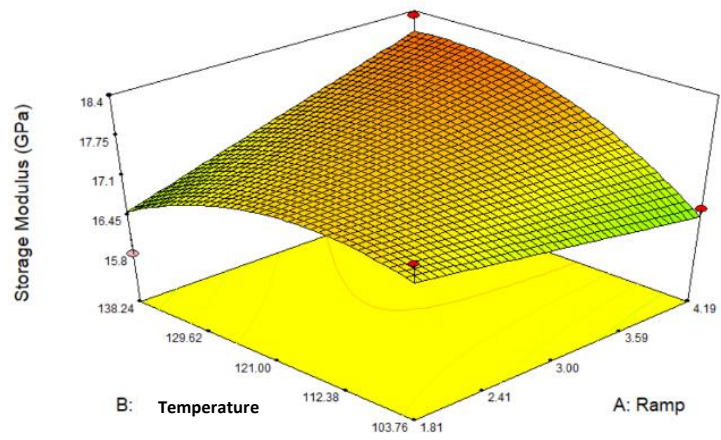
b)



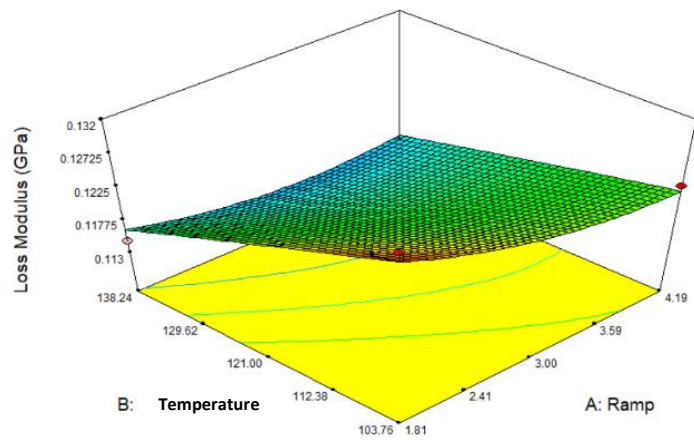
c)



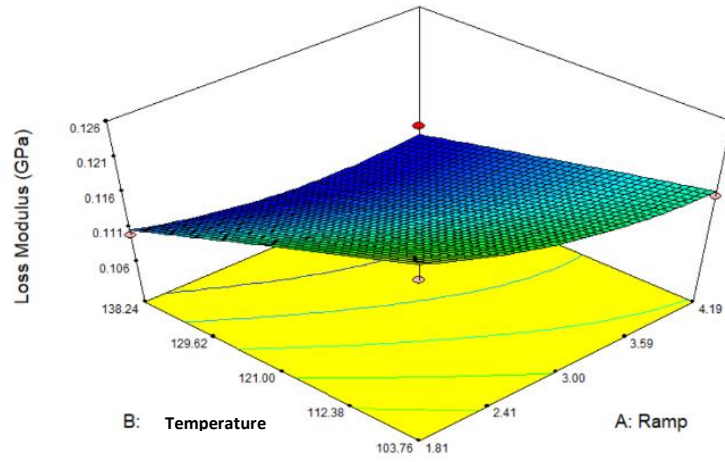
d)



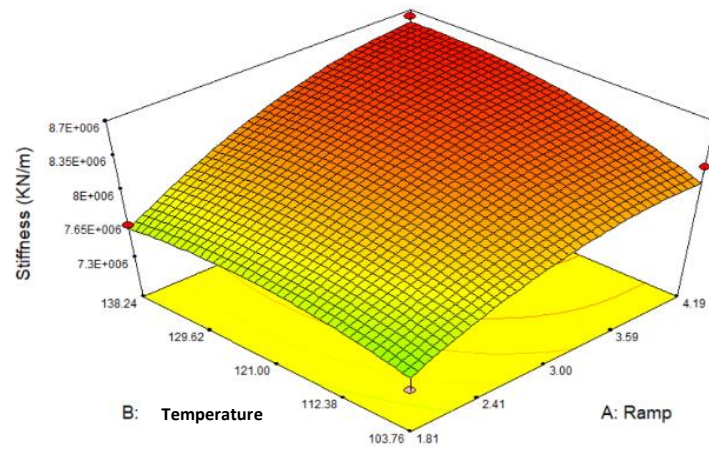
e)



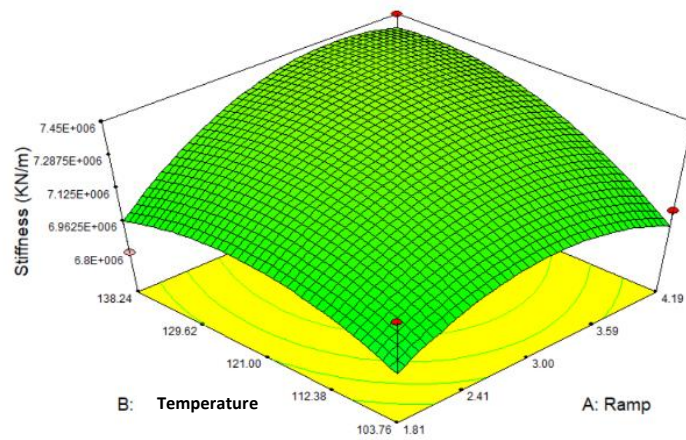
f)



g)



h)



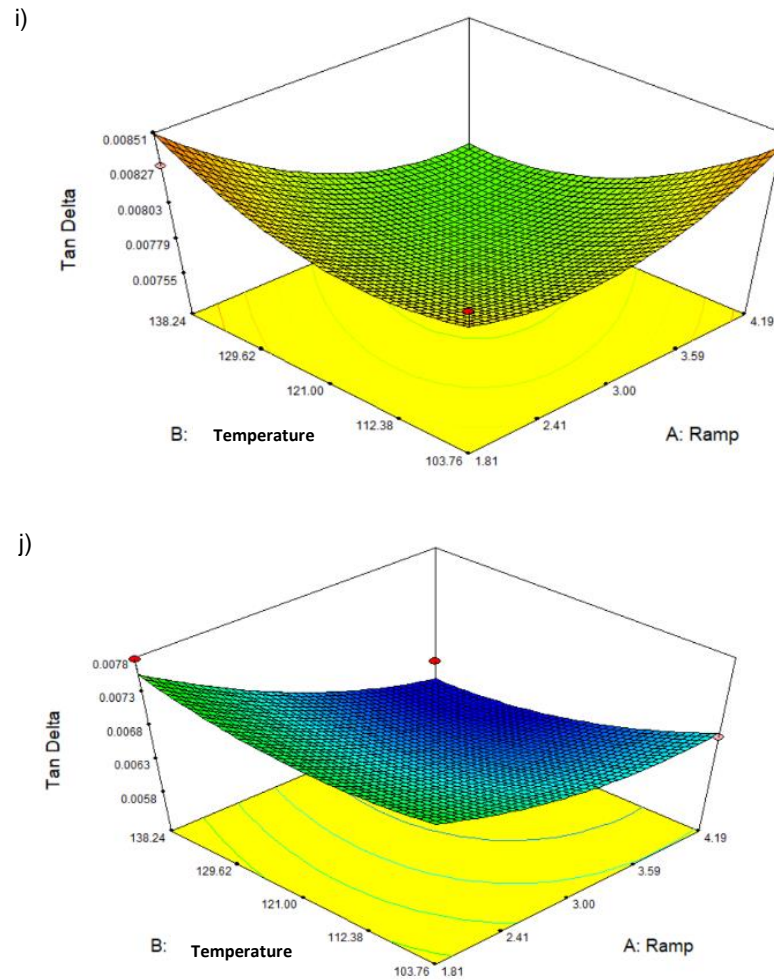


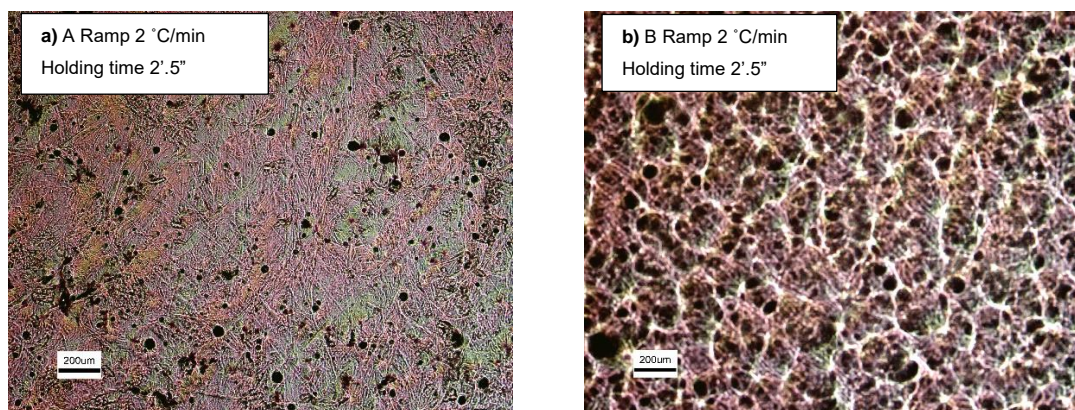
Figure 3.5: Optimization phase analysis part II: a) Desirability plot and contour in type A prepreg (Optimum point number 1), b) Desirability plot and contour in type B prepreg (Optimum point number 11th), c) Storage modulus plot and contour in type A prepreg (Optimum point number 1), d) Storage modulus plot and contour in type B prepreg (Optimum point number 11th), e) Loss modulus plot and contour in type A prepreg (Optimum point number 1), f) Loss modulus plot and contour in type B prepreg (Optimum point number 11th), g) Stiffness plot and contour in type A prepreg (Optimum point number 1), h) Stiffness plot and contour in type B prepreg (Optimum point number 11th), i) $\tan \delta$ plot and contour in type A prepreg (Optimum point number 1), j) $\tan \delta$ plot and contour in type B prepreg (Optimum point number 11th).

It is apparent from the above plots that even in the second phase of the optimization, the optimum value for the A prepreg shows a good improvement in its mechanical properties or in other words in enhancement of responses comparing to the B prepreg as in the eleventh(11th) optimum point shown in Table 3.2. However, only in the stiffness part, type B shows better qualities (showing with the green area rather than the red ones) but overall it would not change the fact that A prepreps are better candidates for industrial and lab scale usage in the curing process. Thus, maximizing the holding time after curing seems to increase the mechanical properties with a recognizable ratio and would not change the fact of using A prepreps instead of the B ones.

3.4.1.2 Optical microscopic figures using the optimization phase for both types of prepreps

It is understood that enhancing the holding time after the curing process could help eliminate pinholes on the surface to some extent. However, reaching 7 hours for the holding time would almost burn the sample and voids and pinholes would be more severe afterwards, while the stiffness of the sample would not be at its highest value. This phenomenon would also happen with the holding time of 3 hours and 39 minutes, second phase of optimization.

As shown in Figure 3.6, the two types of A and B prepreps after the curing process are shown by optical microscopy comparing 2 and 3°C/min as ramp rates and 2 hours and 50 minutes, 3 hours and 39 minutes and 7 hours as their holding time.



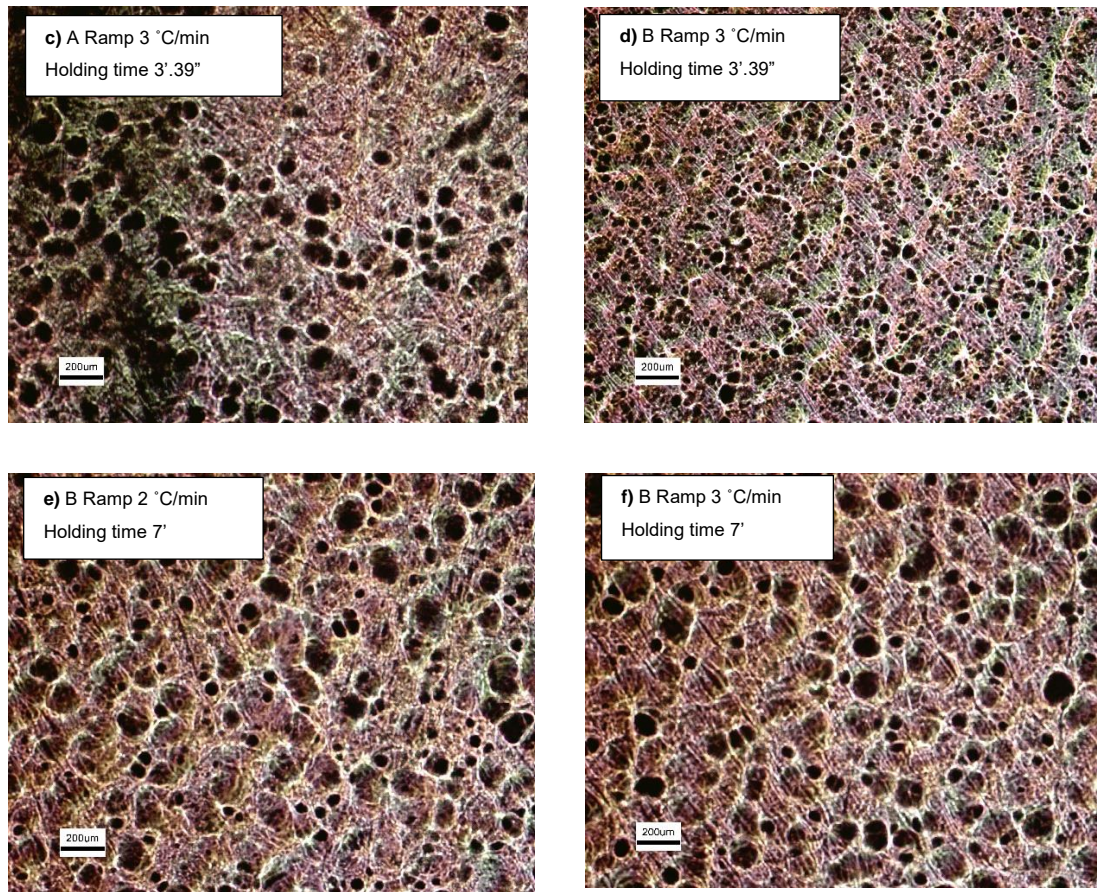


Figure 3.6: Optical Microscopic structure of both A and B preregs in different conditions: a) A with Ramp 2°C/min, Holding time of 2 hours and 50 minutes. b) B with Ramp 2°C/min, Holding time of 2 hours and 50 minutes. c) A with Ramp 3°C/min, Holding time of 3 hours and 39 minutes. d) B with Ramp 3°C/min, Holding time of 3 hours and 39 minutes. e) B with Ramp 2°C/min, Holding time of 7 hours. f) B with Ramp 3°C/min, Holding time of 7 hours.

Accordingly, by increasing the ramping rate to 3°C/min, the mechanical properties of the preregs were improved. However, having 3 hours and 39 minutes as the holding time after the curing process resulted in larger pinholes and more void formation on the surface of the samples. This can result in burnt composite structures and by reaching the extreme of 7 hours would cause severe burnt textures Figure 3.6.

3.4.2 Thermal gravimetry analysis (TGA) for both A and B prepregs indicating the mechanical behavior status of the composites

In this section after curing prepregs of both type A and B following three conditions of: ramp 2°C/min, temperature 121°C and holding time of 2 hours and 50 minutes after the curing process; ramp 3°C/min, temperature 121°C and holding time of 2 hours and 50 minutes and ramp 3°C/min, temperature of 121°C and holding time of 3 hours and 39 minutes, we examine the critical factors determining the tensile behavior of both type A and B prepregs.

Considering the T_g points derived from the DMA device, there is a special relationship between the performed curing temperature of each prepregs and their specific glass transition point that would make our samples either more viscous or brittle compared to each other. Using thermogravimetry analysis (TGA), the resin content before the curing process for type A was 40% whilst the B sample had 35% as the resin content which would make the amount of carbon fiber be higher in B samples rather than the type A ones, 65% and 60% respectively. As a result, we are expecting to have more brittle samples using the B type. To ensure the resin and carbon fiber content, the second TGA batch was run having similar results.

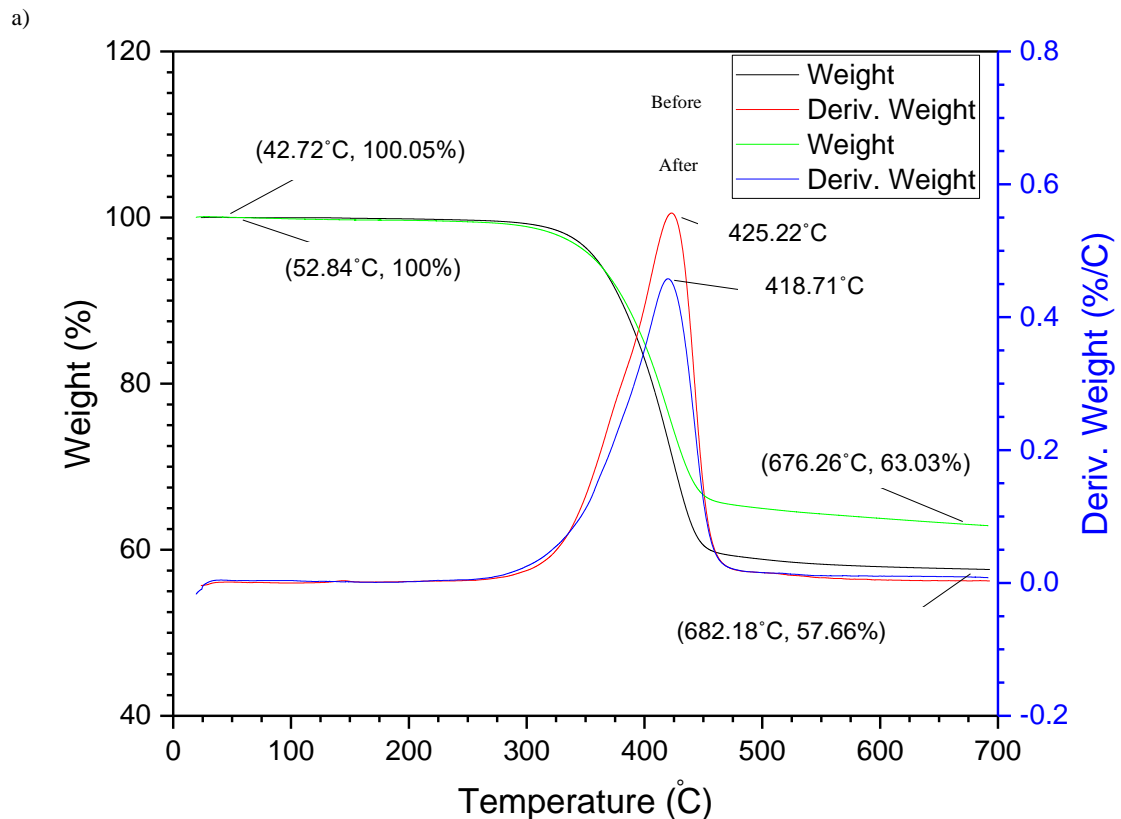
Note that out of 6 conditions for both types of prepregs, the higher holding time factor can make both types more brittle and burnt to some extent. As a result, the focus is comparing both ramps of 2 and 3°C/min by having the same onset curing temperature of 121°C and holding time of 2 hours and 50 minutes. Table 3.3 is addressing the conditions that each sample is facing as a result of the difference between their onset curing temperature and their glass transition points derived from the TGA device.

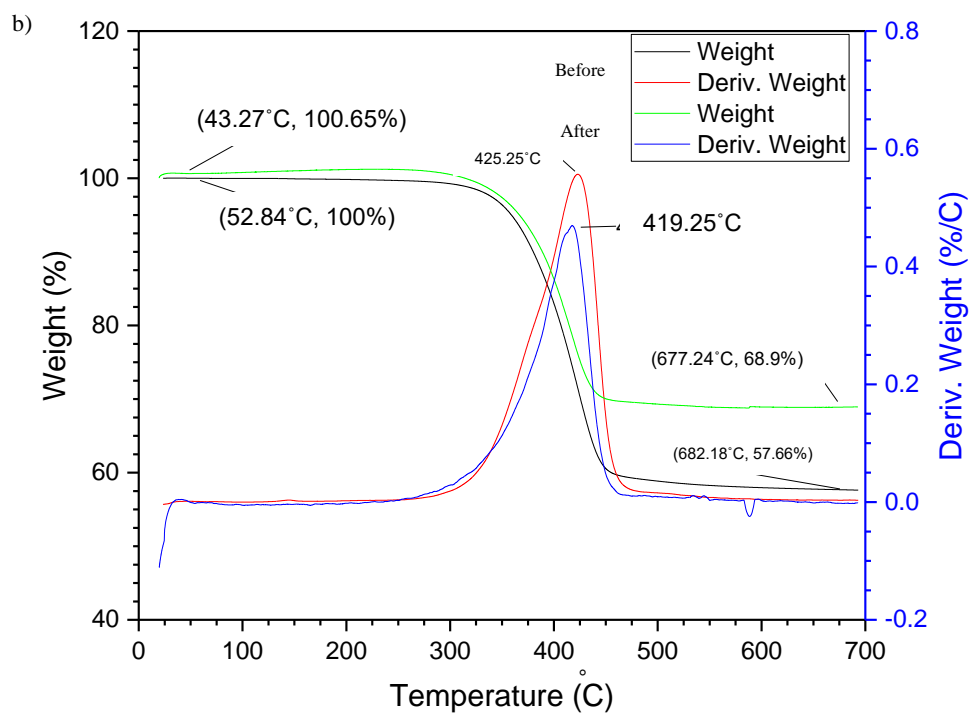
Table 3.3: Addressing types of the prepregs using special relationship between onset curing temperature and the glass transition temperature.

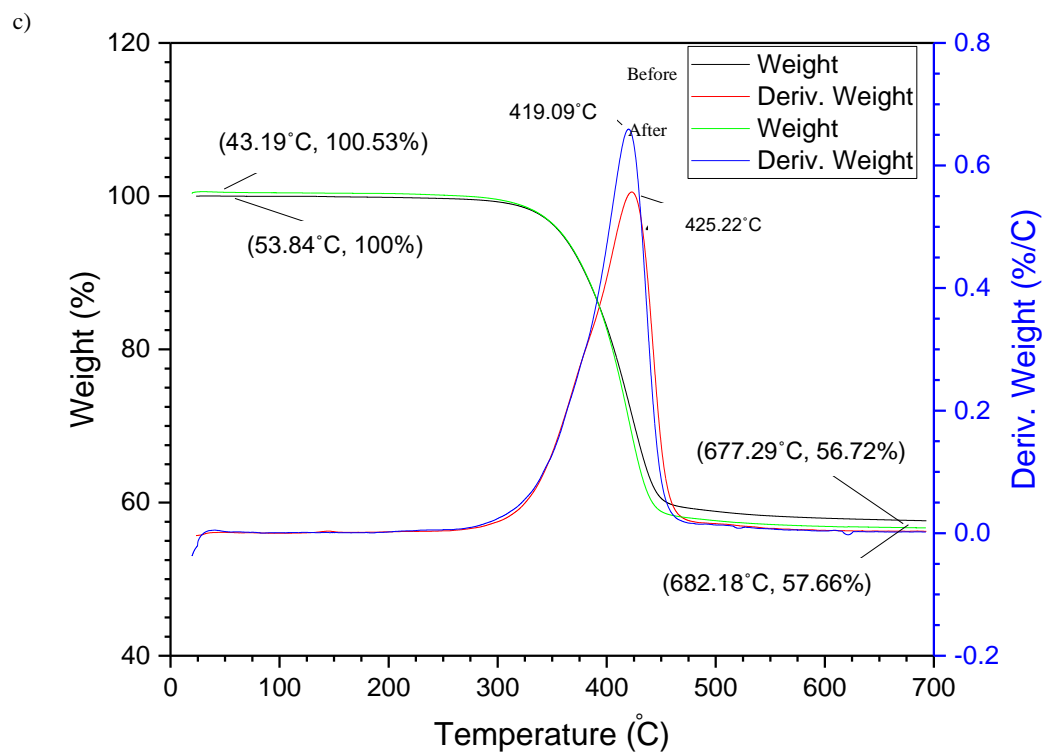
Ramp (°C/min)	Holding time (min)	Prepreg type	Performed curing temperature (T)(°C)	Glass transition temperature (T_g)(°C)	Relationship between the temperatures	Type of samples at that condition
2	170	A	121	105.10	$T > T_g$	More viscous

3	170	A	121	119.92	$T > T_g$	More viscous
3	219	A	121	110.96	$T > T_g$	Burnt
2	170	B	121	147.09	$T_g > T$	More Brittle
3	170	B	121	148.15	$T_g > T$	More Brittle
3	219	B	121	155.03	$T_g > T$	Burnt

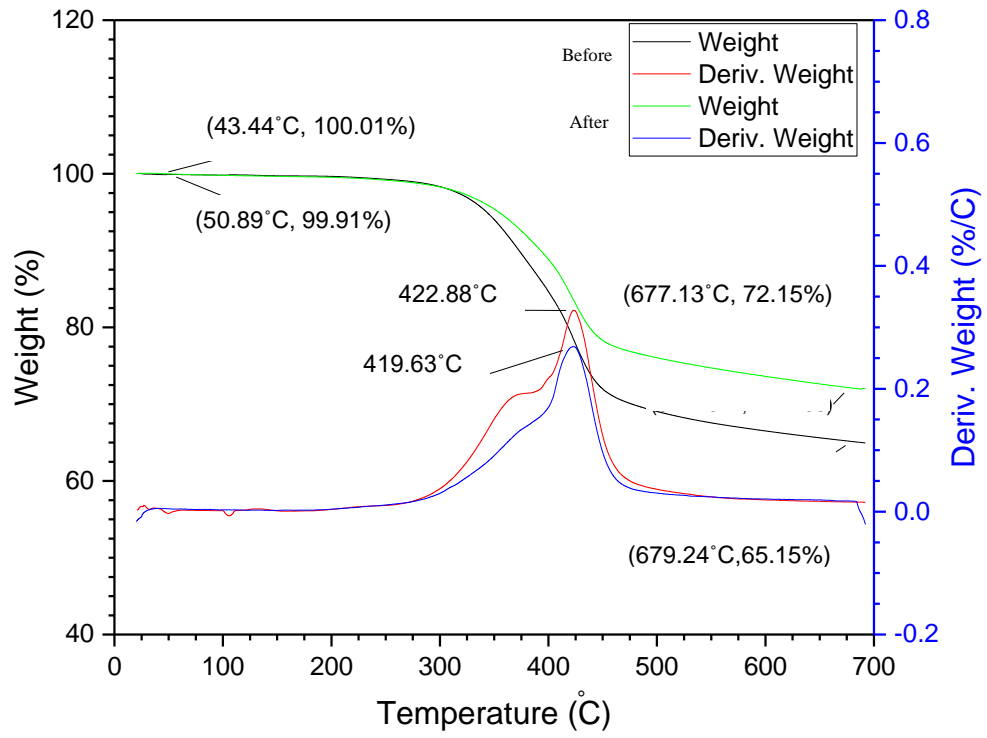
The TGA device was used to run tests for both types of the preregs before and after the curing process. Initially both type A and B preregs had respectively, 40% and 35% resin content which leads to the fact that the amount of carbon fiber for B samples would be 5% higher than the A ones as A and B contain 60% and 65% carbon fiber correspondingly. By overlapping results for each condition versus the initial condition the resin loss was found (Figure 3.7).



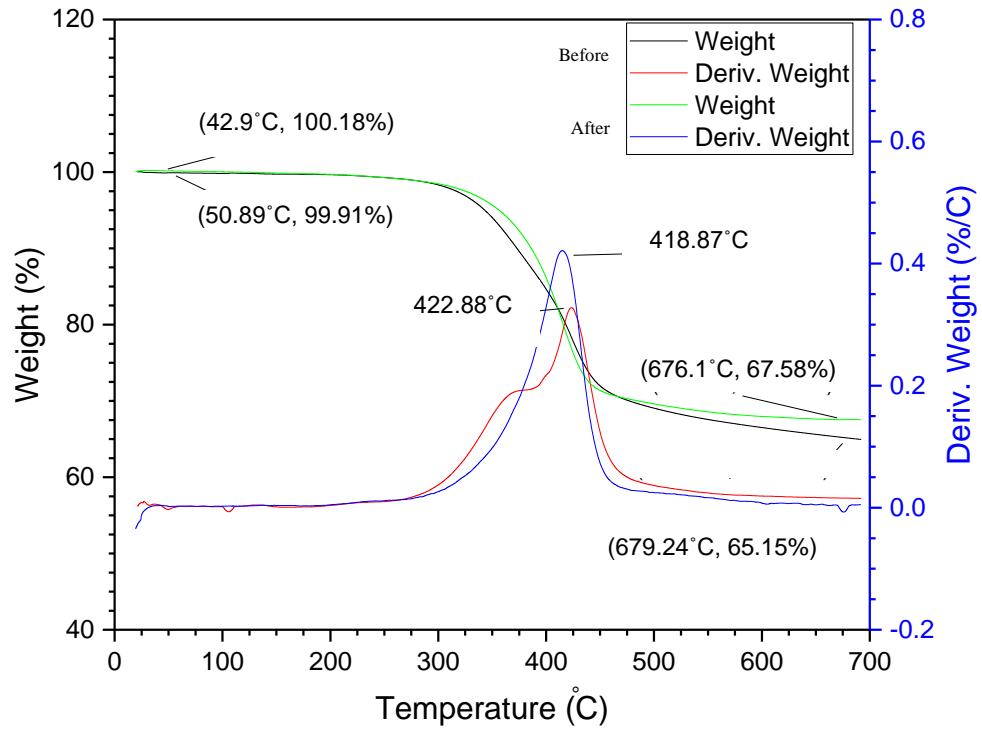




d)



e)



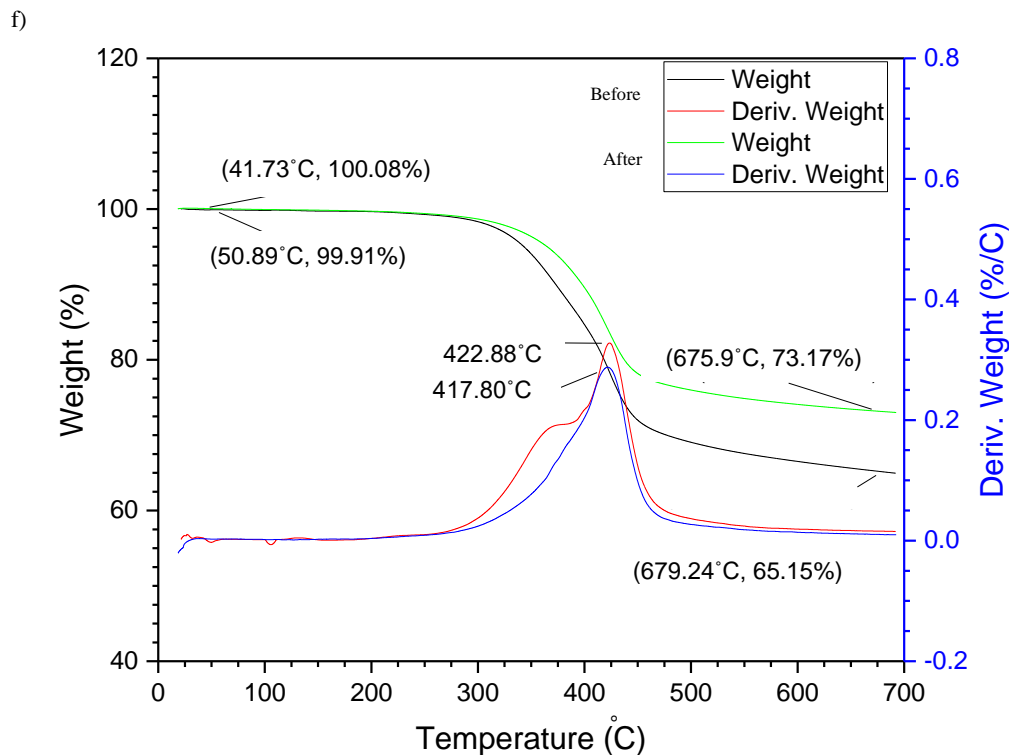
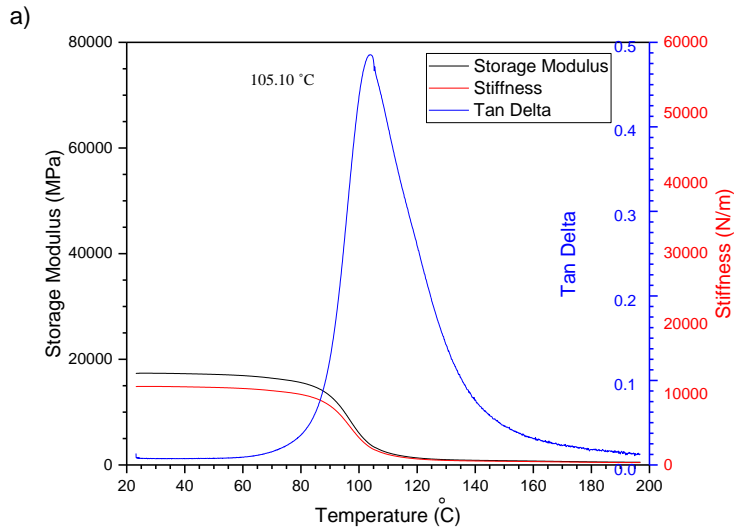


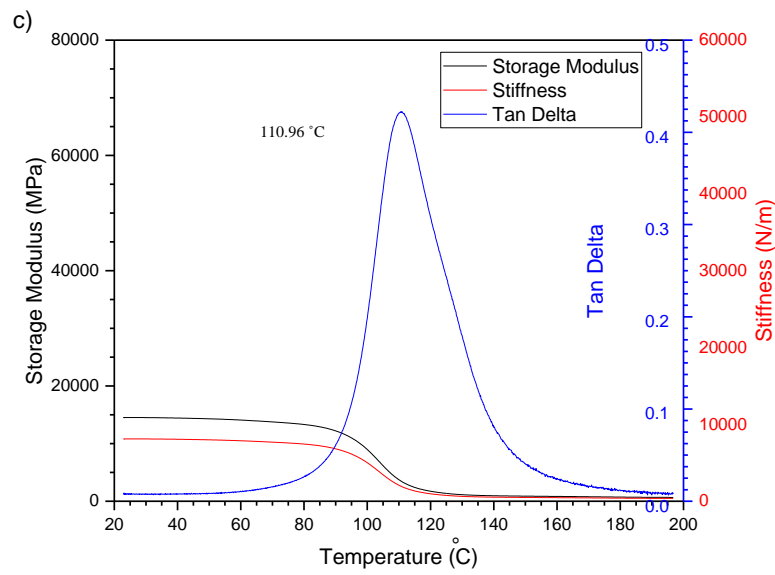
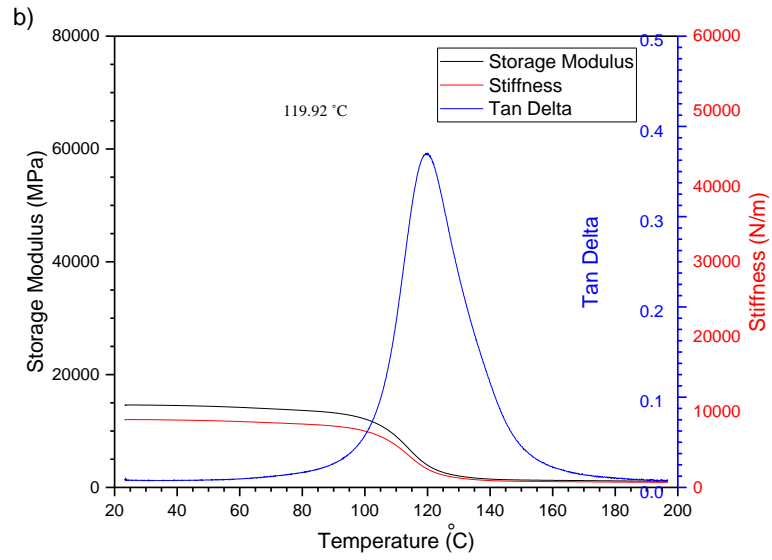
Figure 3.7: The TGA overlapping results before and after the curing process a) A sample, ramp 2°C/min, holding time 2 hours and 50 minutes, b) A sample, ramp 3°C/min, holding time 2 hours and 50 minutes, c) A sample, ramp 3°C/min, holding time 3 hours and 39 minutes, d) B sample, ramp 2°C/min, holding time 2 hours and 50 minutes, e) B sample, ramp 3°C/min, holding time 2 hours and 50 minutes, f) B sample, ramp 3°C/min, holding time 3 hours and 39 minutes.

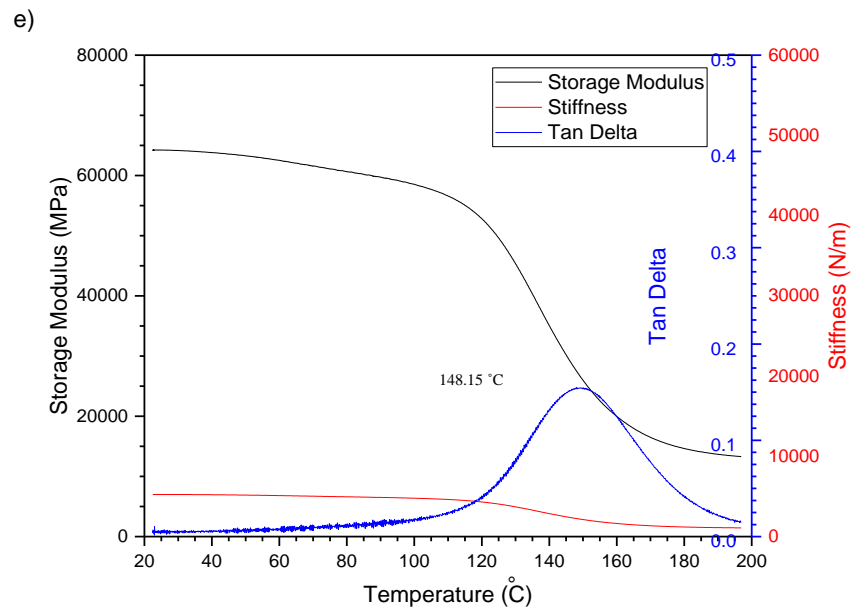
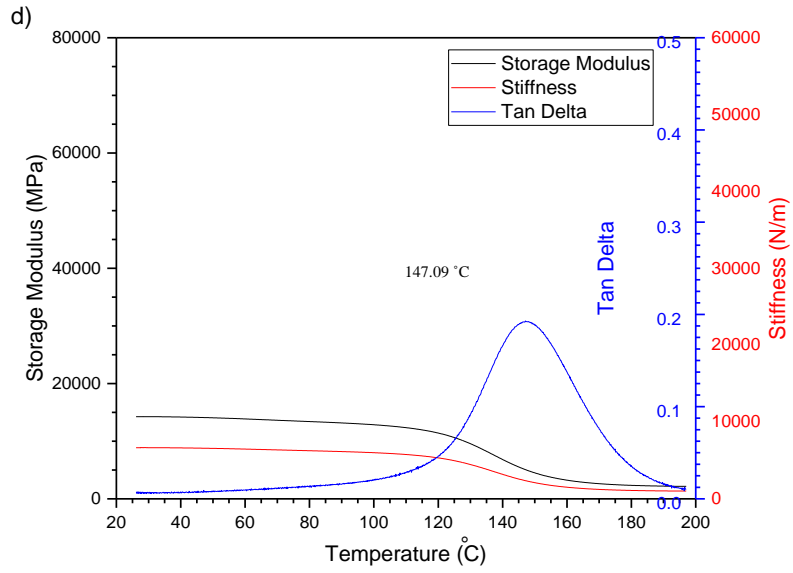
During the process of curing using each condition, the resin content did not change and was nearly the same as before the curing process as the values by the weight plot using TGA is showing close results in (Figure 3.7). Similar results were derived using the peak value of the derivative weight percentage plot, which also indicate that our resin content before and after the curing process are having the same results (Figure 3.7).

3.4.3 Glass transition point values using the (DMA)

Below are the glass transition point values derived from the DMA device. It is clear that by using peak value of the $\text{Tan } \delta$ plot, the T_g points can be determined (Figure 3.8). Comparing both type A and B preregs the T_g point for type B is higher not focusing on the ramping and the holding time after the curing process. This leads to better mechanical properties and better performance for type B samples as the transition temperature between the rigid phase and the rubbery phase is higher. For each prepreg type separately, the glass transition point at ramp $3^\circ\text{C}/\text{min}$ and holding time of 2 hours and 50 minutes are more reliable as the samples would not be burnt compared to the same ramp and holding time of 3 hours and 39 minutes (Figure 3.8).







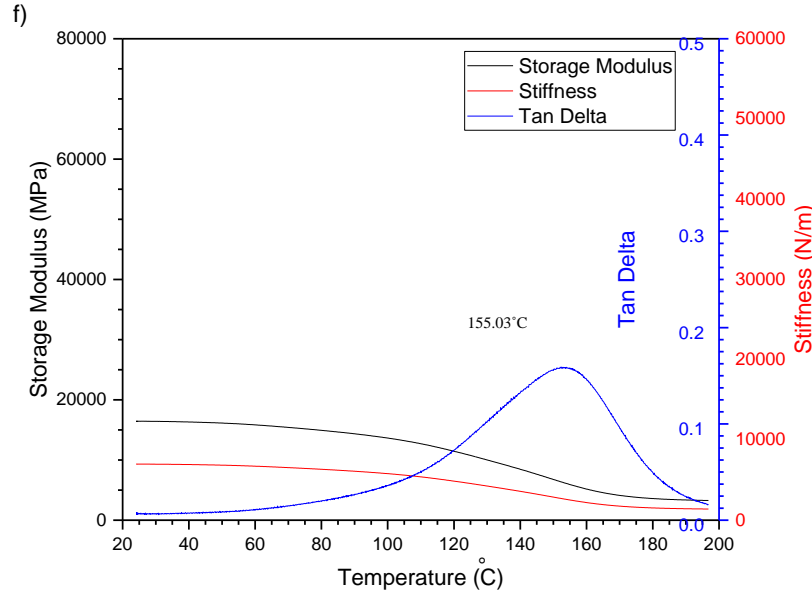


Figure 3.8: a) A sample Ramp $2^{\circ}\text{C}/\text{min}$, temperature 121°C , holding time 2 hours and 50 minutes, b) A sample Ramp $3^{\circ}\text{C}/\text{min}$, temperature 121°C , holding time 2 hours and 50 minutes, c) A sample Ramp $3^{\circ}\text{C}/\text{min}$, temperature 121°C , holding time of 3 hours and 39 minutes, d) B sample Ramp $2^{\circ}\text{C}/\text{min}$, temperature 121°C , holding time 2 hours and 50 minutes, e) B sample Ramp $3^{\circ}\text{C}/\text{min}$, temperature of 121°C , holding time 2 hours and 50 minutes, f) B sample Ramp $3^{\circ}\text{C}/\text{min}$, temperature 121°C , holding time 2 hours and 39 minutes.

The stress-strain curves were plotted for all the 6 initial and optimum conditions using the best values as shown in (Figure 3.9). As the plot shows, type B samples behave in a more brittle format due to having more carbon fiber in their structures. The elastic portion of the plot is longer for type A sample at ramp $3^{\circ}\text{C}/\text{min}$ and holding time of 2 hours and 50 minutes while B samples mostly at ramp $3^{\circ}\text{C}/\text{min}$ with the same holding time are the stiffest prepreg overall.

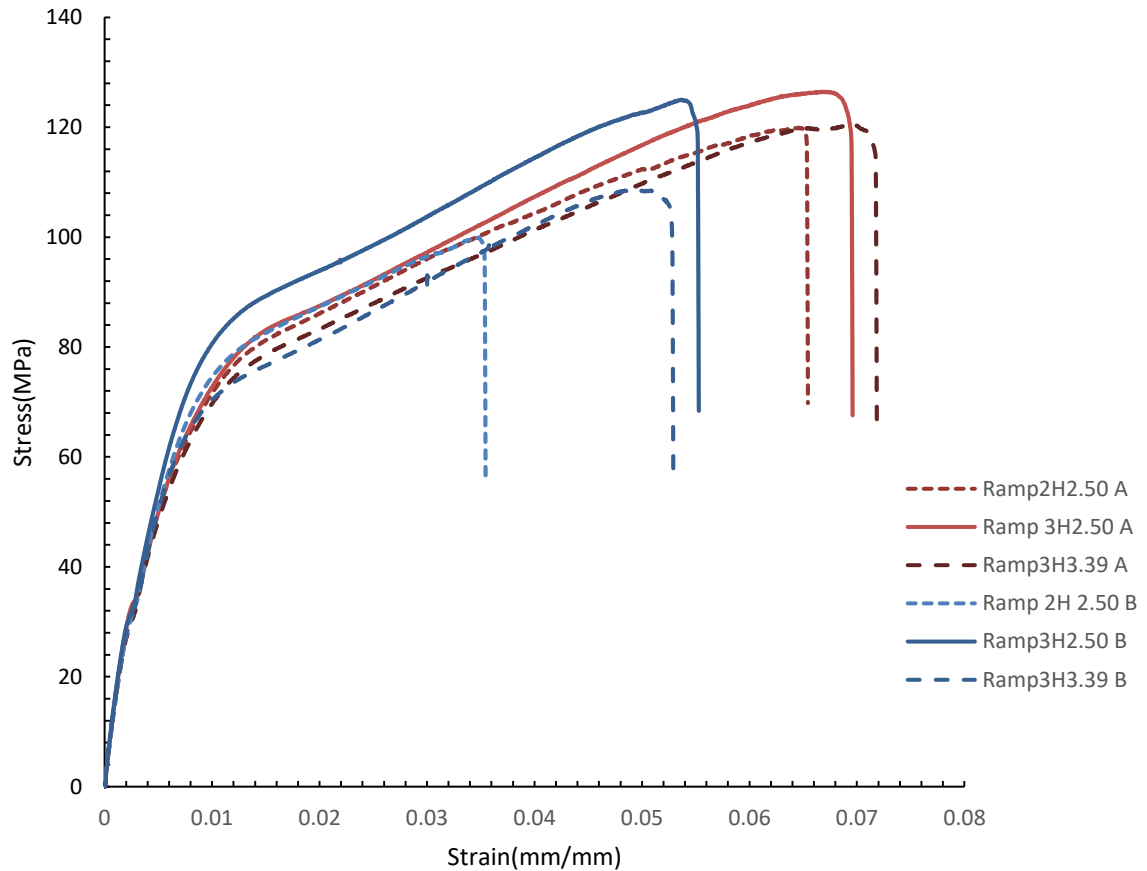


Figure 3.9: Stress-strain curves for preregs having both optimum and initial curing conditions with ramping rate of 2 and 3°C/min and holding time after the curing process value of 2 hours and 50 minutes and 3 hours and 39 minutes for both type A and B preregs.

3.4.4 Tensile Strength

Applying the same factor for both A and B preregs, the tensile strength values were determined using the Instron device with the average values of five samples plotted for each condition (Figure 3.10). Using the second TGA run for all six conditions, the resin loss was calculated for the preregs: a-Figure 3.10. This allowed us to measure the tensile strength and compare the results with the percentage of resin lost. However, as the bar charts are so close in values mostly for comparing preregs at holding time of 2 hours and 50 minutes and 3 hours and 39 minutes, we zoomed in and replotted the values in order to have an accurate conclusion b-Figure 3.10.

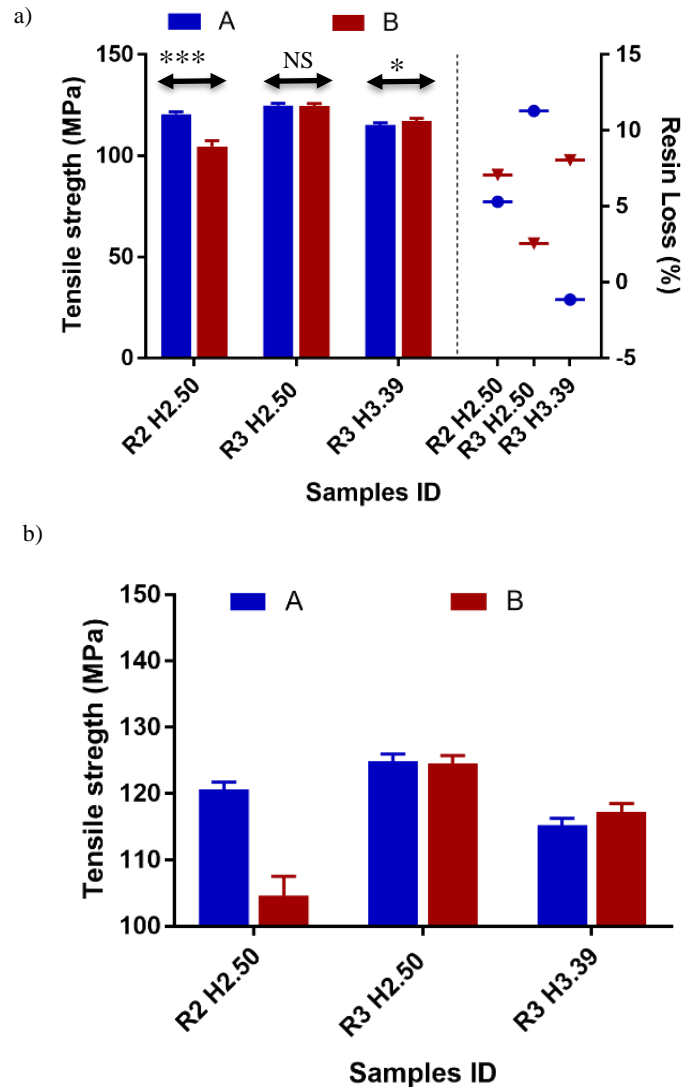


Figure 3.10: a) Tensile strength and percentage of the resin loss bar chart for both preregs considering initial and optimum conditions using Instron, b) Tensile strength zoomed in to accurately compare two preregs at same conditions using Instron.

As is evident from the tensile strength plot, by increasing the ramp to $3^{\circ}\text{C}/\text{min}$ and having the same holding time for the curing, the stress at break point is expected to increase. The tensile strength would increase to a higher extent while working with the A preregs at a ramp rate of $3^{\circ}\text{C}/\text{min}$ and holding time of 2 hours and 50 minutes, as they are having 68% of the carbon fiber content rather than B preregs with 69% of carbon fiber content after the curing process. The A preregs are more viscous after the curing compared to the more

brittle B samples, with the tensile strength values corroborating this. Comparing both of the preregs for higher holding time of 3 hours and 39 minutes while having the same ramp of 3°C/min, the samples would only burn so the tensile strength value for more brittle preregs would decrease to some extent.

In order to analyze the zoomed in plot accurately, a t-test was used to compare the values with each other as shown in Table 3.4. According to the literature, this method would be used for figuring out the difference between the means of two groups¹⁸.

Table 3.4: The t-test results for the tensile strength results using the Holm-Sidak method for the two types of preregs.

	Signif	P value	Mean1	Mean2	Diff	SE of diff	t ratio	DOF	Adj-p value	Status
R2H2.5	Yes	<0.0000 1	120.6	104.6	15.99	1.4	11.43	8	<0.00001	***
R3H2.5	No	0.56954	125	124.6	0.42	0.71	0.59	8	0.56954	NS
R3H3.39	Yes	0.02077	115.3	117.3	-2.04	0.71	2.87	8	0.04112	*

As the results indicate, both the initial and the last conditions give significant differences between the two type of preregs. Also, having the not significant results for ramp 3 °C/min and holding time of 2 hours and 50 minutes agrees to the fact that there is no special difference in using either of the preregs. Note that, while using the Holm-Sidak method, the alpha value was 0.05 and that each row was analyzed individually, without assuming a consistent SD¹⁹.

3.4.5 Elongation percentage to break

Both preregs were found to have better mechanical properties while performing at ramp 3°C/min and the holding time of 2 hours and 50 minutes. As a result, the ultimate elongation, which is the strain on a sample at break point, was found to increase. As the A samples have more resin content, compared to B ones, the elongation for such preregs would be higher by increasing the ramp and having the same holding time as the tensile

strength value. However, when increasing the holding time after curing at the same ramp value, the samples would become more brittle and the ultimate elongation value would decrease. Note that, there was a huge difference between the elongation of the break for both A and B prepregs at ramp $2^{\circ}\text{C}/\text{min}$ which is since type B samples were more brittle at first compared to the A samples and by increasing the ramp at same holding time, we could improve the mechanical properties of the prepregs (Figure 3.11).

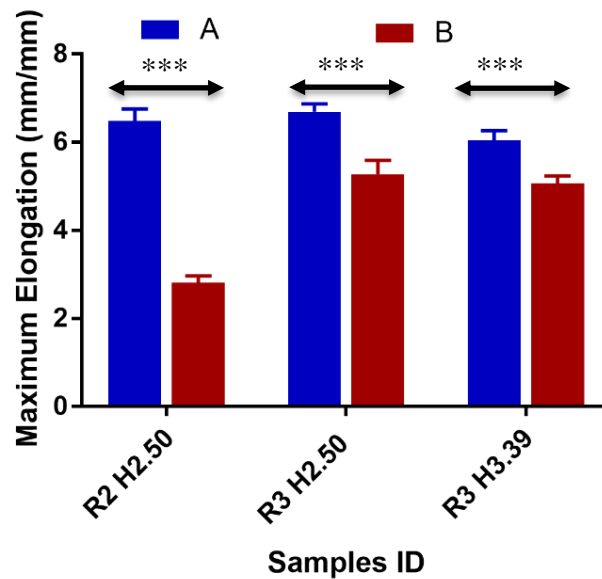


Figure 3.11: Elongation at break point for both A and B prepregs.

Using the same t-test method for the maximum elongation results, the bar charts show significant differences between the samples according to their means. Note that such differences are not due to chance. Therefore, the A prepregs have a higher maximum elongation and at the ramp $3^{\circ}\text{C}/\text{min}$ and holding time of 2 hours and 50 minutes both prepregs are experiencing the highest maximum elongation value Table 3.5.

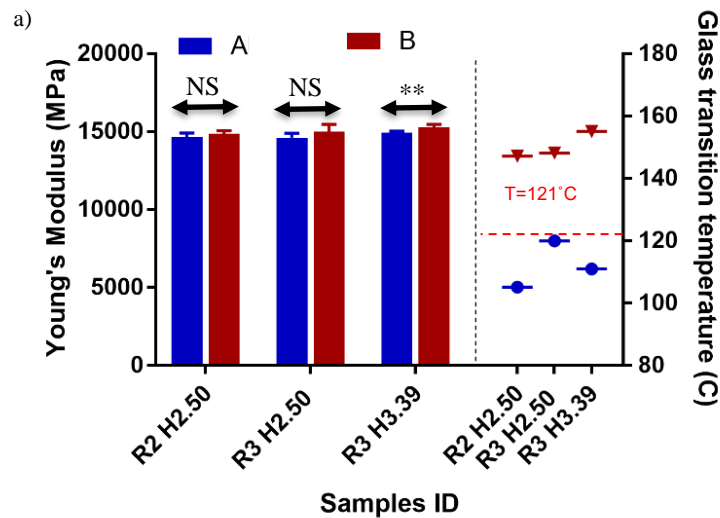
Table 3.5: The t-test results for the maximum elongation value using the Holm-Sidak method by the design expert software for the curing conditions using two types of prepregs.

Signif	P value	Mean1	Mean2	Diff	SE of diff	t ratio	DOF	Adj-p value	Status
--------	---------	-------	-------	------	------------	---------	-----	-------------	--------

R2H2.5	Yes	<0.00001	6.48	2.81	3.67	14.17E ⁻²	25.9	8	<0.00001	***
R3H2.5	Yes	0.00002	6.69	5.28	1.42	16.06E ⁻²	8.83	8	0.00004	***
R3H3.39	Yes	0.00005	6.05	5.07	0.97	12.3E ⁻²	7.91	8	0.00005	***

3.4.6 Young's Modulus

According to the results, type B prepregs have a higher Young's modulus compared to the A ones. This indicates that the higher carbon fiber content in the B prepregs leads to a higher Young's modulus and as a result greater stiffness. As this time, we are more focused on the carbon fiber content, the glass transition temperature was also measured using the DMA device, with the results given in a-Figure 3.12. The glass transition point (T_g) is where the polymer transitions from a hard-glassy material to a soft rubbery one; it is beneficial to have a look at the stiffness region of the materials while categorizing them as either brittle or viscous, recalling that polymers are visco-elastic. As the onset curing temperature was 121°C for both prepregs, the B samples having a higher carbon fiber content showed a more brittle texture compared to the viscous structure of the A samples. Considering the first stage of having the same holding time while improving the ramp to 3°C/min, the A prepregs have a lower Young's modulus value compared to the B samples. This is attributed to them being more viscous, and the ratio of the stress to strain is lower compared to the B prepregs in their more brittle manner b-Figure 3.12.



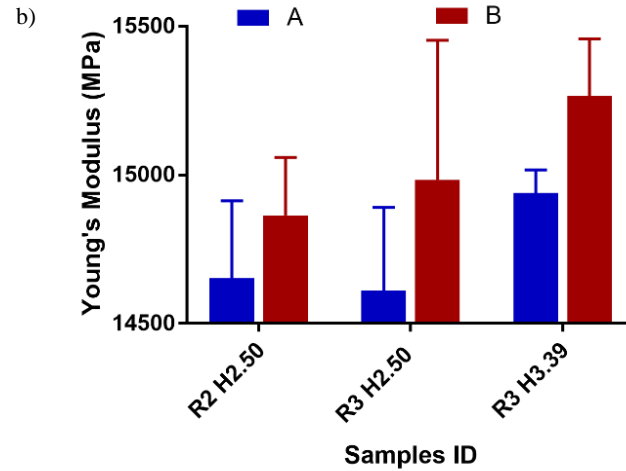


Figure 3.12: a) Young's modulus bar chart for both prepregs considering initial and optimum conditions using Instron, b) Young's modulus zoomed in, to accurately compare two prepregs at same conditions using Instron.

Finally, at the same ramp increasing the holding time would make both parties more brittle therefore, the young's modulus would increase but still the B samples would have higher values as their carbon fiber content is higher compared to the A prepregs.

Having a close difference between the two groups of prepregs, the t-test method was used to compare the differences of the means for each prepreg and whether such alterations were made by chance or not Table 3.6.

Table 3.6: The t-test results for the Young's modulus value using the Holm-Sidak method by the design expert software for the curing conditions using two types of prepregs.

	Signif	P value	Mean1	Mean2	Diff	SE of diff	t ratio	DOF	Adj-p value	Stat us
R2H2.5	No	0.1842	1.47E ⁴	1.49E ⁴	-211.7	145.6	1.45	8	0.3037	NS
R3H2.5	No	0.1653	1.46E ⁴	1.5E ⁴	-373.5	244.6	1.53	8	0.3037	NS
R3H3.39	Yes	0.00773	1.49E ⁴	1.52E ⁴	-326.3	92.43	3.53	8	0.023	**

Accordingly, having the first two curing conditions in the not significant manner show, there would be no difference for using either of the prepregs during the process of curing for both 2 and 3°C/min ramp values at the same holding time of 2 hours and 50 minutes. However, using a ramp rate of 3°C/min and having the 3 hours and 39 minutes as the holding time process of curing would make a good difference in the comparison of the means for two prepreg types and as the B samples are generally more brittle, they would be having a higher Young's modulus.

3.4.7 Modulus of toughness

The sample modulus of toughness was measured using the surface area under the stress vs the strain plot for each of the curing conditions as shown in (Figure 3.13).

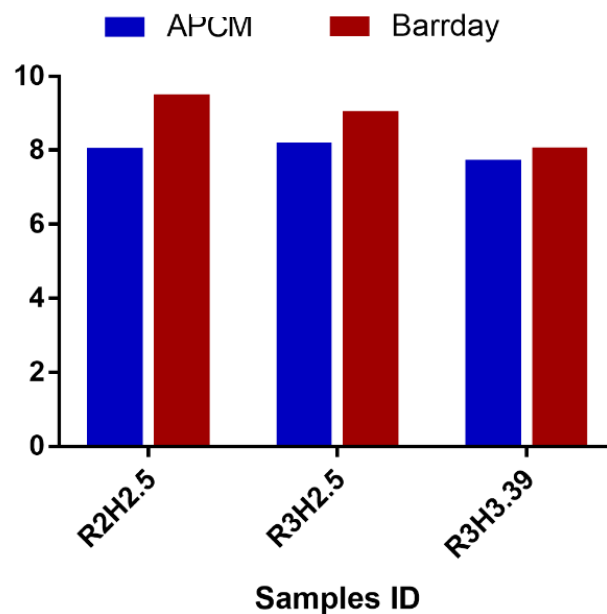


Figure 3.13: Toughness modulus for both type A and B prepregs using the surface area under the stress vs the strain plot.

It is evident that the amount of energy B samples can handle before their breakage point, is higher than the A samples due to the higher carbon fiber content. Therefore, the toughness modulus value for type B prepregs is higher. By increasing the ramp factor to 3°C/min, the modulus of toughness decreased slightly for both of the parties, meaning the

mechanical properties of the samples have improved as we were not looking for the highest toughness modulus overall. Not to mention that by increasing the holding time while having the same ramp, the toughness modulus just diminished due to having burnt samples.

3.4.8 Hardness

Using the aforementioned steps, type B samples have a higher hardness value compared to the A preregs. B samples are having smaller indentations and as a result are mostly harder. As type B samples have a greater carbon fiber content, their resistance toward the plastic deformation is larger. By increasing the ramp to 3°C/min, while having the same holding time, we found that the hardness could be increased for the A samples as well while having a slight decrease in the B type (Figure 3.14).

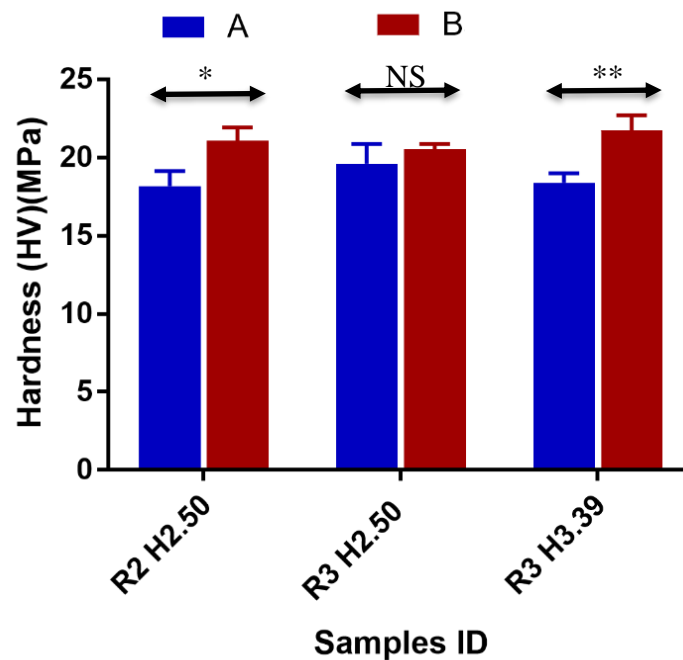


Figure 3.14: Hardness for both A and B type of preregs using the Buehler MicroMet 5100 series hardness device.

Hence, increasing the holding time to 3 hours and 39 minutes led to the samples burning a decrease in the hardness amount for both prepreg types occurred. Overall, the results show

that a ramp rate of 3°C/min and a holding time of 2 hours and 50 minutes made the performance of A samples more efficient.

As the results are close to each other, the t-test was run once again. As predicted earlier, during the ramp 2°C/min and holding time of 2 hours and 50 minutes, the means of the two types have significant differences with each other and the p-value for this step is lower than 0.05, meaning the hardness results in this stage are not made by chance. While increasing the ramp rate to 3°C/min at the same holding time is showing not big of a difference between the prepregs and confirming that such differences are made randomly. Finally, the enhancing of holding time to 3 hours and 39 minutes did bring differences and the p-value using this step is smaller than 0.01 Table 3.7.

Table 3.7: The t-test results for the hardness value using the Holm-Sidak method by the design expert software for the curing conditions using two types of prepregs.

	Signif	P value	Mean1	Mean2	Diff	SE of diff	t ration	DOF	Adi-p value	Status
R2H2.5	Yes	0.017	18.18	21.08	-2.9	0.74	3.912	4	0.034	*
R3H2.5	No	0.278	19.59	20.55	-0.97	0.77	1.253	4	0.278	NS
R3H3.39	Yes	0.007	18.38	21.77	-3.39	0.65	5.182	4	0.02	**

3.4.8.1 Optical microscopy figures using the hardness technique

By examining the different curing conditions using optical microscopy, the results show that the harder the surface the smaller is the indenter mark, with all samples giving a clear diamond shape on the surface of the samples. As shown in the figures at a ramp rate of 2°C/min and holding time of 2 hours and 50 minutes, the sample shows severe voids and pinholes on the surface as well and we could decrease the amount by improving the curing conditions to 3°C/min using the same holding time (Figure 3.15).

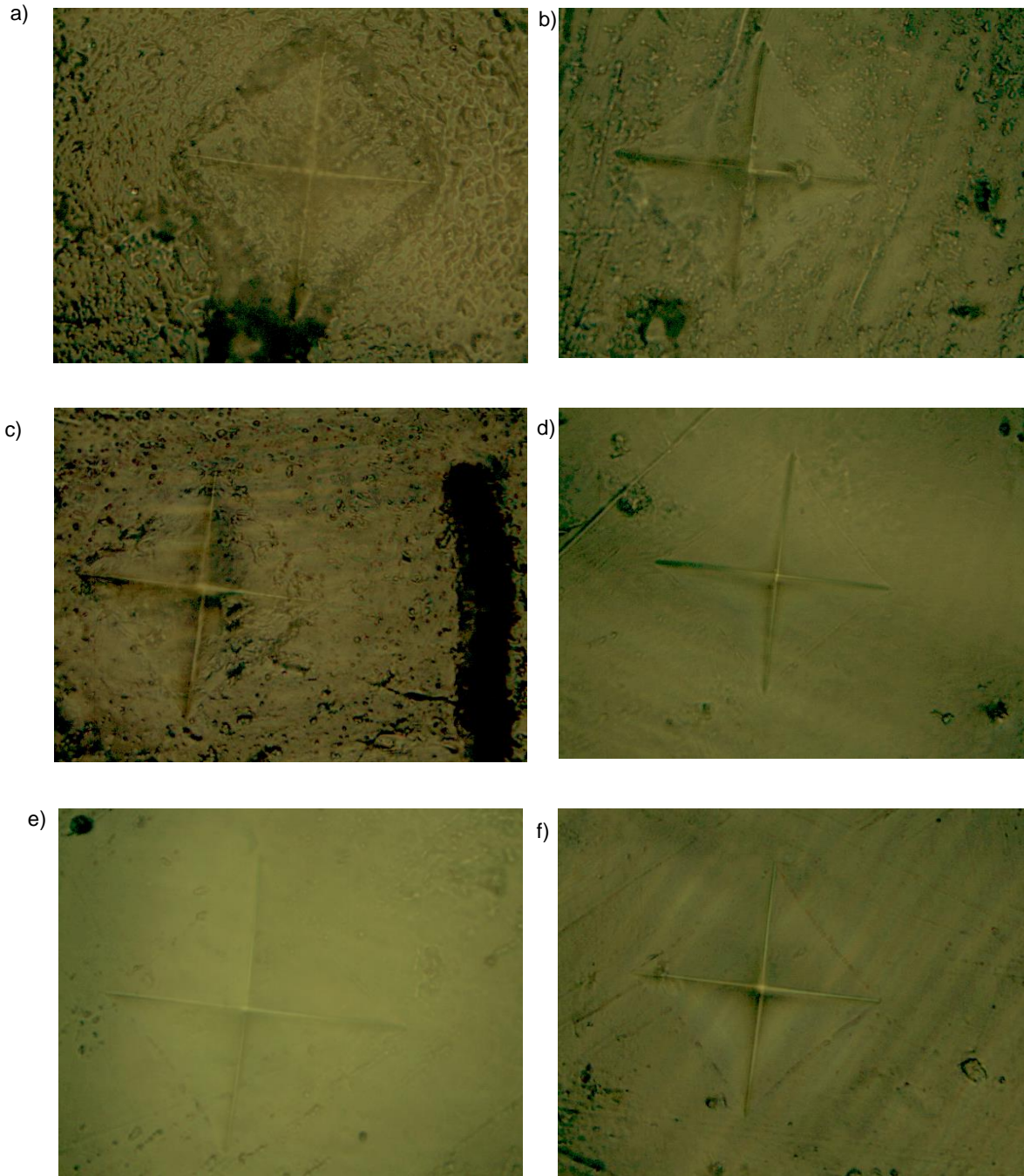


Figure 3.15: Indentation mark on the surface of the samples using Buehler MicroMet 5100 series as hardness device a) A sample, ramp $2^{\circ}\text{C}/\text{min}$, holding time 2 hours and 50 minutes, b) A sample, ramp $3^{\circ}\text{C}/\text{min}$, holding time 2 hours and 50 minutes, c) A sample, ramp $3^{\circ}\text{C}/\text{min}$, holding time 3 hours and 39 minutes, d) B sample, ramp $2^{\circ}\text{C}/\text{min}$, holding

time 2 hours and 50 minutes, e) B sample, ramp 3°C/min, holding time 2 hours and 50 minutes, f) B sample, ramp 3°C/min, holding time 3 hours and 39 minutes.

Note that samples at the last condition using ramp 3°C/min and holding time of 3 hours and 39 minutes are showing more porous surface with larger pinholes and voids as they are burnt even though their mechanical properties slightly improved.

3.5 Summary

It is understood that if delamination happens, it will likely to occur between prepreg and honeycomb for A-boat surface, and between layers of prepreg for B-boat surface. Therefore, as we are mostly focusing on the A prepregs increasing the holding time after the curing process, one of the parameters of the DOE, would decrease the delamination in between the honeycomb and prepreg layer.

From the DMA device, an increase of holding time after the curing process to 7 hours resulted in a noticeable enhancement in the mechanical properties of the prepregs. Thus, for the optimization phase part II the same parameters were being used except we maximized the holding time after the curing process. Values for the second optimization phase indicate that, the optimum points being used for this phase for both A and B prepregs have ramp of 3°C/min, the temperature of 121°C and holding time of 3 hours and 39 minutes after the curing process Table 3.2.

Consequently, using the TGA results before and after the curing cycles for the commercial prepregs indicated that, there is a special relationship between the performed curing temperature of each prepregs and their specific glass transition point that would make our samples either more viscous or brittle compared to each other. Therefore, following this technique type A composites would be more viscous and type B ones would be more brittle Table 3.3 & Figure 3.9.

Working with the tensile strength bar charts while using the Instron device indicate that by increasing the ramp to 3°C/min and having 2 hours and 50 minutes for the holding time parameter, the stress at break point would increase as well, which would agree to the assumption of viciousness/ brittleness of the two types of prepregs. Increasing the holding

time to 3 hours and 39 minutes while having the same ramp would also agree that we are dealing with burnt samples so the tensile strength value for such brittle prepregs would decrease to some extent shown in Figure 3.10.

Checking different mechanical properties led to studying the Young's modulus for the prepreg composites Figure 3.12. Type B prepregs are showing higher values as their carbon fiber content is higher compared to the A prepregs.

Accordingly, results for the modulus of toughness value suggests that, type B prepregs would have higher values. By increasing the ramp factor to $3^{\circ}\text{C}/\text{min}$ the toughness modulus decreased slightly for both composites, meaning the mechanical properties of the samples have improved as we were not looking for the highest toughness modulus overall. Note that increasing the holding time after the curing while having the same parameters demonstrates that modulus of toughness value just decreased as dealing with burnt samples (Figure 3.13).

As Figure 3.15 through the hardness test indicate, we were able to decrease voids and pinholes by switching the conditions from ramp $2^{\circ}\text{C}/\text{min}$ and holding time of 2 hours and 50 to ramp $3^{\circ}\text{C}/\text{min}$ while having the same holding time. Consequently, reaching the condition of ramp $3^{\circ}\text{C}/\text{min}$ and holding time of 3 hours and 39 made the prepregs more porous and burnt texture simultaneously.

All in all, it was understood that type A prepregs are dealing with more viscous texture compared to the brittle structure of B prepregs. Overall, the tensile strength and elongation at the breakage for type A composites would be higher while increasing the ramp to $3^{\circ}\text{C}/\text{min}$ and holding time of 2 hours and 50 minutes. However, working with the young's modulus, toughness modulus and hardness of the samples the behavior would be the opposite and type B prepregs would have higher values. Not to mention that at ramp $3^{\circ}\text{C}/\text{min}$ and increased holding time of 3 hours and 39 minutes, both prepregs would result in burnt samples as they will be having more carbon fiber content during the curing process.

3.6 References

1. Grunenfelder, L.; Dills, A.; Centea, T.; Nutt, S., Effect of prepreg format on defect control in out-of-autoclave processing. *Composites Part A: Applied Science and Manufacturing* **2017**, *93*, 88-99.
2. Hexcel *Hexply Prepreg Technology*.; Hexcel.com, 2017.
3. Hasnine, M., *Durability of Carbon Fiber/Vinylester composites subjected to marine environments and electrochemical interactions*. Florida Atlantic University: 2010.
4. Centea, T., Grunenfelder, L.K. and Nutt, S.R., A review of out-of-autoclave prepregs—Material properties, process phenomena, and manufacturing considerations. . *Composites Part A: Applied Science and Manufacturing* **2015**, *70*, 132-154.
5. Kausar, A., Rafique, I. and Muhammad, B., Aerospace application of polymer nanocomposite with carbon nanotube, graphite, graphene oxide, and nanoclay. . *Polymer-Plastics Technology and Engineering* **2017**, *56(13)*, 1438-1456.
6. Mahmood, I. A.; Shamukh, M. Z., Characteristics and properties of epoxy/polysulfide blend matrix reinforced by short carbon and glass fibers. *Al-Nahrain Journal for Engineering Sciences* **2017**, *20* (1), 80-87.
7. Lionetto, F.; Moscatello, A.; Maffezzoli, A., Effect of binder powders added to carbon fiber reinforcements on the chemoreology of an epoxy resin for composites. *Composites Part B: Engineering* **2017**, *112*, 243-250.
8. Kima, C.; Choa, C. H.; Sona, I.; Leeb, H.; Woo, J.; Hanb, J.-G. K.; Leea, J. H., Effect of microscale oil penetration on mechanical and chemical properties of carbon fiber-reinforced epoxy composites. **2017**.
9. Hexcel *Hexply prepreg technology*; <http://www.hexcel.com/resources/selector-guides>, 2017.
10. Liu, T.; Zhao, Z.; Tjiu, W. W.; Lv, J.; Wei, C., Preparation and characterization of epoxy nanocomposites containing surface-modified graphene oxide. *Journal of Applied Polymer Science* **2014**, *131* (9).
11. ASTM, ASTM D, 4065-12: Standard practice for plastics: dynamic mechanical properties: determination and report of procedures. *ASTM International* **2001**.

12. Standard, A., D3039/D3039M-14. Standard test method for tensile properties of polymer matrix composite materials. West Conshohocken, PA: ASTM International; 2014. 2014, doi: 10.1520/D3039_D3039M-14.
13. ASTM, Standard test method for tensile properties of polymer matrix composite materials. ASTM International. *ASTM Committee D-30 on Composite Materials* **2008**.
14. Appinc Tensile strenght testing.
15. Dalle Vacche, S.; Michaud, V.; Demierre, M.; Bourban, P.; Månson, J. E. In *Curing kinetics and thermomechanical properties of latent epoxy/carbon fiber composites*, IOP Conference Series: Materials Science and Engineering, IOP Publishing: 2016; p 012049.
16. Mravljak, M.; Sernek, M., The influence of curing temperature on rheological properties of epoxy adhesives. *Drvna industrija* **2011**, 62 (1), 19-25.
17. Sarrai, A.; Hanini, S.; Merzouk, N.; Tassalit, D.; Szabó, T.; Hernádi, K.; Nagy, L., Using central composite experimental design to optimize the degradation of tylosin from aqueous solution by photo-fenton reaction. *Materials* **2016**, 9 (6), 428.
18. Mumin, M. A.; Akhter, K. F.; Oyeneye, O. O.; Xu, W. Z.; Charpentier, P. A., Supercritical fluid assisted dispersion of nano-silica encapsulated CdS/ZnS quantum dots in poly (ethylene-co-vinyl acetate) for solar harvesting films. *ACS Applied Nano Materials* **2018**, 1 (7), 3186-3195.
19. software, D. E., T test experiment 2018

Chapter 4

4 Conclusions and Recommendations

4.1 Conclusions

The present research showed that, both commercial prepregs have pros and cons. Using TGA and DSC devices, the type A sample shows better homogeneity (better adhesion between epoxy resin and carbon fiber) but weaker adhesion to Nomex honeycomb core, especially at current processing temperature (121 °C) or higher (150 °C).

Moreover, as we are mostly focusing on type A prepregs increasing the holding time after the curing process, one of the parameters of the DOE, would decrease the delamination in between the honeycomb and prepreg layer. Note that, as we increased the temperature the T_g point increased as well. At ramp 2 °C/min, by increasing the temperature both storage and loss modulus decreased. After the T_g point increased, using same samples at higher ramp (5 °C/min), the pattern is nearly the same with lower values. So, switching to a safer ramp (2.5– 3.5 °C/min) could be the best option.

Later on, the central composite design as our design of experiment was being used. Having 4 parameters in the design for optimizing 4 responses resulted in running 40 tests. The evidence suggested that in order to have the best optimized conditions meaning maximized storage modulus, stiffness and $\tan \delta$ and minimized loss modulus our parameters for the central composite design need to be at ramp 3 °C/min, temperature 121 °C, holding time of 2 hours and 50 minutes after curing for both A and B prepregs.

The DMA device was being used to increase the holding time after the curing process to 7 hours resulting in noticeable enhancement in the mechanical properties of the prepregs. Thus, for the second phase of our optimization the same parameters were being used except we maximized the holding time after the curing process. Results of the second optimization phase indicate that, the optimum points being used for this phase for both A and B prepregs have the ramp of 3 °C/min, temperature of 121 °C and holding time of 3 hours and 39 minutes after the curing process. It is interesting to add that all the contours and 3D plots for the statistical analysis section agreed to the above information except, at higher holding

time (second optimization phase) the stiffness value for B samples were slightly more acceptable and practical compared to the values for A results. Moreover, aiming the optical microscopic, A samples have better uniformity and less holes by enhancement of the ramp factor. Both commercial prepregs at ramp $3^{\circ}\text{C}/\text{min}$ and holding time of 3 hours and 39 minutes reached a burnt texture even though, their mechanical properties seemed to improve at mentioned conditions.

Using the TGA results before and after the curing cycles for the prepregs indicated that, there is a special relationship between the performed curing temperature of each prepregs and their specific glass transition point that would make our samples either more viscous or brittle compared to each other. Therefore, following this hypothesis type A composites would be more viscous and type B ones would be more brittle.

Subsequently, checking different mechanical properties led to studding factors from the tensile strength to the modulus of toughness results using the Instron device. Thus, as type B prepregs are showing higher values in their carbon fiber content than A prepregs, the young's modulus and toughness modulus values would be higher but due to the resin content their elongation at break point would be lower compared to type A prepregs. Working with the tensile strength bar charts indicate that, increasing the ramp to $3^{\circ}\text{C}/\text{min}$ and having 2 hours and 50 minutes for the holding time parameter, the stress at break point would increase, which would agree to the assumption of viciousness/ brittleness of the two types of prepregs.

Following the hardness technique, we were able to decrease voids and pinholes by switching the conditions from ramp $2^{\circ}\text{C}/\text{min}$ and holding time of 2 hours and 50 to ramp $3^{\circ}\text{C}/\text{min}$ while having the same holding time. Consequently, reaching the condition of ramp $3^{\circ}\text{C}/\text{min}$ and holding time of 3 hours and 39 made the prepregs more porous and burnt texture simultaneously.

All in all, it was understood that type A prepregs are better candidates and not only we could increase the ramp of the curing process to up to $3^{\circ}\text{C}/\text{min}$ but also, we could eliminate possible pin holes and sever voids by only increasing the holding time after the curing process mostly to 2 hours and 50 minutes in the lab scale. Not to mention working with the

A type would produce more viscous samples. Increasing the holding time to 3 hours and 39 minutes would make both prepregs resulting burnt samples as they will be having more carbon fiber content during the curing process.

4.2 Recommendations for future works

During the present work, some areas were revealed to be of significant interest for future research; as a result, for the next steps of this project, the following would be taken into consideration:

- Studying the mechanical properties of the initial and optimum curing conditions using the Instron device to learn more about the effect of adhesions in between the prepregs and honeycomb layer.
- Examining the fracture surface of composites using SEM and other imaging techniques to give us good information and accurate measurement on the size of the pinholes and voids of the composite surface.
- Aiming a kinetic model, for the oven curing process of such prepregs.
- Elaborating on the possibility of switching to another resin, for instant, vinyl resins can be prepared at room temperature and normal pressure, so it is reported to strongly depend on the curing temperature, initiators and accelerator levels which are already known and settled for this project.
- Consuming graphene oxide or hemp fibers as the suitable candidate additives to enhance the mechanical properties of the prepregs.

Curriculum Vitae

Name: Rayehe Samimi

**Post-secondary
Education and
Degrees:** Western University
Sharif University of Technology, Iran, Tehran
2012-2016 B.E.Sc.

The University of Western Ontario
London, Ontario, Canada
2017-2019 M.A.

**Honours and
Awards:** Province of Ontario Graduate Scholarship
2017-2019

**Related Work
Experience** Teaching Assistant
The University of Western Ontario
2017-2019

Publications:

Poster presentation at Interamerican congress of Chemical Engineering incorporating the 68th Canadian chemical engineering conference at Toronto, Ontario, Canada